Cracking Performance of Asphalt Mixtures Containing Taconite Tailings using Traditional and Multiple Freeze-Thaw Moisture Conditioning Methods

A THESIS
SUBMITTED TO THE FACULTY OF THE GRADUATE SCHOOL
OF THE UNIVERSITY OF MINNESOTA
BY

Justin Joel Baker

IN PARTIAL FULFILLMENT OF THE REQUIREMENTS
FOR THE DEGREE OF
MASTER OF CIVIL ENGINEERING

Eshan V. Dave

September 2012

Acknowledgements

I would like to thank a few people for their efforts in helping me through the work of my thesis. First of all, I would like to thank my advisor, Dr. Eshan Dave, for his direction, encouragement, and commitment to this project and myself. I would also like to thank Eddie Johnson and the Minnesota Department of Transportation, as well as Martin Marietta Materials for their efforts in providing valuable resources to our project and technical advice. Finally, I would like to thank the University of Minnesota Duluth's Civil Engineering Department for providing an excellent educational experience. The views expressed in this paper are that of the author and do not reflect those of sponsors.

I dedicate this thesis to my parents,

Mark and Sharon.

ABSTRACT

Crushed aggregate resources for use in infrastructural applications are depleting and use of alternative resources is necessary to meet the demand. With annual consumption of approximately 1.2 billion tons of aggregates in the United States, significant environmental impact is caused. Annually, more than 125 million tons of fine grained crushed siliceous material is generated through iron ore mining in Northern Minnesota. This material is typically referred to as "taconite tailings" and usually ends up as landfills near mining operations. Research is being conducted on the potential usage of taconite tailings in asphalt mixtures to improve sustainability of highways.

This study is focused on the key pavement failure mechanism of moisture damage, typically evident in the form of pot-holes during winter and spring seasons. The mechanical performance of asphalt concrete rapidly deteriorates in presence of moisture and is significantly accelerated through incur of freeze-thaw cycles. Currently there are no standardized tests which condition asphalt mixtures through multiple freeze-thaw cycling. Therefore, this study explored a method for subjecting specimens to multiple freeze-thaw cycles using temperatures which better represent actual climatic conditions. A field conditioning method was also employed by placing samples outside over a period of winter and spring months. These proposed conditioning methods were compared with a conventional conditioning process used for AASHTO T-283 procedure. The evaluation of moisture damage in asphalt mixtures containing taconite tailings was conducted using the conventional AASHTO T-283 test procedure and a fracture energy based approach.

Testing results indicate that mix containing taconite tailings has acceptable moisture damage resistance after multiple freeze-thaw and field conditioning, which more accurately represents typical climatic conditions. The mechanical behavior of field and multiple freeze-thaw conditioned samples was quite different as compared to those conditioned in lab using the traditional AASHTO procedure.

TABLE OF CONTENTS

LIST OF TABLES

LIST OF FIGURES

CHAPTER 1: INTRODUCTION AND MOTIVATION

Approximately 1.2 billion metric tons of crushed aggregates were manufactured in the United States in 2010 at the cost of about $11 billion [1]. The crushed aggregate resources for use in infrastructural applications are depleting and use of alternative resources is necessary to meet the demand [2]. The environmental cost of producing crushed aggregates is quite significant [3]. The outcomes of mining and crushing operations further lead to greater ecological and sociological problems [4]. Mining by-products can be utilized to substitute the new crushed aggregates usedin the manufacturingof asphalt concrete.

Annually, about 40 million tons of high grade iron ore, rich in the mineral hematite, is produced in the North-Central portion of United States at the Minnesota Mesabi Iron Range (MMIR) mining operations. This production is about 75% of the total United States' production of iron ore. During processes to enrich the ore, the large blasted rock particles are crushed to finer sizes and iron rich ore particles are extracted through use of magnets. The left behind crushed siliceous aggregate is commonly referred to as "taconite tailings." Typically the tailings are used as backfill material at the open pit mines.Previous studies have indicated that the mechanical properties of taconite aggregate, in particular their crushing resistance and hardness, make them well suited for use in asphalt concrete.

While previous studies have explored viability of using taconite tailing in asphalt mixes and conducted research on aspects related to logistics of using tailings, there is limited information available on mechanical properties of asphalt mixes containing taconite tailings and their performance. Due to the siliceous nature of this aggregate one potential problem can arise from moisture induced damage. Moisture damage primarily occurs due to penetration of moisture between asphalt mastic film and aggregate surface causing stripping of the asphalt film leading to material disintegration. Especially for colder climates where effects of moisture induced damage are exaggerated due to freezing, the material damage can significantly increase the amount of pavement cracking leading to premature failure. This study evaluates moisture damage potential in asphalt mixtures

containing taconite tailings against traditional mix with a perspective on pavement cracking.

Currently there are no standardized tests which subject asphalt mixtures to multiple freeze-thaw cycling as typically seen in the field. This study examined the use of a conditioning process with multiple freeze-thaw cycling using 10 and 20 freeze-thaw cycles with temperatures typically seen in the field. A set of samples were also placed in the field for a period of winter and spring months to examine the effects of natural process. The study intended to make preliminary comparisons between these proposed conditioning methods and current conditioning methods.The standard test method for determining moisture induced damage potential in asphalt concrete is AASHTO T-283 [5]. The AASHTO method is required as part of the Superpave asphalt mix design which has been adopted by several State and local transportation agencies. In recent years the AASHTO procedure has received criticism for being too empirical and not representative of the actual field moisture damage. The mechanical property evaluation for the AASHTO procedure is conducted through indirect tensile strength test conducted at 25°C. For regions of older climate, such as Minnesota, the indirect tensile strength test at 25°C is not representative of typical conditions present during winter and spring months.

The use of fracture energy based measurements of asphalt concrete's cracking resistance has gained popularity in recent years. In this work both the AASHTO procedure using indirect tensile strength and fracture energy measurement using the disk-shaped compact tension (DCT) test were employed. The DCT tests were conducted using the ASTM D7313 [6] test procedure. The moisture conditioning for DCT specimens followed the same process as the AASHTO T-283 as well as testingsamples subjected to multiple freeze-thaw cycling and field conditioning.

Background information through literature review on topics of using taconite tailings in asphalt concrete and moisture damage evaluation are presented in the subsequent section. The testing plan and details on materials are presented thereafter and followed by test results and discussion.

CHAPTER 2: BACKGROUND AND LITERATURE REVIEW

Mining by-products can be utilized to substitute the new crushed aggregates used in manufacture of asphalt concrete. Previous studies have indicated that the mechanical properties of taconite aggregate, in particular their crushing resistance and hardness, make them well suited for use in asphalt concrete. The following includes an extensive literature review which examines taconite tailing aggregates, moisture damage in asphalt pavement, and current mechanical testing and conditioning methods for asphalt mixtures.

2.1 Taconite Tailings

Taconite tailings are a by-product produced from mining taconite. As one of the world's leading producers in mining taconite, 125 million tons of taconite tailings are produced annually on Minnesota's Iron Range [7]. Most of the tailings produced are stored in piles until they are needed. Common sites in which tailings are extracted from include Ispat Inland, Minntac, EVTAC, Hibbing Taconite, and National Steel Pellet Company [8].

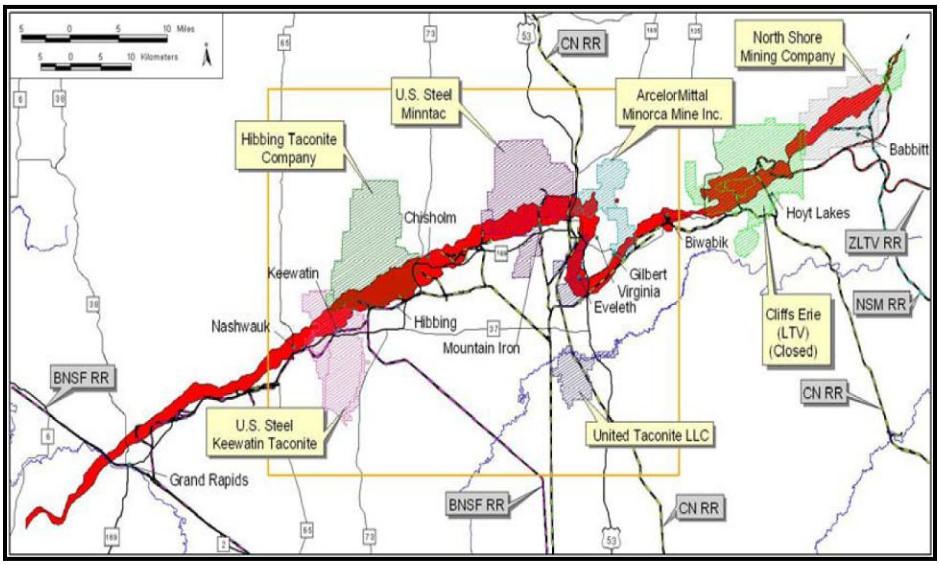

Figure 1: Taconite operations on the Mesabi Range (from reference [10])

Previous studies have indicated that the mechanical properties of taconite aggregate, in particular their crushing resistance and hardness, make them well suited for use in highway pavement applications. Taconite aggregate material testing was completed from the five mining operations listed above by previous researchers [8]. The results revealed

the tailings have superior properties in the area of soundness, sand equivalency, fine aggregate angularity, lightweight particles, R-value, and hydraulic conductivity. Material testing of taconite aggregate has also been performed byMinnesota Department of Transportation (MnDOT). Three materials were tested including railroad ballast, Ispat Tailings, and Minntac Tailings. Tests conducted on the materials included gradation, specific gravity, fine aggregate angularity, and percent crushed. Testing demonstrated the taconite aggregates performed as well or better than conventional aggregates [9].

Taconiteis an iron-bearing sedimentary rock commonly mined on Minnesota's Iron Range [10]. Taconite pellets are extracted from the mining process and used to create steel.During the mining and extraction process, large amounts of waste material are produced, called "tailings," and are stored in piles near the mining operations. Taconite tailings are a very hard, durable material containing large amounts of quartz. Table 1 provides mineral compositions for both Minntac Coarse Tailings and a Martin Marietta Granite aggregate, both used for this study.Tailing's hardness and high compressive strength can be attributed to the iron-formation they were extracted from. These hard, durable aggregates possess other quality properties including skid resistance which plays an important role in the safety of our highways.

Table 1: Mineral composition of aggregate sources used for this study (data reprodcued from Zanko et al. [10])

Mineral	Aggregate Source Mineral Composition [%]	
	Minntac (Coarse Tailings)	Martin Marietta (Granite)
Quartz	85	65
Albite		15
Biotite		5
Augelite		5
Anorthite		5
Sanidine		3
Pargasite		2
Hematite	6	
Minnesotaite	2	
Sepiolite	3	
Clinochlore-1M11b	2	
Siderite	2	

2.1.2 Historical use of Taconite Tailings in Minnesota Roadways

Taconite tailings have been used in Minnesota for construction dating back as early as the 1950s. In the early days, tailings were mainly used on the Iron Range due to their close proximity. By the 1970s and 1980s, they started to move their way down towards southern Minnesota [11]. Even though much of the tailing material is used for operation at the mines, millions of tons of tailings are produced annually which results in a high amount of excess material. Excess material combined with current transportation systems allows for the tailings to be shipped anywhere across the world.

Figure 2: Taconite tailings used for railroad ballast outside of Minot, ND (Enbridge)

Tailings were first used inhighway applications in 1958 [11]. They were used as a stabilizing base material on Trunk Highway 61. By 1961, tailings were being used as fill material as well as in bituminous mixtures. By 1970, a stretch of Highway 61 from Palisade head to just north of Silver Bay, near Illgen City, was constructed completely with taconite aggregate. Tailings were used as base material, as well as the aggregate source in the base course, binder course, and wear course. According to officials, the roadway held up very well but was eventually overlaid by the existing pavement.

Because taconite tailings have very low percentages of fine material, they hold up well with capillary and freeze-thaw action as roadway base materials. Therefore, they were

ideal for the use in low-lying wetland areas. Part of Highway 53 near Virginia used large amount of tailings along a low-lying area.

Tailings possess excellent skid resistance and wearing characteristics, which increased their demand in thin overlays. Overlays that were laid in the 1970s in the Grand Rapids area all the way over to the Moorhead area are still in service.

By the 1980s, the taconite industry saw a downturn due to the closing of mines [11]. This led to the use of tailings in projects closer to the Iron Range. The 1990s saw more use of bituminous mixtures containing tailings. The largest use of tailings in a project occurred during 2004-2005 on the Highway 53 and Highway 169 interchange north of Virginia, MN. Over 1.82 million tons of tailings were used, mostly as embankment fill. The bituminous mixtures contained 10% tailings.

2.1.3 Pavement Test Sections with Taconite Tailings

In 2004 MnDOT started a partnership with Minnesota DNR to evaluate the use of taconite tailings in pavement mixtures [9]. The goal of the project was to asses asphalt mixtures containing taconite aggregate and if they would be suitable for low volume roads in Minnesota. Two test sections were constructed on a Low Volume Road (LVR) at the MnROAD Facility. Both mechanical properties and economic issues were dealt with in the project. Project tasks included assessing pre-existing road sections with taconite tailings, constructing new test sections with taconite tailings, maintenance treatments, demonstration projects, pothole studies, and laboratory testing.

In 2004, a low traffic volume asphalt mixture called Cell 31 and a concrete pavement mixture called Cell 54 were constructed. Cell 31 consisted of 80% Mesabi Select Hard Aggregate which included the coarse and fine aggregate of the mixture. The design included a 100 mm (4 inch) thick mat over 400 mm (16 inches) of aggregate base as specified by MnPAVE software. A PG64-34 binder at 6.4% proportioned by weight was used. A traffic level 2 (< 1 million Equivalent Single Axle Load traffic level) was specified since taconite aggregate did not meet the flat and elongated particles criteria set

forth by MnDOT. The Cell 54 contained Mesabi Select as an aggregate in concrete. The cell included an 8 inch thick concrete layer with various base layers. The pavement was jointed plain with slab dimensions as 3.5 m (12 feet) by 4.5 m (15 feet). The transverse joints were doweled and the longitudinal joint was tied. The main object of Cell 54 was to construct, test, and investigate the usage of taconite aggregate in concrete. This is believed to be the first ever use of taconite aggregate in concrete.

Three test cells were constructed in 2008. Two of the cells were constructed on interstate 94 and the other on the low volume road. The Cell 6 which was constructed on interstate 94 consisted of a 50 mm (2 inch) overlay over a 130 mm (5 inch) newly constructed concrete pavement. The objective was to investigate the performance of a thin layer of asphalt containing taconite aggregate. The HMA was a 4.75 mm mixture containing fine taconite aggregate. Cells 23 and 87 were constructed using taconite railroad ballast as an aggregate base material.

Monitoring of distresses, rutting, ride quality, faulting, falling weight deflectometer, and friction was completed for the test cells by MnDOT. After three years in service, minimal distresses were found in all test cells. Cell 6 has not resisted cracking very well but can be attributed to reflective cracking of the underlying concrete. More cracks appeared in the fall of 2009 but it is unclear if the cracks came from the HMA due to thermal effects or reflected from the concrete layer beneath. In terms of rutting, all cells demonstrated good performance. All cells were close to a Ride Quality Index of 3.0 which is the threshold between good and fair ride performance. The Cell 6, the fine aggregate mixture, had the highest ride quality. No measureable faulting was observed at the time of writing this thesis. The falling weight deflectometer was tested on sections containing taconite ballast as a base material. Test results demonstrated the taconite ballast has a much higher strength compared to MnDOT's typical Class 5 base material. All three cells with taconite aggregates demonstrated very good friction performance.

A summary of the project concluded that taconite aggregate can be successfully used in pavement applications. Quality aggregate base, asphalt, and concrete layers can be

constructed using taconite aggregates. Test sections constructed at MnROAD have performed as well or better than conventional pavements. Further research will continue and is expected that taconite aggregate will provide a durable material for pavement applications.

2.2 Moisture Damage in Asphalt Concrete

The mechanical performance of asphalt concrete rapidly deteriorates in presence of moisture and is significantly accelerated through incur of freeze-thaw cycles. Water can enter the pavement structure through surface cracks, air voids, the subgrade/base, and the sides. The degradation of asphalt concrete properties due to effects of moisture is commonly referred to as moisture damage (Figure 3). The main processes that lead to moisture damage are loss of cohesion, failure of adhesion, and degradation of aggregate. These processes eventually lead to pavement distresses such as stripping, potholing, raveling, and loss of support.

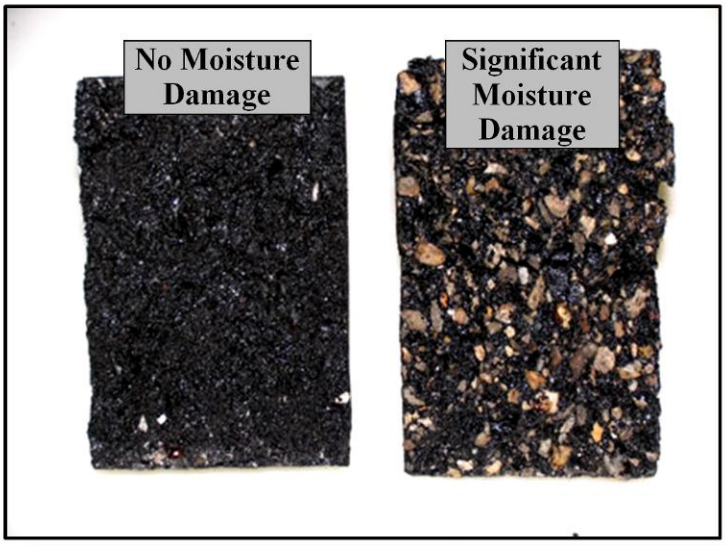

Figure 3: Moisture damage in asphalt mixture (image from pavementinteractive.org)

Factors which affect moisture damage include aggregate type, binder grade, mix design and construction, environment, traffic, and anti-stripping additives. Binder grades have the potential to effect moisture damage. Since stiffer asphalts are harder to peel off of aggregate, they usually have a better resistance to moisture damage. Air void level and

permeability are greatly influenced by mix design and construction methods. A larger amount of air voids and permeability gives way to channels where water can seep into the pavement structure and cause moisture damage. Higher binder contents reduce moisture susceptibility of a mixture since there are fewer voids for water to travel through. Usually, dense graded mixtures have around 15% to 25% air voids. As long as water can completely drain, this is acceptable. Previous researchers haveshownthe nominal maximum aggregate size (NMAS) ratio as one of the key failure mechanisms in rehabilitation methods. When the suggested NMAS ratio was not met, adequate compaction and density was not met and caused a moisture damage failure [12]. The environment is another factor influencing moisture damage. Higher rainfall amounts cause more chance for water to enter the pavement structure. Colder climates can also cause major damage due to freeze-thaw mechanism. Traffic can force water into the pavement structure and cause moisture damage. However, decreased air void levels from traffic decreases permeability and decreases the risk of moisture damage [13].

Stripping is the most common form of moisture damage. Stripping occurs when the asphalt film is "stripped" from the aggregate, usually caused by the presence of water. The loss of strength of a mixture can be related to a loss of adhesion or cohesion. Adhesive failure is defined by the failure of bond between the binder and the aggregate, whereas cohesive failure is the failure withinthe asphalt mastic itself. Moisture damage of asphalt usually starts at the bottom of the asphalt layer. This will eventually cause potholes, raveling, rutting, cracking, etc. [13].

Many tests have been developed to determine moisture susceptibility of asphalt mixes. These include tests performed on aggregates, mixtures, and chemical analysis. Tests on aggregates include static and dynamic immersion, boiling water, detachment tests, etc. Tests on asphalt mixtures include dynamic abrasion, Marshall Immersion, Hveem Stability, indirect tensile tests, elastic modulus, etc. [13].

Warm Mix Asphalt (WMA) is a fairly new process in which asphalt is produced at much lower temperatures than Hot Mix Asphalt (HMA) in order to save on energy use.

Although WMA saves on energy use, there have been reported issues with moisture damage due to inadequate drying of aggregate. Gong and Tao, conducted fracture energy and resilient modulus testing on asphalt samples in which aggregates were either fully or partially dried as well as subjected to moisture conditioning [14]. Resilient modulus tests indicated there was a significant effect of both moisture conditioning as well as incomplete drying of aggregate. Incomplete drying of aggregate as well as moisture conditioning led to a decrease in the resilient modulus. There was no significant difference in the creep compliance test between samples, other than the samples which were subjected to incomplete drying of aggregate as well as moisture conditioning had the largest creep compliance. The same trends as seen with the resilient modulus were seen with the indirect tensile test. Whenever moisture was present, or moisture conditioning occurred, the strength values decreased. The fracture energy test results showed a significant decrease in fracture energy with both the presence of moisture as well as moisture conditioning. This led to the sample that was both moisture conditioned and had incomplete drying to have the lowest ER value [14].

2.3 Moisture Conditioning Processes

Asphalt pavement rapidly deteriorates when moisture is present. In addition to moisture, freeze-thaw action causes acceleration of deterioration. Roadways in northern climates experience higher amounts of freezing and thawing which cause pavements to degrade more quickly. Some testing procedures aim to analyze the effects of moisture conditioning and freeze-thaw action, but none which investigate multiple freeze-thaw cycles.

The most widely accepted moisture damage evaluation method is the modified Lottman procedure that utilizes the tensile strength ratio (TSR). The original method is based on work by Lottman [15]. The method has been revised to make it suitable for Superpave mix design procedure through work by Epps et al. [16]. The current method is specified as the AASHTO T-283 test procedure [5]. There has been some criticism of the test for its high variability and not representative of actual field conditions [16-17].

The procedure entails use of six asphalt specimens that are compacted to achieve an air void level of 7% ± 1%, three of which are conditioned and three are tested unconditioned (dry). The conditioned samples are soaked in water, and then put through one freeze thaw cycle. The samples are then thawed in a water bath before being tested for indirect tensile strength. Details of the conditioning procedure are described in the sections discussing the testing plan.

Currently there are no standardized tests for conditioning asphalt samples with multiple freeze-thaw cycles. In northern climates such as Minnesota, pavements experience many freeze-thaw cycles through the winter and spring months. In a study performed by the Federal Highway Administration, environmental conditions such as deep-freeze with low freeze-thaw cycles and moderate-freeze with high freeze-thaw cycles were tested [18]. Pavement responses of interest included rutting, fatigue cracking, roughness, and transverse cracking. Initially, a higher rate of distress accumulation was found in deep freeze and multiple freeze thaw cycle zones. The study determined that multiple freeze-thaw cycles contributed more to rutting compared to deep-freeze climates, whereas deep-freeze climates had the largest effect on fatigue wheel path cracking. It was also found that the International Roughness Index increased more so in deep-freeze climates with transverse cracking initiating earlier in pavement life. The study determined that cold weather climates with multiple freeze-thaw cycles and deep-freeze conditions create difference responses in pavement. Therefore, pavement mixes that will be exposed to cold weather environments need to be tested under these conditions.

2.4 Mechanical Testing

Moisture damage evaluation of asphalt materials has gained more recognition since the 1970s. Moisture damage is detrimental to pavements and causes rutting, raveling, and cracking which results in poor performance of our highways. With rising interest in moisture damage, standardized tests have been formed. Some of the more common tests conducted on asphalt mixtures include AASHTO T-283, Fracture Energy, and SuperPave indirect tensile strength test (IDT). There are currently two types of moisture susceptibility tests. The first includes subjecting a specimen to moisture conditioning

prior to mechanical loading, such as AASHTO's T-283. The second type subjects a specimen to a mechanical load while being saturated; typically the mechanical loading is cyclic in nature in this category. This simulation can be done using the Hamburg Wheel-Tracking Device or the Asphalt Pavement Analyzer. Previous research implies that the currenttesting methods do not exactly correlate with the same conditions asphalt experiences in the field [19]. Making a direct link between physical parameters regarding moisture susceptibility and engineering properties was determined of critical importance along with determining a time frame over which the moisture induced damage may occur in the field.

2.4.2 Indirect Tensile Strength Test (AASHTO T-283)

One of the most common moisture susceptibility tests for asphalt mixtures is the AASHTO T-283. The test procedure was developed originally to utilize specimens compacted with the Marshall device.The procedure has since been modified to utilize compacted samples using a Superpave gyratory compactor (SGC) with 150 mm diameter as compared to 100 mm diameter samples.Although AASHTO T-283 is a very common test, researchers have found that even though a sample may pass the lab specification requirements, significant damage (such as stripping) is still seen over time [16].

AASHTO T-283 involves subjecting compacted asphalt mixtures to one freeze thaw cycle. The specimens are then tested in an indirect tensile mode at a loading head displacement rate of 50 mm/min until the failure. Six specimens are produced; three that will be tested in a dry state and three that are tested in a conditioned state. All specimens are tested at 25^{o}C. The maximum compressive load is recorded and the maximum indirect tensile stress is calculated using the equation below, where S is the stress (MPa), P is the load (N), D is the diameter (mm), and t is the thickness (mm).

$$S = \frac{2P}{\pi D t}$$

The end result of the test includes calculating the tensile strength ratio (TSR). TSR is calculated by dividing the indirect tensile strength of the conditioned specimens by the

strength of the dry specimens. In order to meet the requirements, specimens need to have a TSR of 85% or greater [20].

2.4.3 Disk Shaped Compact Tension Fracture Test

Fracture cracking is one of the major causes of deterioration in asphalt concrete, especially in colder climates. Fracture cracking is caused by a combination of wheel loading and environmental conditions.

The fracture energy of material is the amount of necessary energy consumed before a crack or discontinuity is formed. It is differentiated from tensile strength in the sense that strength simply gives the peak stress limit at which failure is initiated, whereas, fracture energy is a mechanical property that includes formation of damage, accumulation of damage and formation of a crack. This is especially important in quasi-brittle material like asphalt concrete which exhibit significant material capacity even after the peak stress threshold (strength) is reached.

The Disk Shaped Compact Tension (DCT) Test was developed by Wagoner et al. [21] as a method for determining fracture energy of asphalt concrete. The DCT test can be performed on both cored field samples or laboratory compacted samples.

The specimen preparation for the DCT test involves an intricate procedure. The geometry is created from a 50 mm thick, 150 mm diameter asphalt sample, typically obtained from sawing of gyratory compacted cylindrical sample. A flat face, two 25 mm holes, and a notch are cut to create the specimen geometry. Figure 4 provides the specimen geometry layout from ASTM D7313 specification. The test procedure begins with placing the test specimen at the desired temperature for at least 2 hours and no more than 16 hours. It is recommended that the test temperature be 10^{o}Cwarmer than the low temperature limit of the binder grade. The specimens are then placed into the loading fixtures, as shown in Figure 5. The test is performed at a displacement rate of 0.017 mm/s until the post-peak load level has reduced to 0.1 kN. Results obtained from fracture testing include load and crack mouth opening displacement (CMOD). Plots of

CMOD versus time and load versus CMOD can be created. After the area under the load-CMOD curve is calculated, the fracture energy can be calculated using the equation below. In this equation, G_f is the fracture energy (J/m^2), B is the thickness of the specimen (m), W is the diameter of the specimen (m), and a is the notch length (m) [6]. The difference between W and a is called the "ligament length."

$$G_f = \frac{AREA}{B \cdot (W - a)}$$

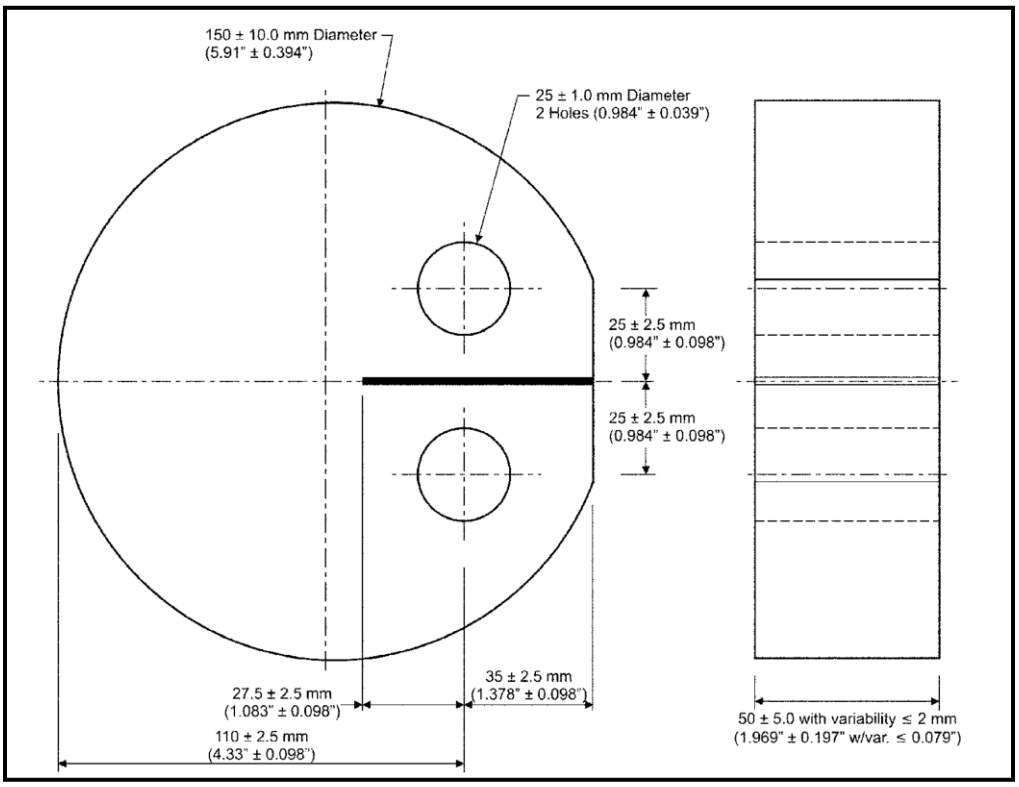

Figure 4: Disk-Shaped Compact Tension Test specimen geometry (from ASTM D7313)

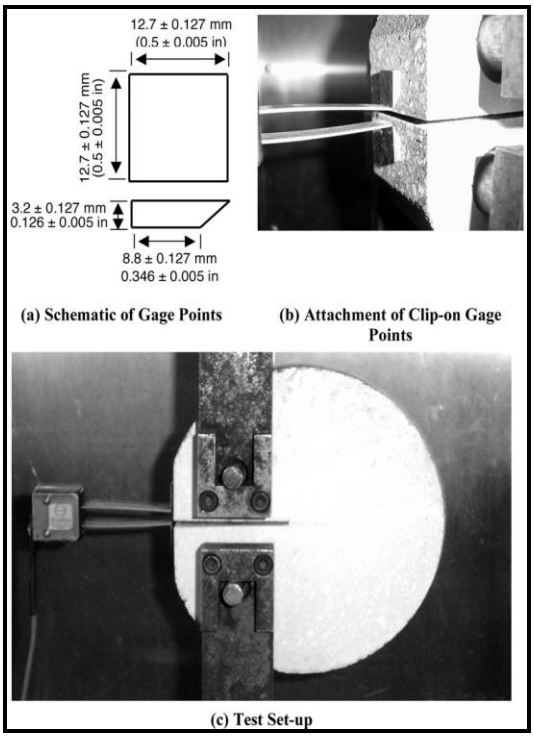

Figure 5: Disk-Shaped Compact Tension test setup (from ASTM D7313)

In recent years the use of fracture energy concepts have become exceedingly popular in linking pavement cracking performance with asphalt mix's mechanical properties. A variety of fracture energy tests and procedures have been proposed, for example, use of indirect tension test [22], disk-shaped compact tension (DCT) test [23], and semi-circular bend (SCB) test [24]. The work by Apeagyei et al. [24] showed the applicability of DCT test in evaluating moisture damage in asphalt mixtures. Use of the energy ratio concept was utilized by Birgisson et al. [26] using IDT fracture tests. The results from this study showed very promising results for using fracture energy ratios.

In a study performed by Birgisson et al., the use of a new performance-based fracture criterion, Energy Ratio (ER), was evaluated for quantifying the effects of moisture damage on the fracture resistance of HMA samples. Current testing for moisture susceptibility only considers a single parameter before and after conditioning, such as tensile strength ratio and modulus ratio. A new performance based fracture parameter, called the energy ratio, was tested in this study. The ER was determined by testing unconditioned and conditioned samples for their fracture resistance. Not only did the study determine that ER is capable of detecting moisture effects, but also the effects of

anti-stripping additives. Samples were conditioned according to AASHTO T-283 specifications and were tested for IDT fracture properties. Fracture energy testing was then conducted on each mixture. The results showed that mixtures with and without anti-stripping additives decrease in fracture energy of conditioned samples. Mixtures with anti-stripping additives had a smaller decrease than mixtures without stripping additives [27].

The DCT and SCB tests have been extensively used for evaluating thermal cracking performance of asphalt pavements [28-30]. The DCT test has also been used extensively in study of reflective cracking in asphalt overlays [31-32]. The DCT fracture energy test has shown very promising results in distinguishing different asphalt mixes in terms of their cracking performance [28, 30] and has been applied to a variety of asphalt mix applications, such as investigating the effects of recycling [33]. Through comprehensive survey of performance tests and material specifications, Dave and Koktan [34] recommended fracture energy tests as most suitable candidates for use as performance test in Minnesota.

The review of previous research described in the preceding write-up helped develop the testing plan for this study. Based on the review it was decided that two types of mixes will be studied; one that utilizes a significant fraction of mineral aggregate in form of taconite tailings and another one that uses commonly used aggregate source from Minnesota. The AASHTO T-283 conditioning procedure was selected due to its popularity and usage over past several decades. For indirect tensile strength tests conducted at 25°C, (AASHTO T-283 procedure) the lab conditioning process recommended by AASHTO T-283 has been used. However, not much information is available as to how this empirical lab condition process fares with fracture properties of materials determined at low temperatures. Thus, it was decided that replicate specimens be conditioned in field by leaving them next to a roadway for duration of one winter and spring season. It was also decided to conduct tests on samples subjected to 10 and 20 freeze-thaw cycles. The field conditioned and multiple freeze-thaw samples will provide more representative results of a pavement in northern Minnesota.

CHAPTER 3: TESTING PLAN AND MATERIALS

3.1 Asphalt Mix Types used in this Study

Asphalt samples were manufactured using previously used mix designs received from the Minnesota Department of Transportation (MnDOT). Aggregate materials were obtained from MnDOT and Martin Marietta Materials.Additional mixtures were tested and include samples from projects on Minnesota trunk highways TH9, TH70, and TH371 along with parking lot mixes from the University of Minnesota Duluth. Mix designs and volumetrics were provided for these mixtures. The following describes each of the asphalt mixtures used in this research along with a brief description of laboratory mix preparation.

3.1.2 Granite and TaconiteMixture Designs

An asphalt mixture made with granite aggregate was used as a baseline to compare against the taconite samples. The mixture was made of 100% granite aggregate from Martin Marietta Materials in St. Cloud, Minnesota with a binder content of 6.90%. The granite material used is made of crushed rock and consists of 100% angular material with very little flat and elongated particles, providing a quality aggregate for asphalt mixtures. The material is well graded as seen in the gradation curve (Figure 7), which provides excellent compaction and load transfer. Asphalt binder graded as PG58-34 from Murphy Oil in Superior, WI was utilized. The PG58-34 grade binder is common to the region of northeastern Minnesota. Volumetric properties for the granite mixture can be seen in Table 2.

The taconite asphalt mixtures were composed of 65% Minntac coarse taconite tailings, 30% laboratory produced composite sand, and 5% fines. The same binder grade of PG58-34 was used at 7.2% binder content. This mix design was simulated after a previously used MnDOT mix design (MnROAD Cell 6). Since the tailings were a very clean material with little fines (Figure 6), a composite sand mixture was created to meet the gradation requirements of the mix. This long and tedious process included separating laboratory sand into specific grain sizes with a set of sieves. Once enough material in

each grain size was produced, percentages for each grain size were calculated and batched to create the composite sand. The composite sand mixed with the tailings and fines produced an aggregate batch that met thegradation requirements (Figure 8). Volumetric properties for the tailings mixture can be seen in Table 2.

Figure 6: Visual comparison of taconite tailings (left) and granite aggregate (right)

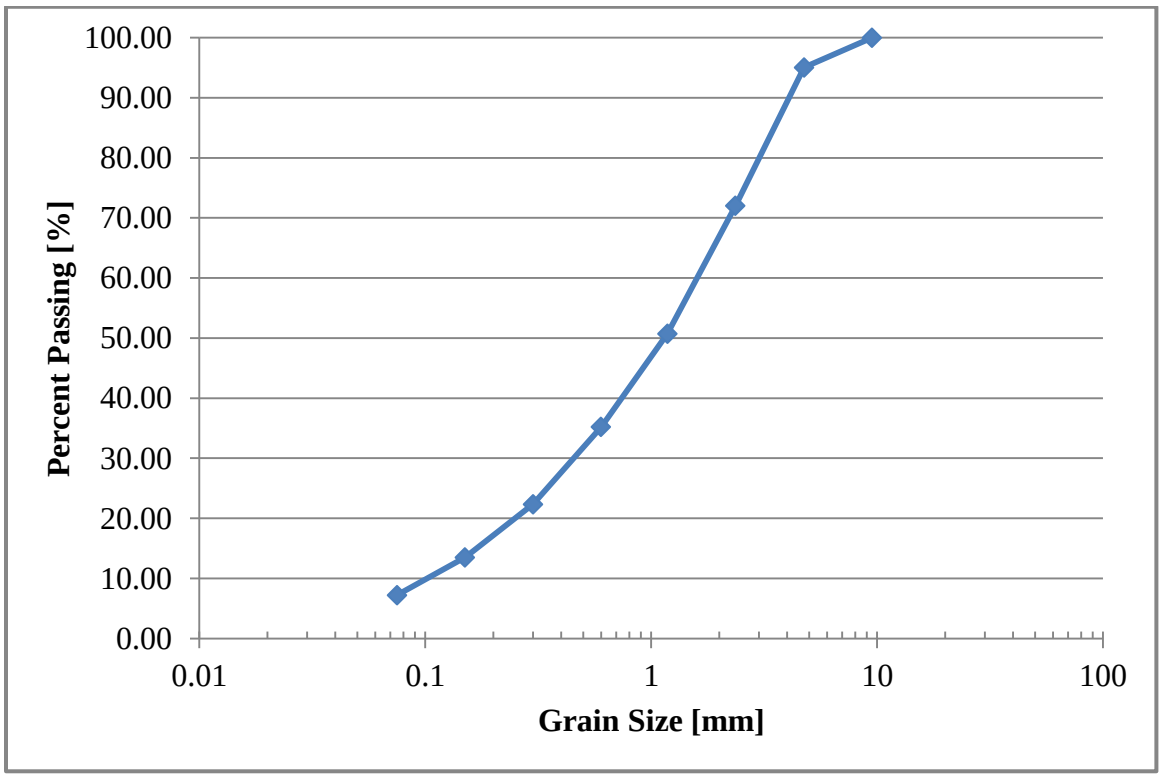

Figure 7: Gradation curve for granite mix (aggregates from Martin Marietta)

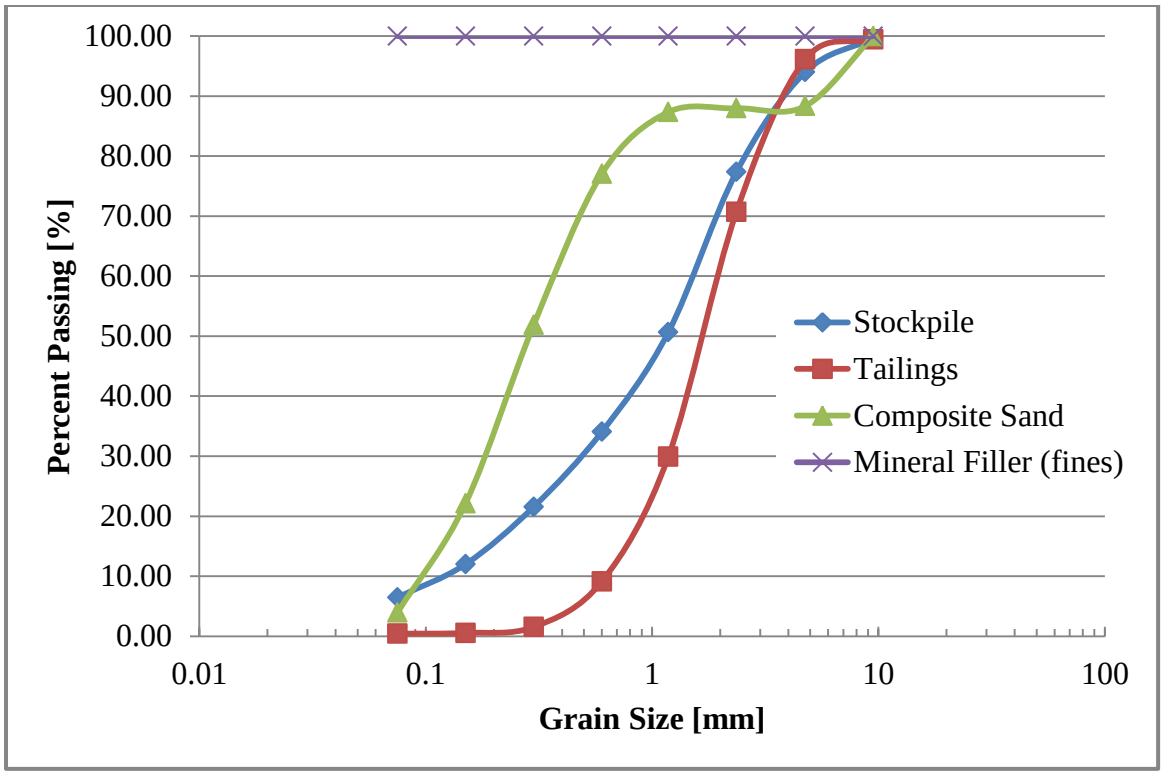

Figure 8: Gradation curve for taconite tailing mix

Table 2: Gradation and volumetric properties for granite and taconite mixtures

Sieve Size (mm)	Percent Passing (%)	
	Granite Mixture	Taconite Mixtures
9.50	100.00	99.63
4.70	95.02	93.98
2.36	72.03	77.36
1.18	50.72	50.65
0.600	35.19	34.06
0.300	22.35	21.57
0.150	13.51	12.01
0.075	7.23	6.47
Binder Content, P_b [%]	6.90	7.21
Adjusted Asphalt Film Thickness (microns)	8.6	9.1

3.1.3 Plant and Field Procured Samples

Field and plant samples from MnDOT and the University of Minnesota Duluth were obtained and tested for measurement of fracture energies. The primary use of these

results was to compare the laboratory prepared granite and taconite mixtures to actual asphalt mixtures typically used in the field.

Loose mix asphaltwas collected on a project for University of Minnesota Duluth parking lots. Wearing and non-wearing coarse mixtures were both collected and tested. Both mixtures contained 20% recycled asphalt pavement (RAP) and had a total binder content of 5.5%.The loose mix was compacted using 60 gyrations as specified by the mix design report, which can be seen in Appendix K.

Additional asphalt samples were received from MnDOT.Loose mix asphalt was received from projects on Minnesota trunk highways TH9 and TH70. TH9, located in west-central Minnesota, runs from Benson, MN to Crookston, MN. The mix was designed for compaction level of 60 gyrations and included 20% RAP and a total binder content of 4.0%. TH70 is located in east-central Minnesota and runs from Mora, MN to the Wisconsin state line.It was also designed for compaction level of 60 gyrations and included 20% RAP, but had a total binder content of 5.2%. Detailed mix designs can be found in Appendix L.

Another set of samples were received from a MnDOT project on trunk highway TH371 near Brainerd, MN. Cored field samples were received from three different sections on TH371, which was constructed in 2004 and 2005. Since then, excessive cracking has been found at specific locations of the highway near reference posts (RP) 17-21. Wearing and non-wearcoarsesamples were received from RP 6, RP 17, and RP 21.5. Cracking was found most prevalent near RP 17 and RP 21.5. Detailed mix designs can be can be found in Appendix L.

3.2 Mixing and Compaction Process

Asphalt is composed of three phases including aggregate, binder, and air. The process of preparing a compacted asphalt sample includes batching materials, mixing, and compaction. Once the mix designs were determined and materials were batched, samples were ready to be mixed and compacted. The first step was to weigh out the required

aggregate and place in the oven at 120^{o} C to dry overnight. Once dry, the aggregate is weighed again and the amount of binder needed is calculated based on the binder content provided. The binder and all tools are placed in the oven at 155^{o} C for 2 hours. The aggregate and binder is then placed in a large bowl and mixed as seen in Figures 9-10. After mixing the materials thoroughly, the asphalt is cured in the oven at 130^{o}C for 4 hours to be prepared for compaction.

Figure 9: Minntac Coarse Tailings and binder prepared for mixing

Figure 10: Mixing of aggregate and binder

Compaction of asphalt samples is completed using a SuperPave Gyratory Compactor (Figure 11). The gyratory compactor simulates the “kneading” and “rolling” action a pavement experiences when compacted with a steam roller. The asphalt undergoes a

pressure of 600 kPa while the specimen gyrates at an angle of 1.25°. The angle simulates the shearing action a steel drummed roller creates. Samples can either be compacted to a specified number of gyrations or a specified height. For this project, samples were compacted to a specified height in order to achieve an air void level of 7% ± 1%. Given required air void level, radius, maximum specific gravity of loose mix, and mass, the height of the specimen can be calculated using the following equation, where M is the mass in grams, G_{mm} is the theoretical maximum specific gravity of the mix, P_a is the air void level in percent, and R is the radius of the gyratory specimen in millimeters.

$$\frac{\frac{M}{G_{mm}} * 10}{\left(1 - \left(\frac{P_a}{100}\right)\right) * \pi * \left(\frac{R}{10}\right)^2}$$

If a specimen was to be compacted in gyration mode, the number of gyrations is usually determined by the amount of traffic the pavement is expected to handle (that is, the higher the amount of traffic the more gyrations required). Once compaction is completed, the sample is then ready to be fabricated for testing (Figure 12).

Figure 11: Pine Superpave gyrator compactor and steel mold

Figure 12: Compacted asphalt specimens

3.3 Mechanical Testing

3.3.2 AASHTO T-283

The AASHTO T-283 test requires specimen geometry that is readily available from lab or field. A gyratory compacted sample is either compacted or cut to a height of 95 ± 5 mm. No additional specimen preparation steps are required. The specimens must have an air void level of 7 ± 1%. Prior to mechanical testing, the conditioning process must be completed. As described before, a total of six specimens are made for the test; three of which are tested in dry condition and three are tested after conditioning by one freeze-thaw cycle.

Indirect tensile strength is obtained after subjecting each specimen to compression along its diameter. All samples are tested at 25^{o}C. Load and displacement data is obtained from the testing and used for data analysis. Other than peak load and strength, load versus displacement curves can be used to determine the amount of work (energy) it takes to cause failure to a specimen. Once the data analysis is completed, tensile strength ratio (TSR) is calculated. The specimen meets the moisture damage resistance requirements if its TSR is 85% or greater. A picture of the test setup can be seen in Figure 13.

Figure 13: AASHTO T-283 test setup

3.3.3 Disk-Shaped Compact Tension Test

The Disk Shaped Compact Tension (DCT) Test is a method for determining fracture energy of asphalt concrete. The DCT test can be performed on both cored field samples or laboratory compacted samples. The DCT has asignificantly complicated geometry requiring demanding fabrication steps as compared to indirect tensile strength test (AASHTO T-283). The specimen is created from a 50 mm thick, 150 mm diameter asphalt sample. First, a 5 mm thick flat face is cut off the edge of the sample. Next, two 25 mm holes are cored. Finally, a 62.5 mm long notch is cut between the two 25 mm holes and perpendicular to the flat face. Figure14providesa picture of an actual DCT specimen ready to be tested.

Figure 14: DCT test specimen

The DCT test procedure begins with placing the specimen at the desired temperature for at least 2 hours but no more than 16 hours. All specimens were tested at 10^{o}Cwarmer than the low temperature Superpave binder grade requirement. For example, the required asphalt binder grade for Duluth, Minnesota is PG58-34. This means that with 98% reliability the pavement surface temperatures will not exceed 58^{o}C in summer and will not drop below -34^{o}C in winter. Therefore, most specimens were tested at -24^{o}C which is 10^{o}C greater than -34^{o}C. Specimens are then placed into the loading fixtures, as shown in Figure 15. An extensometer is attached to the specimen to measure the crack mouth opening displacement (CMOD). Metal gage points were glued to the specimen to hold the extensometer in place (Figure 16). The test is performed at a displacement rate of 0.017 mm/s until the post-peak load level has reduced to 0.1 kN.

Figure 15: DCT specimen placed into loading frame

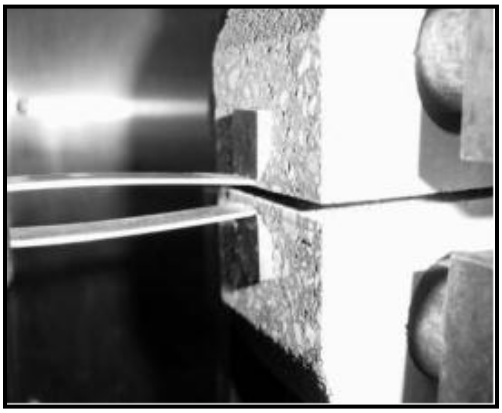

Figure 16: Clip-on gage points for extensometer (from ASTM D7313)

Results obtained from the fracture testing include load and crack mouth opening displacement (CMOD). Plots of CMOD versus time and load versus CMOD were created. To determine fracture energy, area under the load versus CMOD curve is calculated. Fracture energy is then calculated using the previous equation given in the literature review chapter of this paper.

3.4 Conditioning Process

The main objective of this study is to determine how asphalt mixtures containing taconite tailings are affected when exposed to moisture with freezing and thawing. In climates

such as northern Minnesota, pavements experience multiple freeze-thaw cycles throughout the winter and spring months. Currently, there are no standardized tests which subject asphalt samples to multiple freeze-thaw cycles. AASHTO T-283 is one of the only standardized tests which expose asphalt samples to freezing and thawing. In this study, a total of five conditioning levels were used and include:

i) Dry condition
ii) AASHTO T-283 freeze-thaw cycle
iii) 10 freeze-thaw cycles
iv) 20 freeze-thaw cycles
v) Field conditioned samples

Table 3 provides a matrix indicating which conditioning methods were used for each test.

Table 3: Conditioning and testing matrix

	AASHTO T-283 (TSR)	DCT (Fracture Energy)
Unconditioned	X	X
Conditioned: AASHTO T-283	X	X
Field Conditioning	X	X
Conditioned: 5 F-T Cycles		X
Conditioned: 20 F-T Cycles		X

3.4.2 AASHTO T-283 Conditioning

The AASTHO T-283 conditioning process involves subjecting specimens to one freeze-thaw cycle. Before the specimens are put through the freeze-thaw cycle, they are placed in water until 70 to 80 percent saturation is achieved. The specimens are then wrapped with saran wrap and placed in a water tight heavy duty plastic bag with 10 ± 0.5 mL of water. Next, the specimens are placed in a freezer at -18 ± 3^{o}C for a minimum of 16 hours, followed by thawing in a 60 ± 1^{o}C water bath for 24 ± 1 hour. The specimens are then placed in a 25 ± 0.5^{o}C water bath for 2 hours ± 10 minutes.

The single freeze-thaw cycle used for AASHTO T-283 is not very practical, especially in climates like northern Minnesota. In northern Minnesota, pavements will experience

multiple freeze-thaw cycles over the course of winter and spring months. Also, temperatures of -18^{o}C and 60^{o}C are typically not seen in most climates. Using temperatures which represent a region for testing would be a more reasonable way of conducting a freeze-thaw cycle.

3.4.3 Multiple Freeze-Thaw Cycle and Field Conditioning

For the Disk-Shaped Compact Tension Test, specimens were also subjected to multiple freeze-thaw cycling and field conditioning. Field conditioned samples were tested for indirect tensile strength as well.

To keep some consistency, the multiple freeze-thaw samples were prepared in a similar manner to the AASHTO T-283 conditioning process.The only difference was a controlled freeze-thaw chamber was used for running multiple freeze-thaw cycles. This machine allowed for adjustment of high and low temperatures, as well as hold times and number of cycles. Before placing into the chamber, samples were saturated in a similar manner as in AASHTO T-283. Once saturated to desired level, specimens were wrapped in saran wrap and placed in heavy duty plastic bags. The bags were then placed in anti-freezesolution inside the chamber so the samples would not experience mechanical stress caused by expansion of water as it freezes (Figure 17). The chamber was then run to the desired number of cycles.

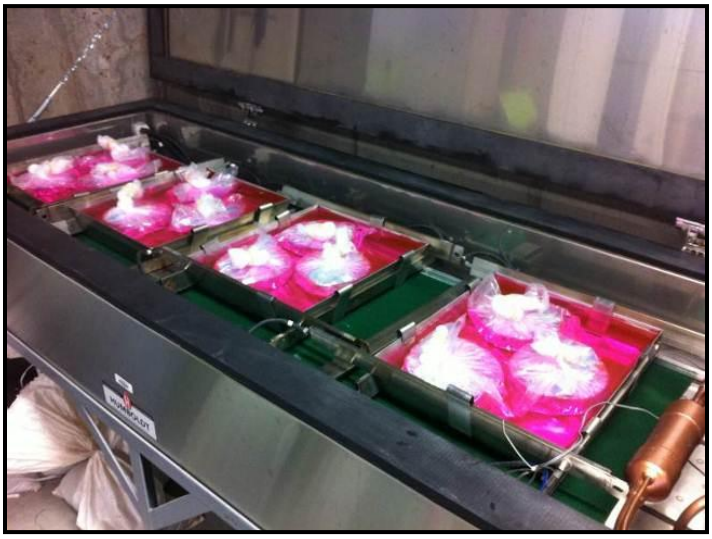

Figure 17: DCT samples prepared for multiple freeze-thaw conditioning

High and low temperature values used for the multiple freeze-thaw cycles were different than AASHTO T-283. Temperature data was obtained from northern Minnesota over a 5 year period. The 5 year maximum and minimum temperatures from November to February were averaged and used for conditioning. A high temperature of 20^{o}C and a low temperature of -20^{o}C were used for the multiple freeze-thaw cycles. These temperature values provide a more realistic scenario for a climate similar to northern Minnesota. Minimum and maximum temperatures were set to be reached in a 4 hour time limit and then held constant for 2 hours. Therefore 1 freeze-thaw cycle was achieved within a 12 hour time interval. It would be ideal to have 1 freeze-thaw cycle run during a 24 hour period but it could not be done due to time restrictions of the freeze chamber.

In order to compare AASHTO conditioning with actual climatic conditioning, gyratory compacted specimens were stored in the field. The specimens were placed on a plywood sheet at a closed weigh-station on Interstate 35 (I-35) located near Cloquet, MN. Figure 18 shows the specimens at the end of conditioning which took place from January 2012 to June 2012.

Figure 18: Specimens placed at closed weight station on Interstate 35 for field conditioning

CHAPTER 4: TESTING RESULTS

4.1 Granite and Taconite Laboratory Samples

The results from laboratory testing of granite and taconite mixes are presented in this section. The results are divided into two sections based on the type of mechanical testing. The results are presented as average of at least three test replicates for each property. The ITS measured using the AASHTO T-283 test protocol is presented first.

4.1.2 Indirect Tensile Strength Test Results

Figure 19 presents the indirect tensile strength (ITS) measurements for both mixes and the three conditioning types. As expected the unconditioned strengths showed the greatest value. It should be noted that the trends of reduction in the ITS of granite and taconite mixes were different with different types of conditioning. Overall the reduction in ITS for either mixes was not very high. The actual reductions are discussed further in the discussion section. The test variability was measured in terms of coefficient of variance (CoV) for each property. The indirect tensile strength (ITS) measurements showed CoV between 1 and 10% with average of 5%.

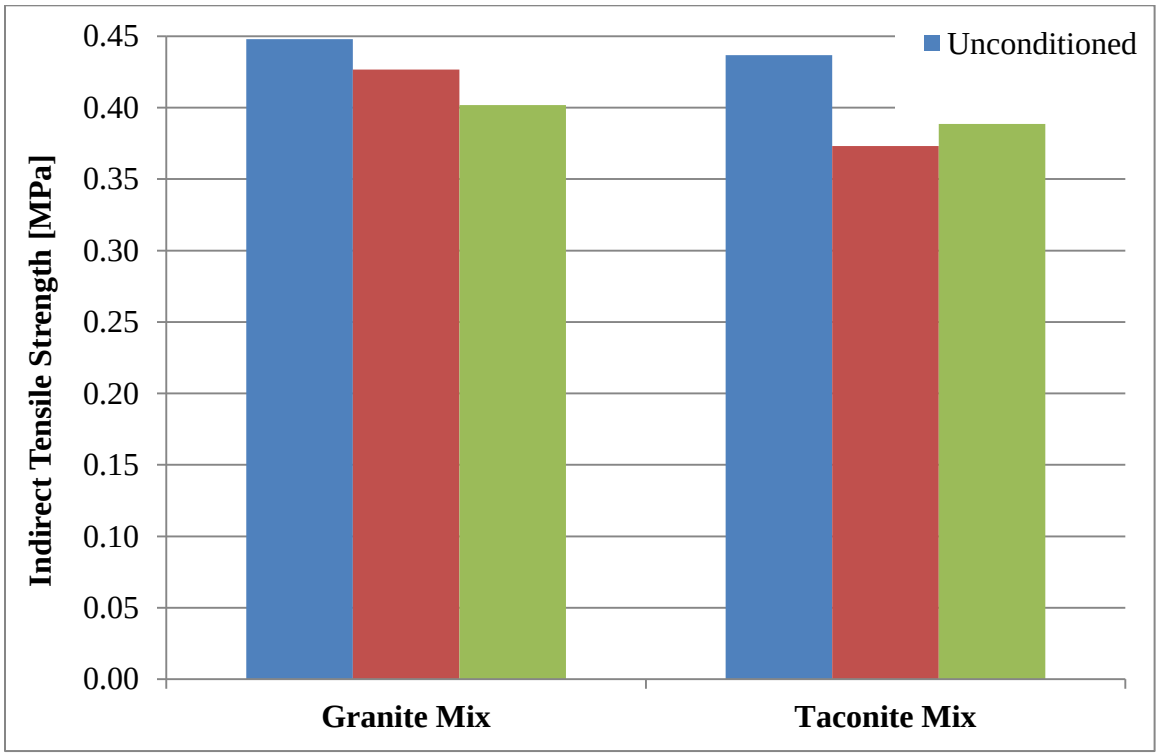

Figure 19: Indirect tensile strength (ITS) results

Figures 20-21 provide stress-displacement curves for both mixes and the three conditioning levels. As expected, the peak stress decreased when the specimens were conditioned. It can be noted that the peak stress for unconditioned and field conditioned samples occurred at the same displacement, but the T-283 conditioned sample's peak stress occurred at a larger displacement. This could be caused by an increase in strain tolerance due to the 60^{o}C thawing temperature in the conditioning phase and causes the material to behavein a more ductile fashion. Therefore, the peak load could occur at a higher displacement.

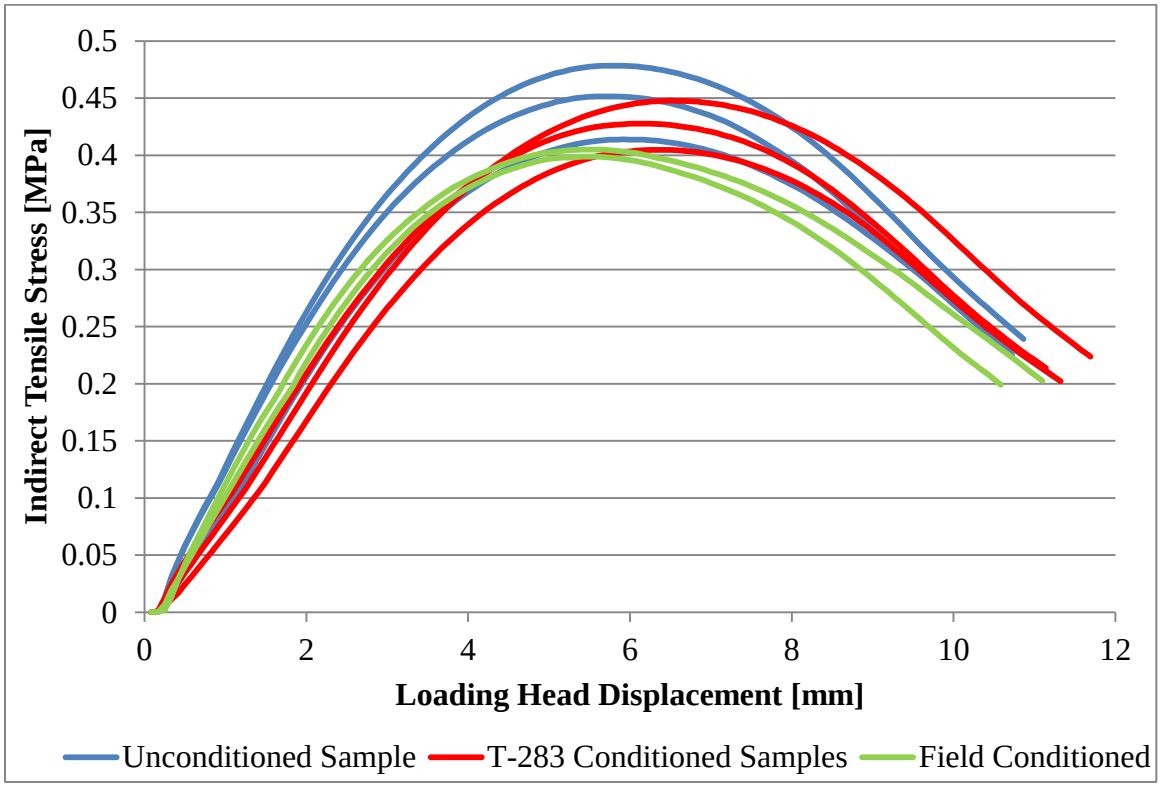

Figure 20: Stress-displacement curves for granitesamples

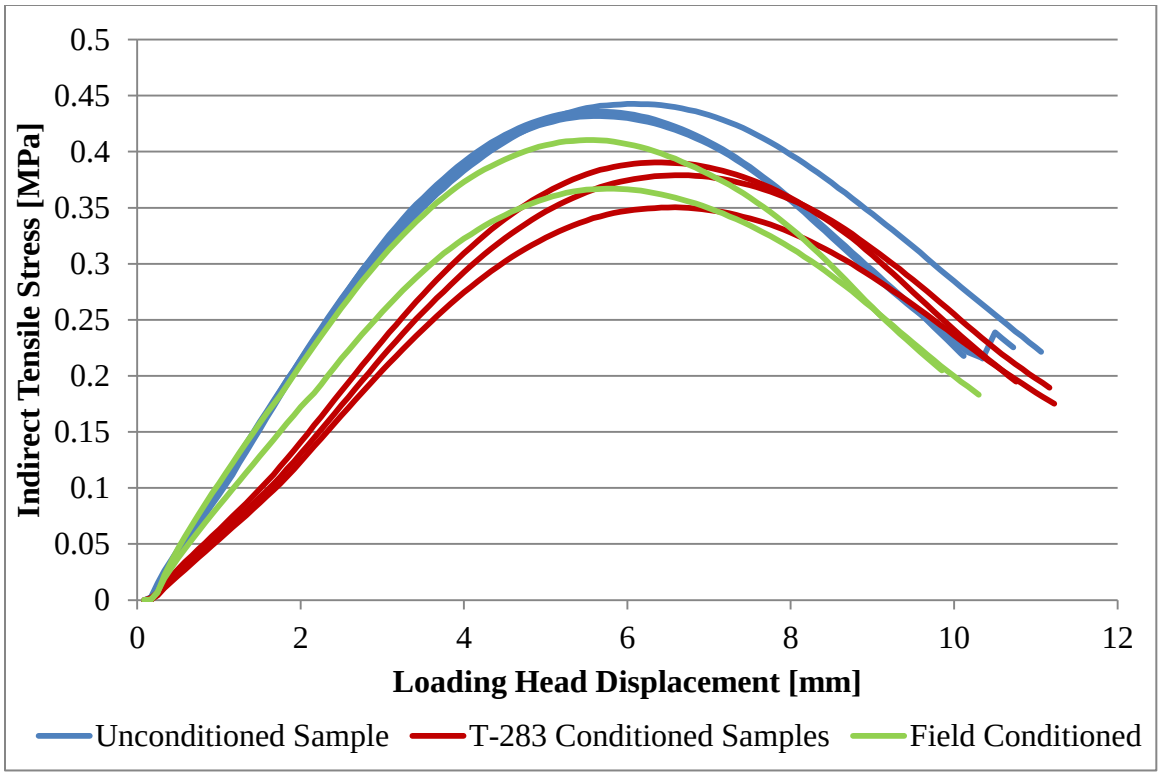

Figure 21: Stress-displacement curves for taconite samples

From stress-displacement curves, the amount of normalized work was calculated till peak stress, as opposed to total work. The normalized work parameter accounts for differences in specimen geometries. A comparison of normalized work values between granite and taconite samples is shown in Figure 22. For taconite mixtures, the amount of work decreases with conditioning. For the granite samples, field conditioning caused a reduction in work but T-283 conditioning resulted in an increase in work required to point of failure (peak load). Further discussions on these results are presented later in this chapter.

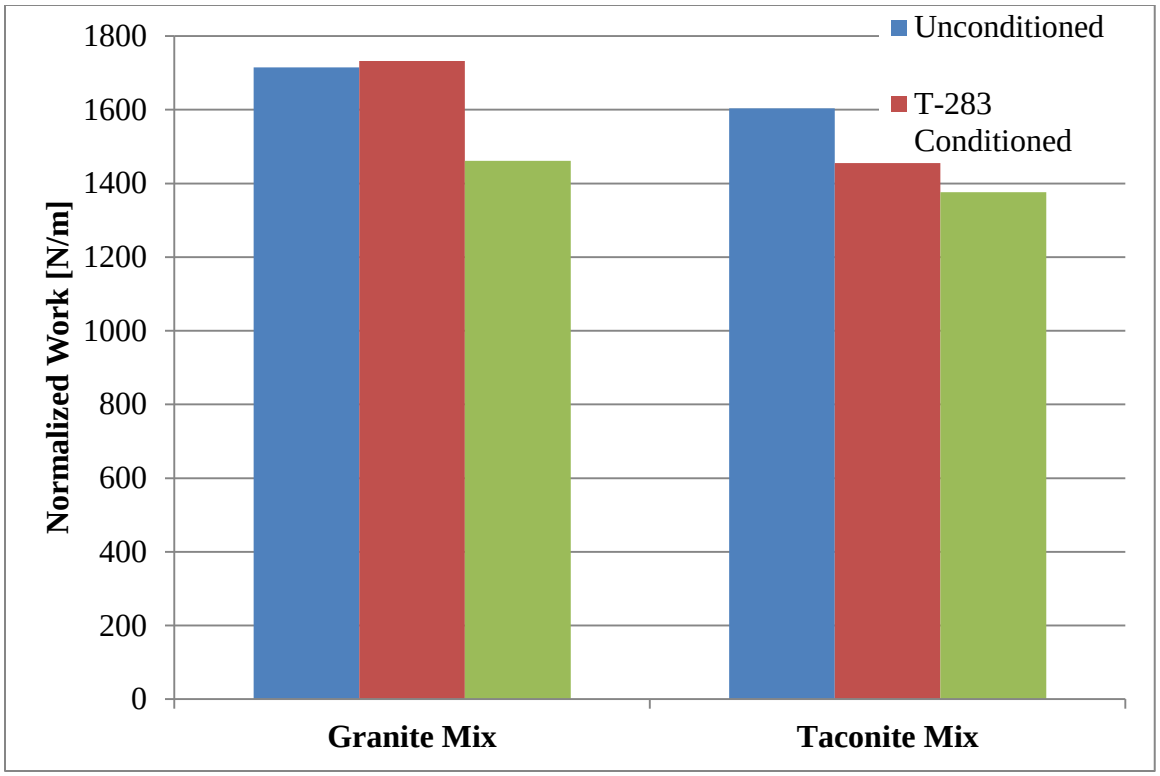

Figure 22: Normalized work results

4.1.3 Disk-Shaped Compact Tension Test Results

The DCT fracture test results were processed to determine the average peak loads and average fracture energies of the materials. The peak load measurement in DCT had a CoV range of 6 to 16% and average of 10%. The fracture energy measurements showed slightly higher variability with CoV range of 10 to 20% and average CoV of 14%. Figure 23 presents the fracture energies for both mixes and all five conditioning levels. The peak loads from the fracture tests are presented in Figure 24. A recently finished comprehensive study on low temperature cracking in asphalt pavements recommended the limiting value of DCT fracture energy for asphalt mixtures as 450 J/m^2 [35]. This recommended limit is also shown in Figure 23. Note that the taconite mix met this requirement narrowly in unconditioned state and after undergoing field conditioning for winter and spring season it failed the recommended limit. The load-CMOD curves for each sample can be found in Appendix H.

Interestingly the material showed significantly different fracture behavior after undergoing the AASHTO T-283 conditioning. The test results indicate significant

increase in the fracture energy and reduction in the peak load. Thus, the material changed to the state where the peak load carrying capacity (strength) reduced but at the same time material exhibited significant strain tolerance against cracking. This is not totally unexpected, the AASHTO T-283 procedure involves freezing of specimen which would induce damage and lower the peak load carrying capacity. Since the freezing is followed by conditioning of the specimen at 60°C for 24 hours, the damaged specimen with a readjusted micro and macro-structure caused due to freezing will heal. This is especially true for softer binder grades such as that used in this study, which is PG 58-34. In general, this type of mechanism (similar to "annealing") tends to increase the ductility or strain tolerance of the material. In other materials such as, metals, ceramics and polymers this type of behavior is often observed. Please note that this type of distinct fracture behavior will not be evident when testing asphalt concrete at temperature of 25°C, as in case with AASHTO T-283 ITS measurement. Since the fracture energy test involves controlled propagation of crack through material it allows to look at fundamental failure characteristic of asphalt mixes and make distinctions between materials that behaves in more brittle versus ductile manner.

While the mechanism of increasing ductility due to AASHTO T-283 conditioning can be explained, it should be noted that the conditioning process itself is quite empirical and not really associated with what may happen in field. For example, in climatic conditions of Minnesota the winter time temperatures of pavement can be significantly below -18°C and a twelve hour continuous high temperature of 60°C may not occur until late spring. The results show that the cracking resistance of material increases several folds as the specimens are conditioned. In reality most studies have indicated significantly reduced cracking resistance as mix is exposed to freeze-thaw cycling in moist conditions. This further indicates that when evaluating cracking resistance of asphalt concrete, the current AASHTO T-283 conditioning process for moisture susceptibility is not appropriate.

The field conditioning of specimens over period of one winter and spring cycle led to small drop in fracture energy and increase in peak load, indicating an increase in brittleness of the mix as well as strengthening. This behavior is similar to previously

reported results by Braham et al. [17] for long term field and lab aged asphalt mixtures. The comparison of AASHTO T-283 and field conditioned specimens also point towards the inapplicability of AASHTO T-283 conditioning process for pavement cracking performance.

Subjecting the specimens to multiple freeze-thaw cycles in an environmental chamber provided different results for each mix. After 10 cycles, the granite samples decreased in fracture energy in a similar manner to the field conditioned samples. After 20 cycles, the granite mixture showed similar results seen with the T-283 conditioned samples in which the fracture energy increases significantly and the peak load decreases indicating the possibility of the material behaving in a more ductile manner. For the taconite mixtures, after 10 and 20 cycles fracture energy increased as compared to the unconditioned samples. The taconite mixtures had the highest peak load after 10 freeze-thaw cycles, with a small decrease after 20 cycles. The 20 freeze-thaw cycle peak load was similar to the peak load for unconditioned taconite samples. For the granite mixtures, 10 freeze-thaw cycle and field conditioning fracture energy values very similar. After 20 cycles, the granite mixture's fracture energy increased significantly. After field and multiple freeze-thaw conditioning, the granite mixture demonstrated higher peak loads compared to unconditioned samples. Interestingly, the largest peak loads for both granite and taconite mixtures occurred when samples were conditioned for 10 freeze-thaw cycles. It should be noted that peak load CoV values for multiple freeze-thaw cycling and field conditioned sampleswere typically in the range of 5-15%. From this, it can be concluded there was no significant differences between peak load values after those conditioning processes and those conditioning process led to similar changes in peak load from unconditioned samples.

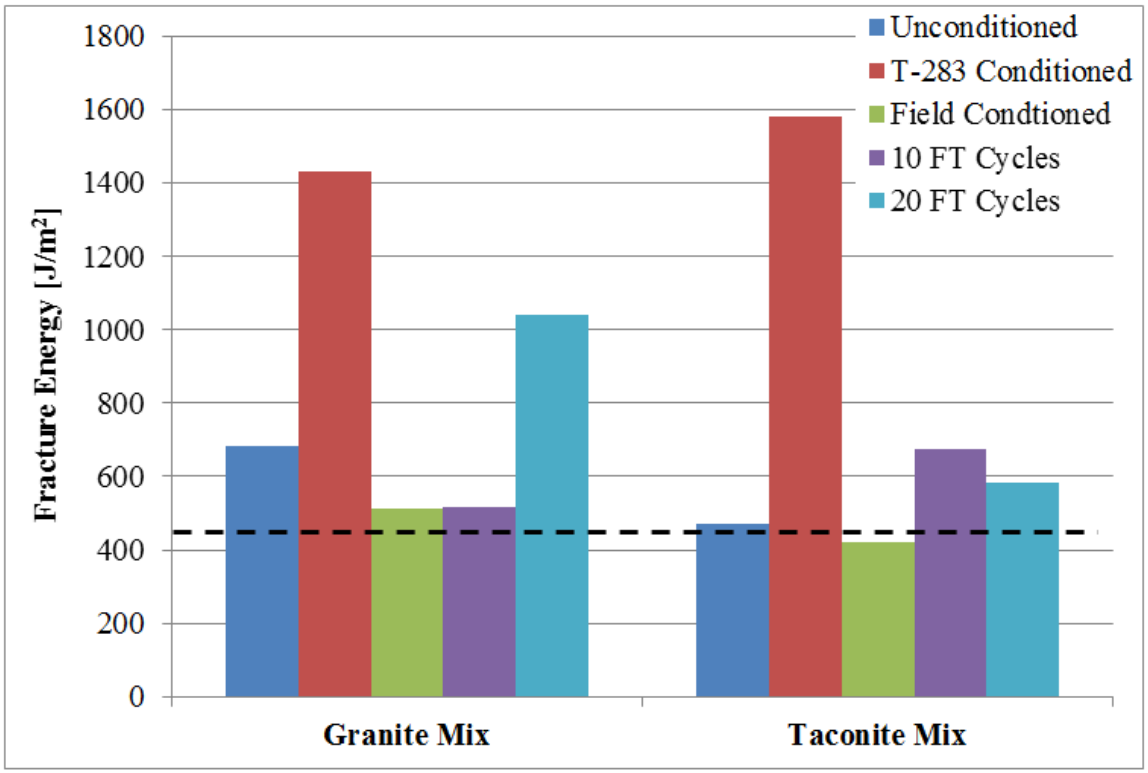

Figure 23: Fracture energy results for granite and taconite mixtures

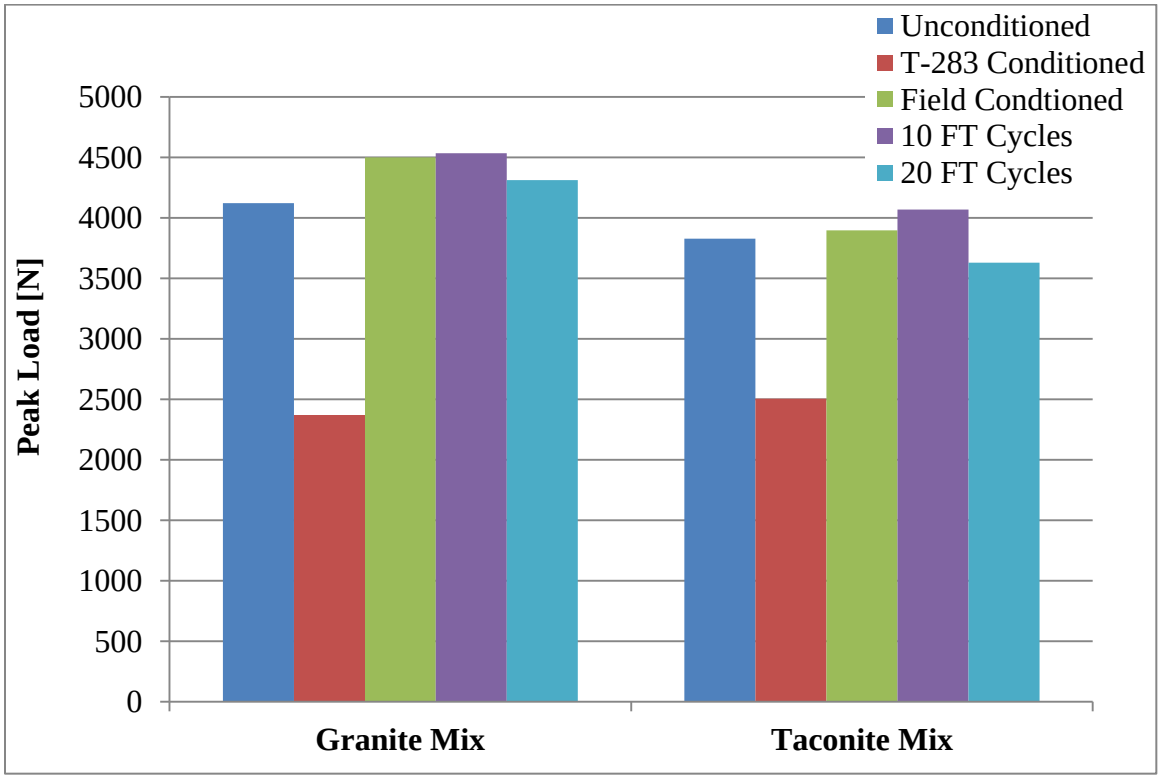

Figure 24: Peak load results for granite and taconite mixtures

Since asphalt behaves differently at different temperatures, DCT testing was performed on unconditioned and field conditioned granite and taconite samples at -18°C in addition to -24°C used in the previous testing. Figures 25-26 provide fracture energy and peak load results. Fracture energies increased dramatically when tested at the higher temperature and peak loads decreased. This is somewhat expected as a higher temperature causes the material to become more ductile and increase its strain tolerance. Also, at higher temperatures the material will not act as stiff and have lower peak load strength. It should be noted that when tested at -18°C, the taconite samples had higher fracture energies compared to the granite samples. At lower temperatures, such as -24°C, more samples tended to have an "abrupt" failure. An "abrupt" failure occurred when the sample would reach peak load and the crack would develop instantaneously. This occurred much less at the higher temperature of -18°C. These results indicate that pavements in colder climates may be more prone to cracking.

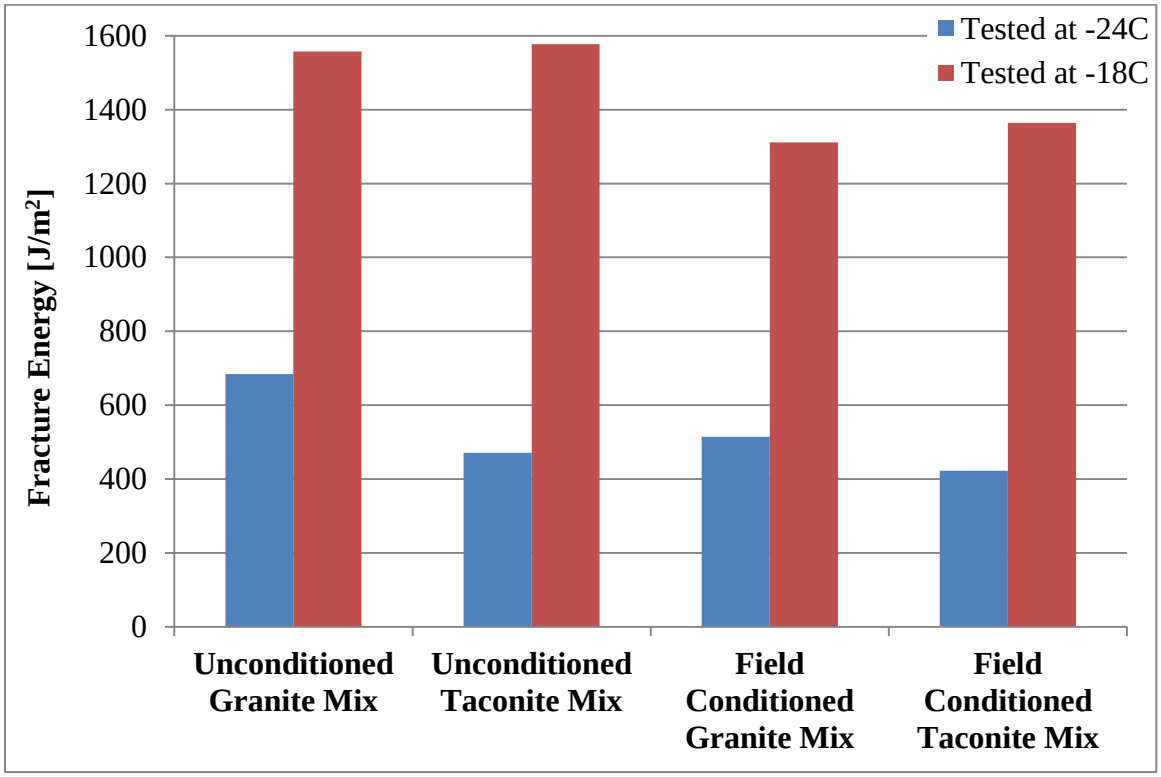

Figure 25: Fracture energy results for granite/taconite samples tested at different temperatures

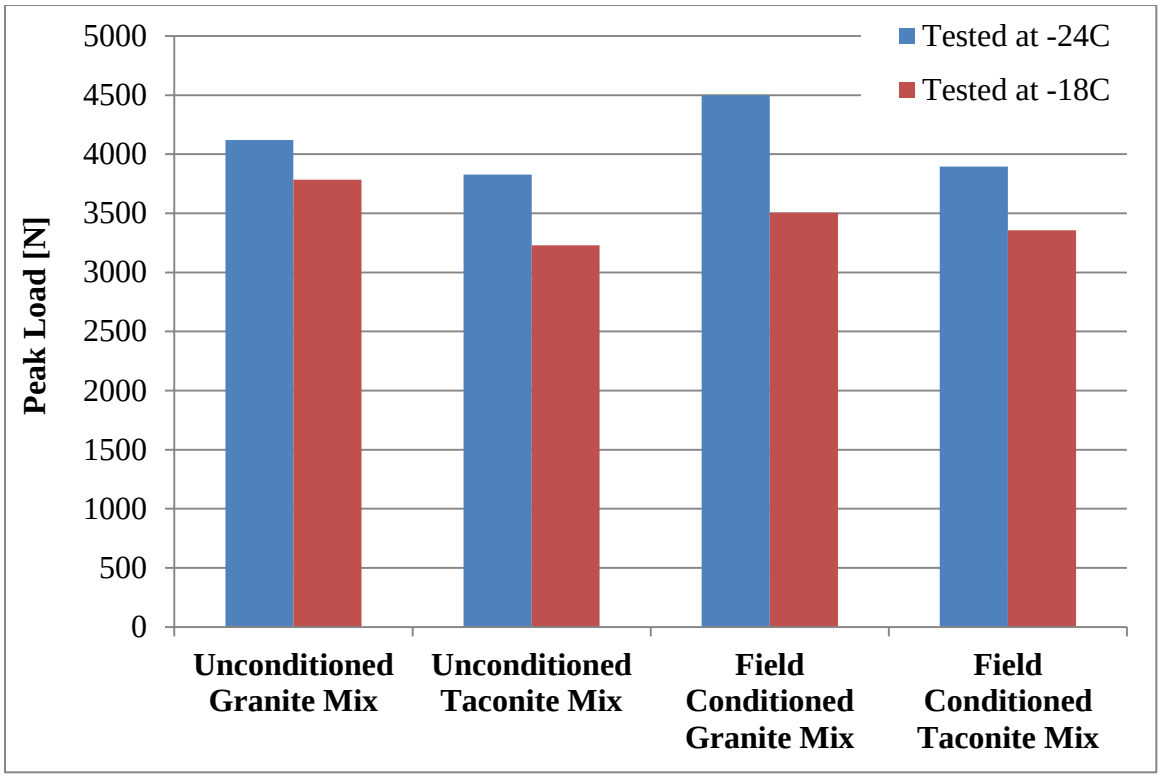

Figure 26: Peak load results for granite/taconite samples tested at different temperatures

4.1.4 Discussion of Results

The previously presented mechanical properties of the two asphalt mixes are converted to a series of ratios; the properties for each mix are normalized against the same property for unconditioned specimens. Table 4 shows the ratios for ITS, DCT fracture energy and DCT peak load. The ITS ratio is commonly referred to as tensile strength ratio (TSR). The Superpave mix design method recommends a minimum TSR of 0.80. The TSR in case of AASHTO T-283 as well as field conditioning met the recommended requirements for both mixes. The mix produced exclusively with granite aggregates showed excellent retention of ITS.

The fracture energy ratios (FER) provide interesting results. In addition to discussions presented previously about the change in material behavior towards significantly ductile manner, the results indicate that mix produced with taconite tailings show significantly higher ductility as compared to granite mix after AASHTO T-283 conditioning. The recommended limits for the FER have not been established as they have been for TSR,

thus if we assume that 0.80 is preferred limit the granite mix actually fails to meet this requirement after the field conditioning over just one winter and spring season. The taconite mix on the other hand retained 90% of fracture energy after field conditioning and is expected to have better retention in cracking resistance. The DCT peak load ratios (PLR) show that taconite mix retained marginally greater strength at low temperatures after undergoing AASHTO T-283 conditioning, whereas granite mixes showed slightly higher PLR after field conditioning. The differences between the two mixes are however relatively small and not greater than the variability associated with testing. In terms of subjecting samples to multiple freeze-thaw cycles, both granite and taconite mixtures showed excellent retention of FER and PLR except when the granite sample was subjected to 10 cycles. The numbers show that granite mixtures were better at retaining peak load but the differences are relatively small and not greater than the variability associated with testing. In all cases, the taconite mix meets the 0.80 threshold as established by AASHTO T-283.

Table 4: Mechanical property ratios for conditioned materials

Type of Conditioning	ITS Ratio (TSR)		DCT Fracture Energy Ratio (FER)		DCT Peak Load Ratio (PLR)	
	Granite Mix	Taconite Mix	Granite Mix	Taconite Mix	Granite Mix	Taconite Mix
AASHTO T-283 Conditioned	0.95	0.85	2.09	3.35	0.58	0.65
Field Conditioned	0.90	0.89	0.75	0.90	1.09	1.02
10 FT Cycle Conditioned	---	---	0.76	1.43	1.10	1.06
20 FT Cycle Conditioned	---	---	1.52	1.24	1.05	0.95

A visual inspection of the specimens after testing was completed. It was clear to see that little stripping had occurred between both granite and taconite mixtures after conditioning the samples. There was a small amount of stripping that could be seen as the conditioning severity increased (i.e. field conditioning, multiple freeze-thaw cycles) as expected. The visual inspection gives another indication that taconite mixtures have potential to resist moisture damage as well as conventional asphalt mixtures, and help reduce the severity of cracking.Figure 27 below show taconite specimens subjected to all conditioning phases as well as the unconditioned phase.

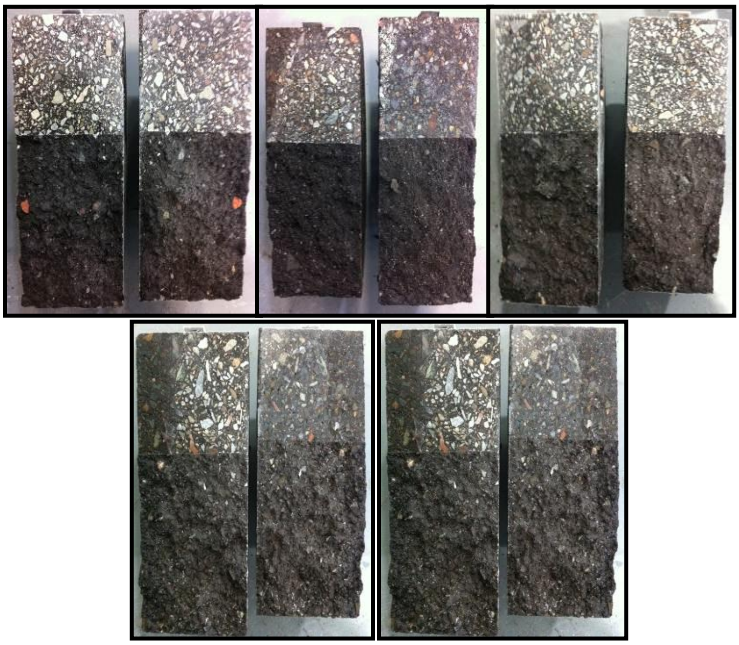

Figure 27: Visual inspection of taconite tailing samples; unconditioned (top left), AASHTO T-283 conditioned (top-center), field conditioned (top-right), conditioned to 10 FT cycles (bottom-left) and conditioned to 20 FT cycles (bottom-right)

Table 5 provides fracture energy and peak load ratios for samples tested at -18^{o}C and -24^{o}C. The ratios are with respect to test temperature -24^{o}C. When samples were tested at the warmer temperature of -18^{o}C, fracture energies more than doubled for the granite mixtures, and more than tripled for the taconite mixtures. Part of this can be attributed to the amount of binder in each mix. The taconite samples had a binder content of 7.2% while the granite samples had a binder content of 6.9%. The increased amount of binder allows for a higher strain tolerance which creates a "softer" material. This higher strain tolerance coupled with the higher test temperature is attributing to the large increase in fracture energy of the taconite samples as well as lower peak loads.

Table 5: Fracture energy/peak load ratios for samples tested at -18^{o}C and -24^{o}C

Sample	Fracture Energy Ratio	Peak Load Ratio
Unconditioned Granite	2.28	0.92
Unconditioned Taconite	3.35	0.84
Field Conditioned Granite	2.55	0.78
Field Conditioned Taconite	3.23	0.86

The following key points can be inferred from the experimental findings:

- The traditional TSR measurement using AASHTO T-283 specifications shows that the granite mix has slightly better damage resistance as compared to taconite mix, however, both mixes meet the recommended thresholds. The field conditioning show different trends for TSR as compared with AASHTO recommended conditioning. In this case the taconite mix shows slightly better damage resistance. Once again, the indirect tensile strength measurement at 25°C is a composite measure of material's resistance to deformation, indirect tensile failure and crushing and shearing failure. Thus it may not be a well suited property to determining the resistance to cracking as a fracture test conducted at low temperatures.

- The fracture energy ratios indicate that the AASHTO T-283 conditioning process might be ill-suited for determining changes in cracking resistance of material due to environmental effects. The taconite mix showed superior retention in fracture resistance of asphalt mixtures after field conditioning as compared to control mix developed using granite aggregate. This is a significant finding as it provides confidence in use of taconite aggregates from mining operations without worry of accelerated deterioration in cracking resistance due to effect of moisture and climatic cycling.

- The reduction in material strength at low temperatures is expected to be comparable between the granite and taconite mixes. Once again the AASHTO T-283 conditioning shows too severe drop, whereas field and multiple freeze-thaw conditioning shows slight improvement. The slight improvement in DCT peak load for field conditioned samples is in agreement with previous research on the topic.

- Taconite mixes proved to have excellent retention of fracture energy and peak loads after subjected to multiple freeze-thaw cycle conditioning. If the

recommended value of 0.80 is implemented, (as used by AASHTO T-283) all samples were able to meet and exceed the limit.

- Fracture energy and peak load results were found to be dramatically different when tested at different temperatures. At higher temperatures, fracture energies increased and peak loads decreased, as expected. This further reinforces that asphalt pavement will perform differently in areas of differing climates. These results also indicate that pavements in colder climates are more prone to cracking.

- The asphalt mixtures were often described as behaving in either a more ductile or brittle manner after conditioning. Mixtures which behave in a more ductile manner after conditioning may have propensity for having future rutting problems. Whereas mixtures which act in a brittle manner after conditioning may have propensity for having future cracking problems. This cannot be fully determined until more testing, such as rutting and fatigue tests, are performed.

4.2 Field and Plant Mixed Samples

The results from field and plant mixed samples tested for fracture energies are presented in this section. Samples were obtained from parking lots of the University of Minnesota Duluth, as well as MnDOT loose mixtures and cored field samples. The results are separated by the type of asphalt mixture used for each project. The primary use of these results is to compare the laboratory prepared granite and taconite mixtures to actual asphalt mixtures used in the field.

4.2.2 University of Minnesota Duluth Parking Lot Samples

Figures28-29 provide fracture energy and peak load results from DCT testing of both base and wearing course mixtures. The DCT fracture energies were higher for the wearing course compared to the base course. Peak loads (Figure 29) were higher for the base course samples compared to the wearing course. The fracture energy measurements showed a CoV range of 8.5 to 10.5% and average of 9.5%. Peak load results had a CoV range of 7 to 8% with an average CoV of 7.5%.

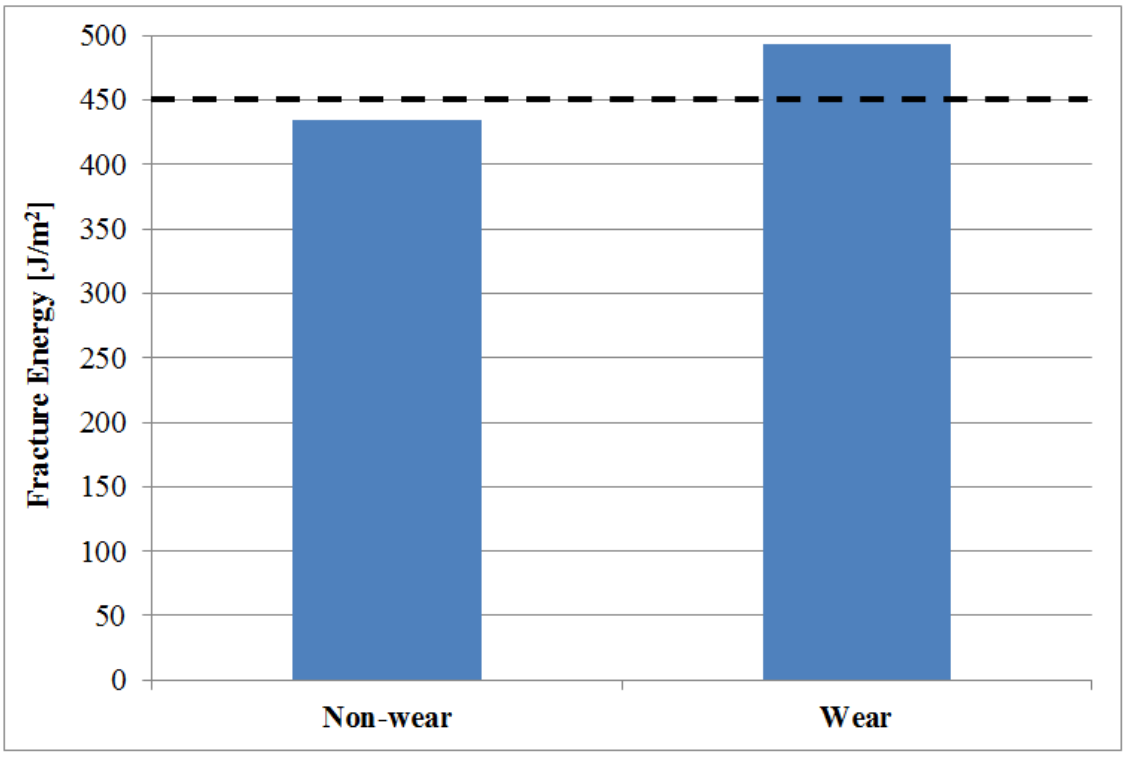

Figure 28: DCT fracture energy results for parking lot samples

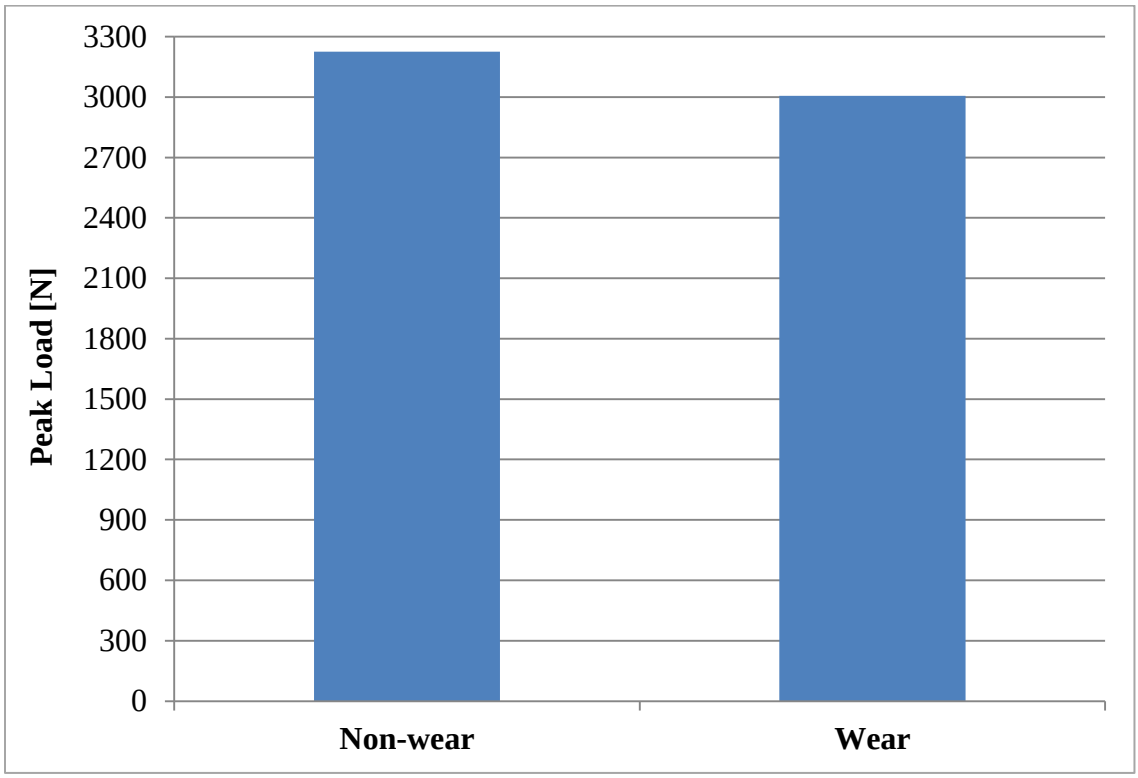

Figure 29: DCT peak load results for parking lot samples

4.2.3 MinnesotaTrunk Highway 9 and Trunk Highway 70 Samples

Figures 30-31 provied fracture energy and peak load results for highway 9 and highway 70 samples. The samples were tested at -24^{o}C and -18^{o}C to examine the effects of temperature on cracking resistance. The fracture energy results showed a very large CoV range of 1 to 39% and average of 21%. Peak load results had a CoV range of 5 to 13% with an average CoV of 7.5%. From the results, it is plain to see that samples tested at -18^{o}C provide superior results in both fracture energy and peak load. It is expected that fracture energy would be greater at higher temperatures because the sample is anticipated to act more ductile, thus having more strain tolerance. It was unexpected to see a higher peak load at the higher temperature. Usually at lower temperatures materials act more brittle and have a higher load capacity, with less ductility.TH70 results provided significantly higher fracture energies compared to TH9. Both samples provided similar results in peak loads at both test temperatures. Going back to the mix design portion of the report, TH9 samples had a total binder content of 4%, with a small percentage of binder from RAP. A 4.0% binder content is very low for typical asphalt mixtures, so it was expected TH9 samples would perform worse compared to TH70 samples. TH70 samples had a total binder content of 5.2%. It should be noted that both mixes had the same adjusted asphalt film thickness (AFT) of 8.5 microns. The AFT method was recently adopted by MnDOT and used for the design of these mixtures. The following results indicate the AFT method may not be completely reliable in predicting pavement cracking, and parameters such as VMA and binder content are equally important.

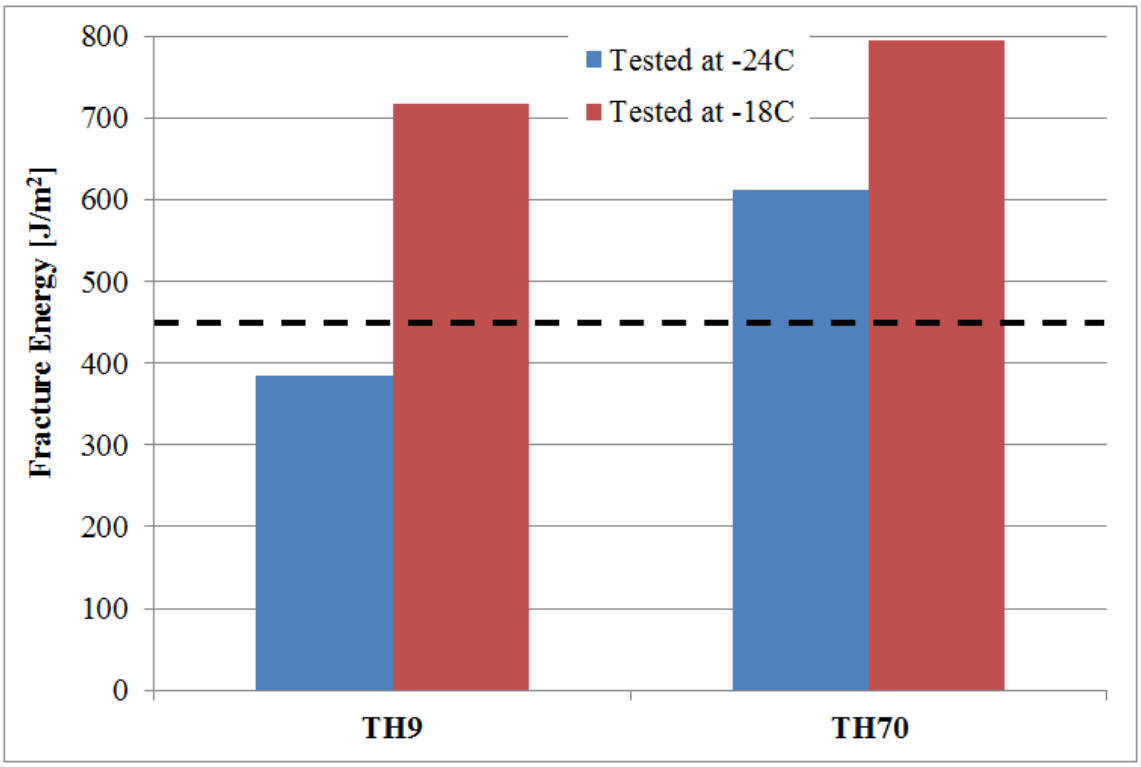

Figure 30: DCT fracture energy results for TH9 and TH70 samples

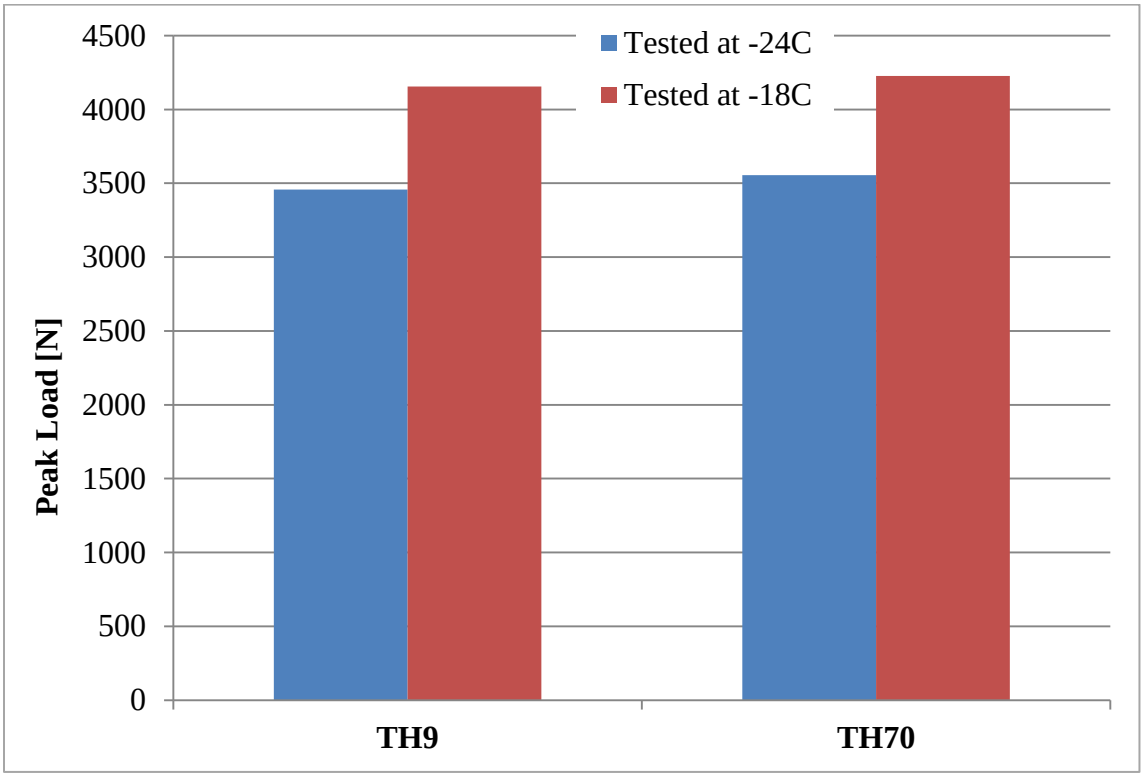

Figure 31: DCT peak load results for TH9 and TH70 samples

4.2.4 Trunk Highway 371 Samples

Figures 32-33 provide fracture energy and peak load results for Minnesota Trunk Highway 371 samples. Fracture energies decreased further towardsthe reference post 21.5. As described in the materials portion of the report, excessive cracking was found between RP 17 and RP 21.5. These fracture energies are below the 450 J/m^2 threshold explained previously for wear and non-wear samples, indicating poor performance. RP 6 sample fracture energies barely reached the 450 J/m^2 threshold for both wear and non-wear. Peak load results showed very small differences between all samples. It should be noted that RP 17 and 21.5 samples had slightly higher peak loads. The higher peak loads and lower fracture energies may indicate the mixture used near RP 17 and 21.5 is a stiff, brittle mix compared to RP 6. The stiffer mixtures may lead to early and excessive cracking.

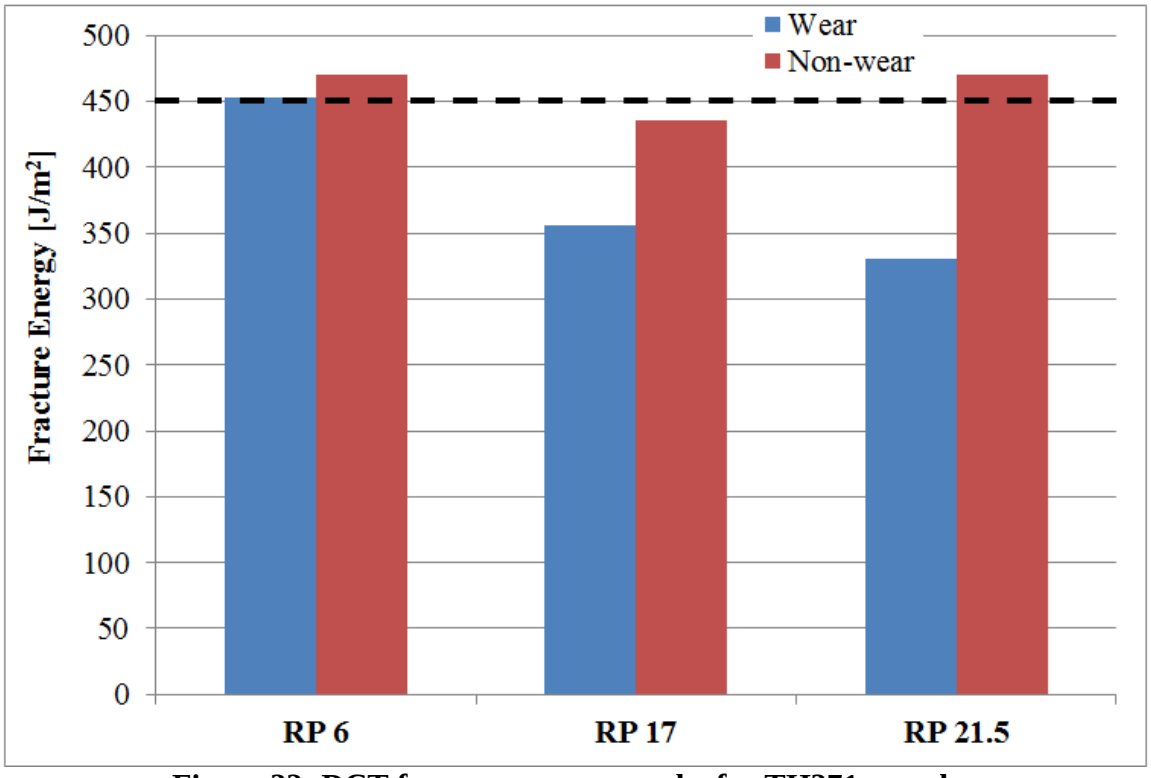

Figure 32: DCT fracture energy results for TH371 samples

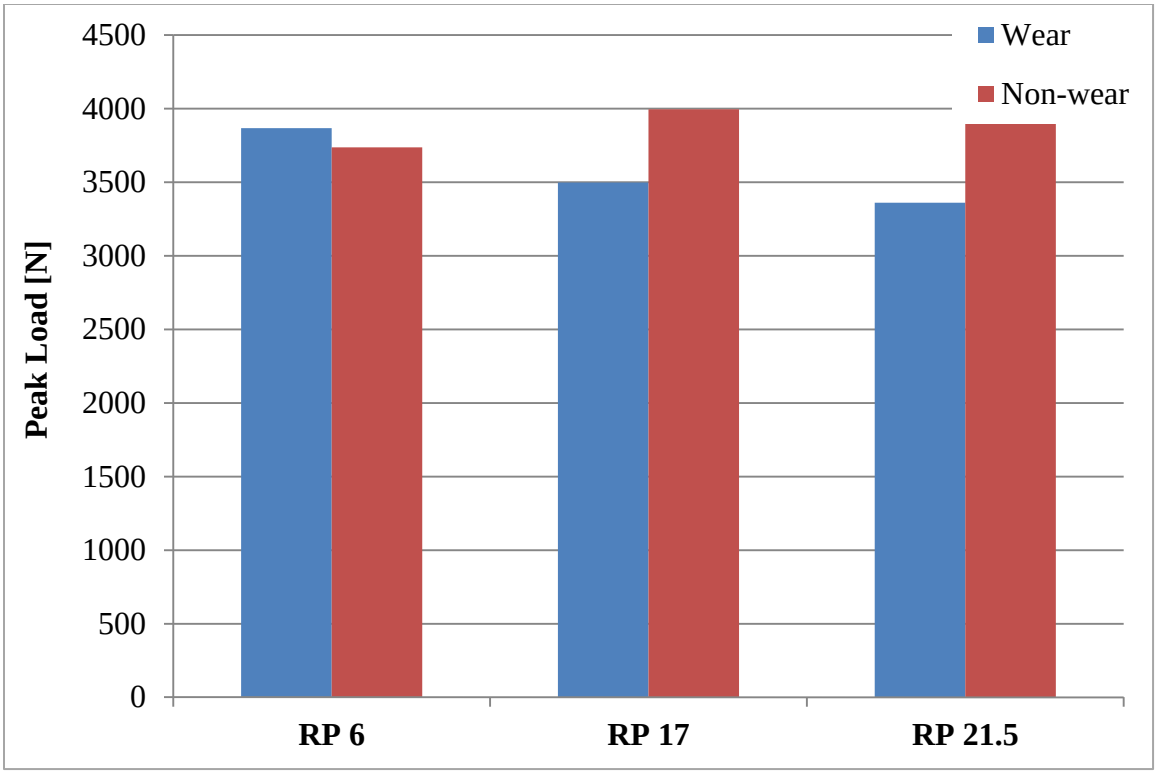

Figure 33: DCT peak load results for TH371 samples

The number of cracks found on TH371 near the reference posts can be seen in Table 6 along with their corresponding fracture energies. All non-wear samples have somewhat similar fracture energies and are close to the 450 J/m^2 threshold. It should be noted that the fracture energy values decrease significantly from reference post 6 to reference post 21.5. This also corresponds to an increasing amount of cracks seen in the field, especially in the south bound lane. This further indicates the DCT test has the ability to correlate laboratory data to actual field cracking performance.

Table 6: DCT fracture energy results versus cracking seen in the field on TH371

RP	North Bound Crack Count	South Bound Crack Count	Fracture Energy [J/m^2]	
			Wear Coarse	Non-wear
6	3	4	453.44	470.02
17	12	8	356.18	435.05
21.5	10	57	330.59	470.45

4.2.5 Discussion of Results

The testing of field procured asphalt mixtures was beneficial for multiple reasons. One of the reasonsis thatfracture energy results could be obtained for asphalt mixtures actually used in the field. The other being that these resultscould be compared to laboratory prepared granite and taconite samples. The following key points can be taken from testing of field samples.

- Highway 70 samples performed the best overall in both fracture energy and peak load compared to the parking lot, TH9, andTH371 samples. This was true for both test temperatures of -18^{o}C and -24^{o}C.

- TH9 samples performed much worse compared to TH70 samples. As indicated previously, TH9 samples had a binder content of only 4.0% with a small percentage being from RAP. From the results, it was determined that a mixture with such a low binder amount will result in low fracture energies and have poor cracking resistance. This is partially due to the lack of ductility the binder provides to the sample. Recently, MnDOT started using the adjusted asphalt film thickness (AFT) method for mix designs. Both TH9 and TH70 samples had identical AFTs but very different binder contents. Therefore, according to these preliminary results, the AFT method needs further evaluation, and parameters such as VMA and binder content should also be considered.

- The wearing coarse samples for TH371 had the lowest fracture energies, especially near reference points 17 and 21.5. Theses samples also had higher peak loads. This indicates the possibility of a brittle mixture which may be susceptible to premature and excessive cracking, as being seen in the field.

- Laboratory data was compared to crack counts taken in the field on TH371. DCT testing results provided lower fracture energies for sections of TH371 experience high amount of cracking. This further indicates the DCT test method has the ability to correlate laboratory testing to actual field performance.

- Granite and taconite samples performed as well or better in fracture energy and peak load performance. Even after conditioning, granite-taconite samples were able to retain this performance. This indicates that mixtures with taconite tailings will perform well in the field in terms of cracking performance.

CHAPTER 5: SUMMARY, CONCLUSIONS AND RECOMMENDATIONS

5.1 Summary

A comparative lab evaluation of moisture induced damage potential for asphalt mixes produced with high amount of taconite tailings against a mix produced with traditional granite aggregates is conducted in this study. The taconite tailings are a by-product from mining and ore enrichment process. The testing efforts included use of conventional AASHTO test procedures as well as fracture mechanics based test. A multiple freeze-thaw conditioning method, which is not a standardized procedure for moisture damage evaluation of asphalt concrete, was explored. This new methodology,along with field conditioned samples,was used to compare against AASHTO T-283 procedure. The main finding of this work is that asphalt mixes containing taconite tailings are not expected to suffer moisture induced damage problems in the field. Through testing efforts it was also realized that there is need for improvement in the moisture conditioning of asphalt specimens. The use of multiple freeze-thaw cycles as means to simulate moisture damage was evaluated and has shown promising results.

5.2 Conclusions

The results of laboratory testing led to the following conclusions:

- The asphalt mixture produced with taconite tailings is not expected to have moisture induced problems. This is based on modified Lottman tests (AASHTO T-283) as well as fracture energy tests. The specimens conditioned using newly proposed multiple freeze-thaw cycling procedure also showed that moisture induced damage is not of concern for deterioration of cracking resistance of asphalt mixes containing taconite tailings. The field conditioned specimens showed that mix with taconite tailings has slightly better performance than granite mix when evaluating moisture damage using fracture properties.

- The conditioning process recommended by the AASTHO T-283 test may not closely replicate the moisture damage occurring in the field. Fracture testing at low temperatures show significantly different behavior of unconditioned and conditioned specimens. It is anticipated that the curing of specimens at 60°C causes significant amount of healing and may not be realistic for propensity of pavement cracking occurring during colder climates. During colder climates the freezing of absorbed moisture in asphalt concrete would cause significant microscopic damage.

- While the AASHTO T-283 recommended conditioning process seems not applicable when using fracture energy testing as the recommended performance test, if it were applicable the increased potential for pavement cracking due to moisture damage is not anticipated. Both granite and taconite mixes showed significant increases in strain tolerance and ductility after undergoing lab conditioning.

- The testing of plant and field samples was beneficial for the comparison of results against laboratory produced granite and taconite samples. The results indicated the DCT test procedure is capable of correlating laboratory results with actual field performance of asphalt pavement.

- The newly proposed moisture condition method involving use of multiple freeze-thaw cycles and temperatures related to actual field conditions showed very good potential. The fracture results for specimens that underwent the method proposed herein showed results closer to field conditioned samples.

5.3 Recommendations

While the focus of this study was to evaluate moisture induced damage potential for asphalt mix with taconite tailings, several observations were made during the course of this research that enable the authors to make practical as well as research related recommendations:

- The taconite tailings in asphalt mixes should be used to substitute mineral aggregates and increase sustainability of pavement infrastructure. Such mixes are not anticipated to have durability problems due to moisture induced damage.

- The AASHTO T-283 conditioning process should be modified to account for actual climatic conditions of the pavement site. The thaw period of the current procedure might be too severe for mixes in colder climates that use softer binder grades.

- The AASHTO procedure only simulates a single freezing and thawing cycle. Typically an asphalt mix undergoes several freeze-thaw cycles during each winter season. The effect of multiple freeze-thaw cycling on asphalt mix durability should be explored further. This study provided very good start to this approach and will form basis for future research efforts.

- The DCT fracture energy test show very good promise for use as a proof test to screen mixtures with potential for moisture induced damage. The DCT test has recently been recommended by a national pooled fund study for specification purposes to ensure good low temperature cracking performance. The moisture damage testing using the DCT test should be added to this proposed specification.

- The fracture testing of field specimens showed that the DCT fracture energy threshold of 450 J/m^2 distinguished good and poor performing pavement sections from perspective of transverse cracking. Also, preliminary evaluation of mixes with the same adjusted asphalt film thickness showed that the low binder content mixes were more prone to cracking.

- It will be necessary to gather more information and conduct other tests to analyze the effects of moisture damage on other distresses such as rutting and fatigue cracking. Rutting, fatigue cracking, and other tests can be performed to determine these effects.

CHAPTER 6: REFERENCES

[1] U.S. Geological Survey (2011), "Mineral Commodity Summaries 2011," U.S. Geological Survey, 198 p., Washington DC.

[2] Tepordei, V. V., and Bolen, W. P. (2006), "Aggregate Economics: Natural Aggregates – A Fundamental Building Block of Modern Society - Are a Major Component of the U.S. Economy", *Aggregates Manager*, Vol. 11, No. 4, pp. 14-23.

[3] McIntyre, J., Spatari, S., and MacLean, H. L. (2009), "Energy and Greenhouse Gas Emissions Trade-Offs of Recycled Concrete Aggregate use in Nonstructural Concrete: A North American Case Study", *Journal of Infrastructure Systems*, Vol. 15, No. 4, pp. 361-370.

[4] Barksdale R. D. (Ed.) (2005), "The Aggregate Handbook", National Stone, Sand and Gravel Association, 800 p., Alexandria VA.

[5] AASHTO (2011), "Standard Method of Test for Resistance of Compacted Hot Mix Asphalt (HMA) to Moisture-Induced Damage," AASHTO T 283-07, American Association of State Highway and Transportation Officials, 8 p., Washington DC.

[6] ASTM (2011), "Standard Test Method for Determining Fracture Energy of Asphalt-Aggregate Mixtures Using the Disk-Shaped Compact Tension Geometry," ASTM D7313-07a, ASTM International, 7 p., West Conshohocken, PA.

[7] Oreskovich, J. A., Patelke, M. M., Zanko, L. M. (2007), "Documenting The Historical Use Of Taconite Byproducts As Construction Aggregates In Minnesota," Natural Resources Research Institute, University of Minnesota Duluth, Technical Summary Report NRRI/TR-2007/22.

[8] Zanko, L. M., Niles, H. B., Oreskovich, J. A. (2003), "Properties And Aggregate Potential Of Coarse Tailings From Five Minnesota Taconite Operations," Minnesota Department of Transportation, St. Paul, MN.

[9] Clyne, T., Johnson, E., and Worel, B. (2010), "Use of Taconite Aggregates in Pavement Applications," Minnesota Department of Transportation, 18 p., St. Paul, MN.

[10] Zanko, L. M. et al. (2012), "Performance of Taconite Aggregates in Thin Lift HMA," Report Number FHWA-HIF-12-025, Final Report – January 31, 2012: Natural Resources Research Institute, University of Minnesota Duluth, Technical Report NRRI/TR-2012/04, 125 p.

[11] Oreskovich, J.A. (2007), "A Brief History of the Use of Taconite Aggregate (Mesabi Hard Rock™) in Minnesota (1950s – 2007)," Natural Resources Research Institute, University of Minnesota Duluth, Technical Summary Report NRRI/TSR-2007/05, 8 pp.

[12] Scholz, T. V., Hunt, E., Shippen, N. (2011), "Forensic Investigation of Moisture-Related Pavement Failures On Interstate Highways In Oregon," Transportation Research Board, Washington DC.

[13] Stuart, K. D. (1990), "Moisture Damage in Asphalt Mixtures -- A State-of-the-Art Report," U.S. Department of Transportation, Federal Highway Administration, McLean, VA.

[14] Gong, W., Tao, M., (2012), "Investigation of Moisture Susceptibility of Warm Mix Asphalt (WMA) Mixes Through Laboratory Mechanical Testing," Transportation Research Board, Washington DC.

[15] Lottman, R. P. (1978), "Predicting Moisture-Induced Damage to Asphaltic Concrete," NCHRP Report 192, Transportation Research Board, National Research Council, Washington, DC.

[16] Epps, J. A., Sebaaly, P. E., Penaranda, J., Maher, M. R., McCann, M. B., and Hand, A. J. (2000), " Compatibility of a Test for Moisture-Induced Damage with Superpave Volumetric Mix Design," NCHRP Report 444, Transportation Research Board, National Research Council, Washington, DC.

[17] Kringos, N., Azari, H., and Scarpas, A. (2010), "Identification of Parameters Related to Moisture Conditioning That Cause Variability in Modified Lottman Test," *Transportation Research Record,* No. 2127, pp. 1-11.

[18] Jackson, N., Puccinelli, J., (2006), "Effect of Multiple Freeze Thaw Cycles and Deep Frost Penetration on Pavement Performance and Cost," Federal Highway Administration, Mclean, Va.

[19] Kringos, N. et al. (2010), "A New Asphalt Concrete Moisture Susceptibility Test Methodology," Tranportation Research Board 2011 Annual Meeting, Washington, D.C.

[20] "Resistance of Compacted Asphalt Mixtures to Moisture Induced Damage - AASHTO T-283." Indiana Department of Transportation. Web. 31 May 2012. <http://www.in.gov/indot/files/283.pdf>.

[21] Wagoner, M. P., Buttlar, W. G., Paulino, G. H., (2005), "Disk Shaped Compact Tension Test for Aspahlt," Department of Civil Engineering, University of Illinois, Urbana-Champaign, IL.

[22] Zhang, Z., Roque, R., and Birgisson, B. (2001), "Identification and Verification of a Suitable Crack Growth Law," *Journal of the Association of Asphalt Paving Technologists,* Vol. 70, pp. 206–241.

[23] Wagoner, M.P., Buttlar, W. G., and Paulino, G. H. (2005), "Disk-Shaped Compact Tension Test for Asphalt Concrete Fracture," *Experimental Mechanics*, Volume 45, pp. 270-277.

[24] Li, X., Marasteanu, M. O., Iverson, N., and Labuz, J. F. (2006), "Observation of Crack Propagation in Asphalt Mixtures with Acoustic Emission," *Transportation Research Record,* No. 1970, pp. 171-177.

[25] Apeagyei, A., Buttlar, W., and Dempsey, B. (2006), "Moisture Damage Evaluation of Asphalt Mixtures using AASHTO T283 and DC(T) Fracture Test," Proceedings of the 10th Internaitonal Conference on Asphalt Pavements (ISAP Quebec 2006), International Society of Asphalt Pavements, ISBN: 978-1-61782-084, pp. 862-873, Red Hook NY.

[26] Birgisson, B., Roque, R., and Page, G. C. (2004), "Performance-Based Fracture Criterion for Evaluation of Moisture Susceptibility in Hot-Mix Asphalt," *Transportation Research Record,* No. 1891, pp. 55–61.

[27] Birgisson, B., Roque, R., Page, G. C., (2004), "Performance-Based Fracture Criterion for Evaluation of Moisture Susceptibility in Hot-Mix Asphalt," Department of Civil and Coastal Engineering, University of Florida, Gainesville, FL.

[28] Marasteanu M. O. et al. (2007), "Investigation of Low Temperature Cracking in Asphalt Pavements", National Pooled Fund Study 776, Final report, Minnesota Department of Transportation, St. Paul MN.

[29] Zofka, A., an Braham, A. (2009), "Comparison of Low-Temperature Field Performance and Laboratory Testing of 10 Test Sections in the Midwestern United State," *Transportation Research Record,* No. 2127, pp. 107-114.

[30] Dave, E. V., Braham, A. F., Buttlar, W. G., Paulino, G. H., and Zofka, A. (2008), "Integration of Laboratory Testing, Field Performance Data, and Numerical Simulations for the Study of Low-Temperature Cracking," Proceedings of the 6th RILEM International Conference on Cracking in Pavements, Chicago, USA, Eds. Al-Qadi, Scarpas, and Loizos, CRC Press Taylor and Francis Group, New York, ISBN: 978-0-415-4757-54, pp.369-378.

[31] Wagoner, M. P., Buttlar, W. G., Paulino, G. H., and Blankenship, P. (2006), "Laboratory Testing Suite for Characterization of Asphalt Concrete Mixtures Obtained from Field Cores," Journal of the Association of Asphalt Paving Technologists, Vol. 75, p. 815-851.

[32] Dave, E. V. and Buttlar, W. G. (2010), "Thermal Reflective Cracking of Asphalt Concrete Overlays," *International Journal of Pavement Engineering*, 11(6), pp. 477-488.

[33] Behnia, B., Dave, E. V., Ahmed, S., Buttlar, W. G., and Reis, H. (2011), "Investigation of Effects of the Recycled Asphalt Pavement (RAP) Amounts on Low Temperature Cracking Performance of Asphalt Mixtures using Acoustic Emissions (AE)," *Transportation Research Record*, No. 2208, pp. 64-71.

[34] Dave, E. V., and Koktan, P. D. (2011), "Synthesis of Performance Testing of Asphalt Concrete," Minnesota Department of Transportation, Report MN/RC 2011-22, 90 p., St. Paul MN.

[35] Marasteanu et al. (2012), "Investigation of Low Temperature Cracking in Asphalt Pavements – Phase II," Draft Final Report, Pooled Fund Study TPF-5(132).

CHAPTER 7: APPENDICES

Appendix A: Volumetric Properties for Indirect Tension Testing

Table A1: ITS volumetric properties for unconditioned/AASHTO T-283 conditioned granite samples

Sample ID	A	B	C	D	E	F
Loose Mix Dry Weight [grams]	1088.0	1088.0	1088.0	1088.0	1088.0	1088.0
Loose Mix Sub. Weight [grams]	1535.4	1535.4	1535.4	1535.4	1535.4	1535.4
Loose Mix SSD Weight [grams]	2172.4	2172.4	2172.4	2172.4	2172.4	2172.4
Compacted Dry Weight[grams]	3750.7	3718.2	3709.9	3721.0	3725.5	3725.2
Compacted Sub. Weight [grams]	2165.9	2150.7	2139.2	2145.5	2152.9	2150.2
Compacted SSD Weight [grams]	3826.1	3809.6	3801.4	3807.0	3811.4	3808.5
G_{mm}	2.412	2.412	2.412	2.412	2.412	2.412
G_{mb}	2.259	2.241	2.232	2.239	2.246	2.246
Percent Water Absorbed [%]	4.54	5.51	5.50	5.18	5.18	5.02
Percent Air Voids [%]	6.35	7.09	7.48	7.17	6.88	6.88
Percent Binder [%]	6.89	6.89	6.89	6.89	6.89	6.89
Percent Aggregate [%]	93.11	93.11	93.11	93.11	93.11	93.11
G_{sb}	2.636	2.636	2.636	2.636	2.636	2.636
G_{se}	2.682	2.682	2.682	2.682	2.682	2.682
VMA [%]	20.21	20.84	21.17	20.90	20.66	20.66
VFA [%]	68.56	65.97	64.66	65.71	66.69	66.70
P_{ba} [%]	0.67	0.67	0.67	0.67	0.67	0.67
P_{be} [%]	6.27	6.27	6.27	6.27	6.27	6.27
P_d	7.23	7.23	7.23	7.23	7.23	7.23
Dust/Binder Ratio	1.15	1.15	1.15	1.15	1.15	1.15
Asphalt Film Thickness [microns]	8.6	8.6	8.6	8.6	8.6	8.6

Table A2: ITS volumetric properties for unconditioned/AASHTO T-283 conditioned taconite samples

Sample ID	A	B	C	D	E	F
Loose Mix Dry Weight [grams]	1067.6	1067.6	1067.6	1067.6	1067.6	1067.6
Loose Mix Sub. Weight [grams]	1534.5	1534.5	1534.5	1534.5	1534.5	1534.5
Loose Mix SSD Weight [grams]	2178.1	2178.1	2178.1	2178.1	2178.1	2178.1
Compacted Dry Weight[grams]	3899.7	3875.9	3888.1	3862.1	3879.9	3893.8
Compacted Sub. Weight [grams]	2326.3	2310.1	2315.4	2302.7	2311.5	2332.0
Compacted SSD Weight [grams]	3981.4	3964.4	3972.0	3960.7	3967.5	3983.8
G_{mm}	2.518	2.518	2.518	2.518	2.518	2.518
G_{mb}	2.356	2.343	2.347	2.329	2.343	2.357
Percent Water Absorbed [%]	4.94	5.35	5.06	5.95	5.29	5.45
Percent Air Voids [%]	6.41	6.94	6.77	7.48	6.94	6.37
Percent Binder [%]	7.21	7.21	7.21	7.21	7.20	7.20
Percent Aggregate [%]	92.79	92.79	92.79	92.79	92.80	92.80
G_{sb}	2.769	2.769	2.769	2.769	2.769	2.769
G_{se}	2.840	2.840	2.840	2.840	2.840	2.840
VMA [%]	21.04	21.49	21.34	21.94	21.48	21.00
VFA [%]	69.52	67.68	68.26	65.91	67.69	69.67
P_{ba} [%]	0.923	0.923	0.922	0.922	0.921	0.921
P_{be} [%]	6.35	6.35	6.35	6.35	6.35	6.35
P_d	6.47	6.47	6.47	6.47	6.47	6.47
Dust/Binder Ratio	1.02	1.02	1.02	1.02	1.02	1.02
Asphalt Film Thickness [microns]	9.1	9.1	9.1	9.1	9.1	9.1

Table A3: ITS volumetric properties for field conditioned granite samples

Sample ID	D-T	D-B
Loose Mix Dry Weight [grams]	1088.0	1088.0
Loose Mix Sub. Weight [grams]	1535.4	1535.4
Loose Mix SSD Weight [grams]	2172.4	2172.4
Compacted Dry Weight[grams]	2028.4	2008.2
Compacted Sub. Weight [grams]	1172.9	1160.1
Compacted SSD Weight [grams]	2070.9	2037.9
G_{mm}	2.412	2.412
G_{mb}	2.259	2.288
Percent Water Absorbed [%]	4.73	3.39
Percent Air Voids [%]	6.37	5.17
Percent Binder [%]	6.90	6.90
Percent Aggregate [%]	93.10	93.10
G_{sb}	2.636	2.636
G_{se}	2.682	2.682
VMA [%]	20.23	19.20
VFA [%]	68.52	73.09
P_{ba} [%]	0.67	0.67
P_{be} [%]	6.27	6.27
P_d	7.23	7.23
Dust/Binder Ratio	1.15	1.15
Asphalt Film Thickness [microns]	8.6	8.6

Table A4: ITS volumetric properties for field conditioned taconite samples

Sample ID	D-T	D-B
Loose Mix Dry Weight [grams]	1067.6	1067.6
Loose Mix Sub. Weight [grams]	1534.5	1534.5
Loose Mix SSD Weight [grams]	2178.1	2178.1
Compacted Dry Weight[grams]	2191.4	2143.0
Compacted Sub. Weight [grams]	1311.4	1279.6
Compacted SSD Weight [grams]	2232.5	2176.5
G_{mm}	2.518	2.518
G_{mb}	2.379	2.389
Percent Water Absorbed [%]	4.47	3.73
Percent Air Voids [%]	5.50274	5.10177
Percent Binder [%]	7.20	7.20
Percent Aggregate [%]	92.80	92.80
G_{sb}	2.769	2.769
G_{se}	2.840	2.840
VMA [%]	20.27	19.93
VFA [%]	72.86	74.41
P_{ba} [%]	0.921	0.921
P_{be} [%]	6.35	6.35
P_d	6.47	6.47
Dust/Binder Ratio	1.02	1.02
Asphalt Film Thickness [microns]	9.1	9.1

Appendix B: Volumetric Properties for Fracture Energy Testing

Table B1: DCT volumetric properties for unconditioned/AASHTO T-283 conditioned granite samples

Sample ID	A-T	A-B	B-T	B-B	C-T	C-B
Loose Mix Dry Weight [grams]	1088.0	1088.0	1088.0	1088.0	1088.0	1088.0
Loose Mix Sub. Weight [grams]	1535.4	1535.4	1535.4	1535.4	1535.4	1535.4
Loose Mix SSD Weight [grams]	2172.4	2172.4	2172.4	2172.4	2172.4	2172.4
Compacted Dry Weight[grams]	2007.6	2006.5	2013.2	1950.9	2047.2	1998.0
Compacted Sub. Weight [grams]	1161.1	1156.0	1154.0	1119.9	1168.5	1144.4
Compacted SSD Weight [grams]	2056.7	2042.4	2048.6	1979.8	2075.9	2021.0
G_{mm}	2.412	2.412	2.412	2.412	2.412	2.412
G_{mb}	2.242	2.264	2.250	2.269	2.256	2.279
Percent Water Absorbed [%]	5.47	4.04	3.96	3.36	3.16	5.023
Percent Air Voids [%]	7.07	6.16	6.71	5.96	6.48	5.52
Percent Binder [%]	6.90	6.90	6.90	6.90	6.90	6.90
Percent Aggregate [%]	93.10	93.10	93.10	93.10	93.10	93.10
G_{sb}	2.636	2.636	2.636	2.636	2.636	2.636
G_{se}	2.682	2.682	2.682	2.682	2.682	2.682
VMA [%]	20.82	20.05	20.52	19.87	20.32	19.50
VFA [%]	66.05	69.27	67.28	70.03	68.11	71.69
P_{ba} [%]	0.67	0.67	0.67	0.67	0.67	0.67
P_{be} [%]	6.28	6.28	6.28	6.28	6.28	6.28
P_d	7.23	7.23	7.23	7.23	7.23	7.23
Dust/Binder Ratio	1.15	1.15	1.15	1.15	1.15	1.15
Asphalt Film Thickness [microns]	8.6	8.6	8.6	8.6	8.6	8.6

Table B2: DCT volumetric properties for unconditioned/AASHTO T-283 conditioned taconite samples

Sample ID	A-T	A-B	B-T	B-B	C-T	C-B
Loose Mix Dry Weight [grams]	1067.6	1067.6	1067.6	1067.6	1067.6	1067.6
Loose Mix Sub. Weight [grams]	1534.5	1534.5	1534.5	1534.5	1534.5	1534.5
Loose Mix SSD Weight [grams]	2178.1	2178.1	2178.1	2178.1	2178.1	2178.1
Compacted Dry Weight[grams]	2071.3	1991.4	2147.6	2030.4	2161.5	2054.8
Compacted Sub. Weight [grams]	1221.3	1194.0	1279.2	1212.2	1290.2	1225.8
Compacted SSD Weight [grams]	2108.0	2042.3	2196.3	2077.5	2212.4	2101.8
G_{mm}	2.518	2.518	2.518	2.518	2.518	2.518
G_{mb}	2.336	2.348	2.342	2.346	2.344	2.346
Percent Water Absorbed [%]	4.14	5.99	5.31	5.45	5.52	5.36
Percent Air Voids [%]	7.22	6.76	7.00	6.81	6.91	6.83
Percent Binder [%]	7.21	7.21	7.21	7.21	7.20	7.20
Percent Aggregate [%]	92.79	92.79	92.79	92.79	92.80	92.80
G_{sb}	2.769	2.769	2.769	2.769	2.769	2.769
G_{se}	2.840	2.840	2.840	2.840	2.840	2.840
VMA [%]	21.72	21.33	21.53	21.37	21.46	21.39
VFA [%]	66.75	68.32	67.51	68.15	67.79	68.07
P_{ba} [%]	0.923	0.923	0.922	0.922	0.921	0.921
P_{be} [%]	6.35	6.35	6.35	6.35	6.35	6.35
P_d	6.47	6.47	6.47	6.47	6.47	6.47
Dust/Binder Ratio	1.02	1.02	1.02	1.02	1.02	1.02
Asphalt Film Thickness [microns]	9.1	9.1	9.1	9.1	9.1	9.1

Table B3: DCT volumetric properties for field conditioned granite samples

Sample ID	A-T	A-B	B-T	B-B	C-T	C-B
Loose Mix Dry Weight [grams]	1088.0	1088.0	1088.0	1088.0	1088.0	1088.0
Loose Mix Sub. Weight [grams]	1535.4	1535.4	1535.4	1535.4	1535.4	1535.4
Loose Mix SSD Weight [grams]	2172.4	2172.4	2172.4	2172.4	2172.4	2172.4
Compacted Dry Weight[grams]	1998.2	2048.5	2086.9	2085.7	2093.8	2016.4
Compacted Sub. Weight [grams]	1154.0	1183.9	1207.1	1205.8	1210.0	1163.4
Compacted SSD Weight [grams]	2027.4	2090.2	2130.4	2115.1	2135.7	2044.9
G_{mm}	2.412	2.412	2.412	2.412	2.412	2.412
G_{mb}	2.288	2.260	2.260	2.294	2.262	2.287
Percent Water Absorbed [%]	3.34	4.60	4.71	3.23	4.52	3.23
Percent Air Voids [%]	5.16	6.31	6.30	4.92	6.24	5.18
Percent Binder [%]	6.90	6.90	6.90	6.90	6.90	6.90
Percent Aggregate [%]	93.10	93.10	93.10	93.10	93.10	93.10
G_{sb}	2.636	2.636	2.636	2.636	2.636	2.636
G_{se}	2.682	2.682	2.682	2.682	2.682	2.682
VMA [%]	19.20	20.17	20.17	18.99	20.12	19.21
VFA [%]	73.13	68.74	68.76	74.10	68.97	73.04
P_{ba} [%]	0.67	0.67	0.67	0.67	0.67	0.67
P_{be} [%]	6.27	6.27	6.27	6.27	6.27	6.27
P_d	7.23	7.23	7.23	7.23	7.23	7.23
Dust/Binder Ratio	1.15	1.15	1.15	1.15	1.15	1.15
Asphalt Film Thickness [microns]	8.6	8.6	8.6	8.6	8.6	8.6

Table B4: DCT volumetric properties for field conditioned taconite samples

Sample ID	A-T	A-B	B-T	B-B	C-T	C-B
Loose Mix Dry Weight [grams]	1067.6	1067.6	1067.6	1067.6	1067.6	1067.6
Loose Mix Sub. Weight [grams]	1534.5	1534.5	1534.5	1534.5	1534.5	1534.5
Loose Mix SSD Weight [grams]	2178.1	2178.1	2178.1	2178.1	2178.1	2178.1
Compacted Dry Weight[grams]	2182.1	2076.1	2161.5	2084.4	2169.5	2126.1
Compacted Sub. Weight [grams]	1302.7	1238.5	1291.7	1243.5	1295.9	1266.5
Compacted SSD Weight [grams]	2235.3	2117.2	2210.6	2120.8	2226.1	2168.9
G_{mm}	2.518	2.518	2.518	2.518	2.518	2.518
G_{mb}	2.340	2.363	2.352	2.376	2.332	2.356
Percent Water Absorbed [%]	5.71	4.67	5.35	4.14	6.08	4.74
Percent Air Voids [%]	7.07	6.15	6.58	5.63	7.37	6.42
Percent Binder [%]	7.21	7.21	7.21	7.21	7.20	7.20
Percent Aggregate [%]	92.79	92.79	92.79	92.79	92.80	92.80
G_{sb}	2.769	2.769	2.769	2.769	2.769	2.769
G_{se}	2.84	2.84	2.84	2.84	2.840	2.840
VMA [%]	21.60	20.82	21.18	20.38	21.85	21.04
VFA [%]	67.26	70.44	68.93	72.37	66.28	69.50
P_{ba} [%]	0.923	0.923	0.922	0.922	0.921	0.921
P_{be} [%]	6.35	6.35	6.35	6.35	6.35	6.35
P_d	6.47	6.47	6.47	6.47	6.47	6.47
Dust/Binder Ratio	1.02	1.02	1.02	1.02	1.02	1.02
Asphalt Film Thickness [microns]	9.1	9.1	9.1	9.1	9.1	9.1

Table B5: DCT volumetric properties for multiple freeze-thaw conditioned granite samples

Sample ID	A-T	A-B	B-T	B-B	C-T	C-B
Loose Mix Dry Weight [grams]	1088.0	1088.0	1088.0	1088.0	1088.0	1088.0
Loose Mix Sub. Weight [grams]	1535.4	1535.4	1535.4	1535.4	1535.4	1535.4
Loose Mix SSD Weight [grams]	2172.4	2172.4	2172.4	2172.4	2172.4	2172.4
Compacted Dry Weight[grams]	2012.1	2031.0	2036.0	2026.6	2030.1	1999.6
Compacted Sub. Weight [grams]	1146.7	1174.2	1177.0	1174.0	1171.0	1159.1
Compacted SSD Weight [grams]	2034.4	2066.1	2078.0	2058.9	2069.5	2035.4
G_{mm}	2.412	2.412	2.412	2.412	2.412	2.412
G_{mb}	2.267	2.277	2.260	2.290	2.259	2.282
Percent Water Absorbed [%]	2.51	3.94	4.66	3.65	4.39	4.09
Percent Air Voids [%]	6.04	5.61	6.32	5.07	6.34	5.41
Percent Binder [%]	6.89	6.89	6.89	6.89	6.89	6.89
Percent Aggregate [%]	93.11	93.11	93.11	93.11	93.11	93.11
G_{sb}	2.636	2.636	2.636	2.636	2.636	2.636
G_{se}	2.682	2.682	2.682	2.682	2.682	2.682
VMA [%]	19.94	19.57	20.18	19.11	20.20	19.41
VFA [%]	69.73	71.36	68.68	73.48	68.60	72.10
P_{ba} [%]	0.67	0.67	0.67	0.67	0.67	0.67
P_{be} [%]	6.27	6.27	6.27	6.27	6.27	6.27
P_d	7.23	7.23	7.23	7.23	7.23	7.23
Dust/Binder Ratio	1.15	1.15	1.15	1.15	1.15	1.15
Asphalt Film Thickness [microns]	8.6	8.6	8.6	8.6	8.6	8.6

Table B6: DCT volumetric properties for multiple freeze-thaw conditioned taconite samples

Sample ID	A-T	A-B	B-T	B-B	C-T	C-B
Loose Mix Dry Weight [grams]	1067.6	1067.6	1067.6	1067.6	1067.6	1067.6
Loose Mix Sub. Weight [grams]	1534.5	1534.5	1534.5	1534.5	1534.5	1534.5
Loose Mix SSD Weight [grams]	2178.1	2178.1	2178.1	2178.1	2178.1	2178.1
Compacted Dry Weight[grams]	2125.6	2056.6	2147.9	2054.7	2149.7	2089.6
Compacted Sub. Weight [grams]	1272.9	1232.2	1284.3	1227.1	1285.3	1253.0
Compacted SSD Weight [grams]	2176.6	2102.7	2197.0	2098.3	2202.9	2136.2
G_{mm}	2.518	2.518	2.518	2.518	2.518	2.518
G_{mb}	2.352	2.362	2.353	2.359	2.343	2.366
Percent Water Absorbed [%]	5.64	5.30	5.37	5.00	5.80	5.28
Percent Air Voids [%]	6.57	6.17	6.52	6.32	6.95	6.03
Percent Binder [%]	7.21	7.21	7.21	7.21	7.20	7.20
Percent Aggregate [%]	92.79	92.79	92.79	92.79	92.80	92.80
G_{sb}	2.769	2.769	2.769	2.769	2.769	2.769
G_{se}	2.840	2.840	2.840	2.840	2.840	2.840
VMA [%]	21.17	20.82	21.12	20.95	21.48	20.71
VFA [%]	68.94	70.39	69.11	69.83	67.64	70.88
P_{ba} [%]	0.923	0.923	0.922	0.922	0.921	0.921
P_{be} [%]	6.35	6.35	6.35	6.35	6.35	6.35
P_d	6.47	6.47	6.47	6.47	6.47	6.47
Dust/Binder Ratio	1.02	1.02	1.02	1.02	1.02	1.02
Asphalt Film Thickness [microns]	9.1	9.1	9.1	9.1	9.1	9.1

Table B7: DCT volumetric properties for unconditioned granite samples tested at -18°C

Sample ID	A-T	A-B	B-T	B-B
Loose Mix Dry Weight [grams]	1088.0	1088.0	1088.0	1088.0
Loose Mix Sub. Weight [grams]	1535.4	1535.4	1535.4	1535.4
Loose Mix SSD Weight [grams]	2172.4	2172.4	2172.4	2172.4
Compacted Dry Weight[grams]	2009.0	2032.1	2057.2	2046.6
Compacted Sub. Weight [grams]	1167.2	1181.6	1188.1	1181.3
Compacted SSD Weight [grams]	2058.2	2077.9	2095.2	2085.7
G_{mm}	2.412	2.412	2.412	2.412
G_{mb}	2.255	2.267	2.268	2.263
Percent Water Absorbed [%]	5.53	5.11	4.19	4.32
Percent Air Voids [%]	6.53	6.02	5.99	6.20
Percent Binder [%]	6.89	6.89	6.89	6.89
Percent Aggregate [%]	93.11	93.11	93.11	93.11
G_{sb}	2.636	2.636	2.636	2.636
G_{se}	2.682	2.682	2.682	2.682
VMA [%]	20.36	19.92	19.90	20.07
VFA [%]	67.91	69.80	69.89	69.13
P_{ba} [%]	0.67	0.67	0.67	0.67
P_{be} [%]	6.27	6.27	6.27	6.27
P_d	7.23	7.23	7.23	7.23
Dust/Binder Ratio	1.15	1.15	1.15	1.15
Asphalt Film Thickness [microns]	8.6	8.6	8.6	8.6

Table B8: DCT volumetric properties for unconditioned taconite samples tested at -18°C

Sample ID	A-T	A-B	B-T	B-B
Loose Mix Dry Weight [grams]	1067.6	1067.6	1067.6	1067.6
Loose Mix Sub. Weight [grams]	1534.5	1534.5	1534.5	1534.5
Loose Mix SSD Weight [grams]	2178.1	2178.1	2178.1	2178.1
Compacted Dry Weight[grams]	2101.0	2120.9	2142.4	2055.9
Compacted Sub. Weight [grams]	1250.4	1259.5	1272.7	1224.3
Compacted SSD Weight [grams]	2145.5	2164.3	2180.2	2096.4
G_{mm}	2.518	2.518	2.518	2.518
G_{mb}	2.347	2.344	2.361	2.357
Percent Water Absorbed [%]	4.97	4.80	4.17	4.64
Percent Air Voids [%]	6.77	6.90	6.24	6.36
Percent Binder [%]	7.21	7.21	7.21	7.21
Percent Aggregate [%]	92.79	92.79	92.79	92.79
G_{sb}	2.769	2.769	2.769	2.769
G_{se}	2.840	2.840	2.840	2.840
VMA [%]	21.33	21.44	20.88	20.99
VFA [%]	68.27	67.81	70.13	69.68
P_{ba} [%]	0.923	0.923	0.922	0.922
P_{be} [%]	6.35	6.35	6.35	6.35
P_d	6.47	6.47	6.47	6.47
Dust/Binder Ratio	1.02	1.02	1.02	1.02
Asphalt Film Thickness [microns]	9.1	9.1	9.1	9.1

Appendix C: ITS Pre-Test Data for Granite-Taconite Samples

Table C1: Indirect tension pre-test data for granite samples

	Unconditioned Subset			T-283 Conditioned Subset		
	B	C	D	A	E	F
Thickness [mm]	95.1	95.2	95.2	95.4	95.1	95
Diameter [mm]	150	150	150	150	150	150
Volume of Specimen [cm^3]	1680.6	1682.3	1682.3	1685.9	1680.6	1678.8
Volume of Voids [cm^3]	119.2	125.8	120.6	107.1	115.6	115.5
Dry Weight [g]	3718.2	3709.9	3720.9	3750.7	3725.5	3725.2
SSD Weight [g]	---	---	---	3828.0	3807.9	3806.4
Volume absorbed [cm^3]	---	---	---	77.3	82.4	81.19
Degree of Saturation [%]	---	---	---	72.2	71.3	70.3

Table C2: Indirect tension pre-test data for taconite samples

	Unconditioned Subset			T-283 Conditioned Subset		
	A	C	F	B	D	E
Thickness [mm]	95.1	95.1	94.9	95.1	95.1	95.1
Diameter [mm]	150	150	150	150	150	150
Volume of Specimen [cm^3]	1680.6	1680.6	1677.0	1680.6	1680.6	1680.6
Volume of Voids [cm^3]	107.7	113.8	106.8	116.6	125.7	116.6
Dry Weight [g]	3899.7	3888.1	3893.8	3875.9	3862.1	3879.9
SSD Weight [g]	---	---	---	3966.0	3955.5	3968.5
Volume absorbed [cm^3]	---	---	---	90.18	93.4	88.7
Degree of Saturation [%]	---	---	---	77.3	74.3	76.0

Table C3: Indirect tension pre-test data for field conditioned samples

	Granite Samples		Taconite Samples	
Specimen ID	D-T	D-B	D-T	D-B
Thickness [mm]	51.4	50.2	52.5	51.1
Diameter [mm]	150	150	150	150

Appendix D: DCT Pre-Test Data for Granite-Taconite Samples

Table D1: DCT pre-test data for unconditioned/T-283 conditioned granite samples

	Unconditioned Subset			T-283 Conditioned Subset		
Sample ID	A-T	B-T	C-T	A-B	B-B	C-B
Thickness [mm]	51.2	51.1	51.8	50.7	49.3	50.07
Diameter [mm]	150	150	150	150	150	150
Ligament Length [mm]	88.8	89.5	87.9	89.25	88.3	89.6

Table D2: DCT pre-test data for unconditioned/T-283 conditioned taconite samples

	Unconditioned Subset			T-283 Conditioned Subset		
Sample ID	A-T	B-T	C-T	A-B	B-B	C-B
Thickness [mm]	50.9	52.5	52.8	48.7	49.8	50.2
Diameter [mm]	150	150	150	150	150	150
Ligament Length [mm]	88.0	89.3	90.9	87.5	89.2	87.9

Table D3: DCT pre-test data for field conditioned granite samples

Specimen ID	A-T	A-B	B-T	B-B	C-T	C-B
Thickness [mm]	49.9	51.6	52.5	52.0	52.7	50.4
Diameter [mm]	150	150	150	150	150	150
Ligament Length [mm]	88.6	87.5	89.4	88.7	88.4	87.1

Table D4: DCT pre-test data for field conditioned taconite samples

Specimen ID	A-T	A-B	B-T	B-B	C-T	C-B
Thickness [mm]	53.1	50.1	52.4	50.0	52.8	51.4
Diameter [mm]	150	150	150	150	150	150
Ligament Length [mm]	87.2	87.2	87.2	86.3	89.6	88.0

Table D5: DCT pre-test data for multiple freeze-thaw cycle conditioned granite samples

Conditioning Level	10 Freeze-Thaw Cycles			20 Freeze-Thaw Cycles		
Sample ID	A-T	B-T	C-T	A-B	B-B	C-B
Thickness [mm]	50.8	51.5	51.4	51.1	50.7	50.2
Diameter [mm]	150	150	150	150	150	150
Ligament Length [mm]	88.6	87.8	89.3	87.1	88.7	88.9

Table D6: DCT pre-test data for multiple freeze-thaw cycle conditioned taconite samples

Conditioning Level	10 Freeze-Thaw Cycles			20 Freeze-Thaw Cycles		
Sample ID	A-T	B-T	C-T	A-B	B-B	C-B
Thickness [mm]	52.0	52.5	52.8	50.1	50.0	50.7
Diameter [mm]	150	150	150	150	150	150
Ligament Length [mm]	88.4	89.2	88.9	87.6	88.7	88.1

Table D7: DCT pre-test data for uncondtioned samples tested at -18^{o}C

Conditioning Level	Granite Samples				Taconite Samples			
Sample ID	A-T	A-B	B-T	B-B	A-T	A-B	B-T	B-B
Thickness [mm]	50.9	51.3	51.7	51.8	51.2	52.0	51.9	50.0
Diameter [mm]	150	150	150	150	150	150	150	150
Ligament Length [mm]	89.0	88.3	90.2	88.5	86.6	87.4	87.2	88.0

Appendix E: DCT Pre-Test Data for Field and Plant Samples

Table E1: DCT pre-test data for parking lot base samples

Sample ID	B1-T	B1-B	B2-T	B2-B	B3-T	B3-B
Thickness [mm]	51.2	50.5	51.4	50.8	51.7	51.1
Diameter [mm]	150	150	150	150	150	150
Ligament Length [mm]	91.4	86.8	92.1	87.6	86.0	87.7

Table E2: DCT pre-test data for parking lot wear samples

Sample ID	W1-T	W1-B	W2-T	W2-B	W3-T	W3-B
Thickness [mm]	51.1	50.8	21.3	51.1	51.3	51.2
Diameter [mm]	150	150	150	150	150	150
Ligament Length [mm]	87.4	87.6	88.6	88.6	86.1	89

Table E3: DCT pre-test data for TH9 samples

Sample ID	A-T	A-B	B-T	B-B	C-T (-18^{o}C)	C-B (-18^{o}C)
Thickness [mm]	52.8	49.7	51.2	50.6	52.9	51.9
Diameter [mm]	150	150	150	150	150	150
Ligament Length [mm]	88.6	88.5	87.7	86.6	85.7	86.8

Table E4: DCT pre-test data for TH70 samples

Sample ID	A-T	A-B	B-T	B-B	C-T (-18oC)	C-B (-18oC)
Thickness [mm]	52.3	51.5	52.4	50.9	51.4	51.8
Diameter [mm]	150	150	150	150	150	150
Ligament Length [mm]	87.4	86.5	86.8	88.0	86.8	88.0

Table E5: DCT pre-test data for TH371 RP6 samples

	Wear			**Non-wear**		
Sample ID	A	B	C	A	B	C
Thickness [mm]	53	52.9	51	51.7	52.4	52.2
Diameter [mm]	145	145	145	145	145	145
Ligament Length [mm]	82.6	80.8	81.8	81.8	82.7	82.6

Table E6: DCT pre-test data for TH371 RP17 samples

	Wear			**Non-wear**		
Sample ID	A	B	C	A	B	C
Thickness [mm]	52.8	50.8	52.1	52.7	52.8	53.5
Diameter [mm]	145	145	145	145	145	145
Ligament Length [mm]	81.5	81.7	83.5	84.9	81.4	82.4

Table E7: DCT pre-test data for TH371 RP21.5 samples

	Wear			Non-wear		
Sample ID	A	B	C	A	B	C
Thickness [mm]	53.3	51.3	51.8	52.6	52.4	52.6
Diameter [mm]	145	145	145	145	145	145
Ligament Length [mm]	81.7	83.4	81.4	82.5	82.3	83.1

Appendix F: ITS Results

Table F1: Granite mixture peak load results from Indirect Tensile Test

Specimen	Dry/Conditioned	Max Load [N]	Average Max Load [N]	CoV [%]
B	Unconditioned	9275	10046	7.29
C		10130		
D		10732		
A	T-283 Conditioned	9098	9569	4.84
E		9586		
F		10023		
D-B	Field Conditioned	4719	4812	2.74
D-T		4905		

Table F2: Taconite mixture peak load results from Indirect Tensile Test

Specimen	Dry/Conditioned	Max Load [N]	Average Max Load [N]	CoV [%]
A	Unconditioned	9799	9791	1.15
C		9675		
F		9899		
B	T-283 Conditioned	7850	8364	5.53
D		8495		
E		8746		
D-B	Field Conditioned	4418.3	4747.72	9.81
D-T		5077.14		

Table F3: Granite mixture strength results from Indirect Tensile Test

Specimen	Dry/Conditioned	Peak Stress [MPa]	Average Stress [MPa]	CoV [%]
B	Unconditioned	0.414	0.448	7.24
C		0.452		
D		0.479		
A	T-283 Conditioned	0.405	0.427	5.04
E		0.428		
F		0.448		
D-B	Field Conditioned	0.399	0.402	1.07
D-T		0.405		

Table F4: Taconite mixture strength results from Indirect Tensile Test

Specimen	Dry/Conditioned	Peak Stress [MPa]	Average Stress [MPa]	CoV [%]
A	Unconditioned	0.436	0.437	1.26
C		0.432		
F		0.443		
B	T-283 Conditioned	0.350	0.373	5.53
D		0.379		
E		0.390		
D-B	Field Conditioned	0.367	0.3887	7.90
D-T		0.4104		

Table F5: Granite mixture work (energy) results from Indirect Tensile Test

Specimen	Dry/Conditioned	Work [J/m^2]	Average Work [J/m^2]	CoV [%]
B	Unconditioned	1577.27	1714.53	8.36
C		1703.05		
D		1863.27		
A	T-283 Conditioned	1629.24	1732.42	6.28
E		1722.04		
F		1845.99		
D-B	Field Conditioned	1470.52	1461.40	0.88
D-T		1452.27		

Table F6: Taconite mixture work (energy) results from Indirect Tensile Test

Specimen	Dry/Conditioned	Work [J/m^2]	Average Work [J/m^2]	CoV [%]
A	Unconditioned	1555.90	1603.44	7.18
C		1519.67		
F		1734.75		
B	T-283 Conditioned	1386.34	1455.61	4.15
D		1483.30		
E		1497.17		
D-B	Field Conditioned	1318.05	1376.23	5.98
D-T		1434.41		

Appendix G: DCT Results for Granite-Taconite Samples

Table G1: DCT results for unconditioned granite and taconite mixtures

Sample	Fracture Energy [J/m^2]		Peak Load [N]	
	Granite Mix	Taconite Mix	Granite Mix	Taconite Mix
1	803.97	387.68	3833.71	3550.70
2	585.97	537.84	4353.96	3689.93
3	662.02	488.48	4173.53	4239.55
Average	683.99	471.34	4120.40	3826.73
CoV [%]	16.18	16.24	6.41	9.52

Table G2: DCT results for T-283 conditioned granite and taconite mixtures

Sample	Fracture Energy [J/m^2]		Peak Load [N]	
	Granite Mix	Taconite Mix	Granite Mix	Taconite Mix
1	1395.65	1509.71	2479.54	2472.75
2	1162.51	1784.63	1987.10	2933.15
3	1733.03	1443.91	2643.73	2108.46
Average	1430.40	1579.41	2370.13	2504.79
CoV [%]	20.05	11.44	14.42	16.50

Table G3: DCT results for field conditioned granite and taconite mixtures

Sample	Fracture Energy [J/m^2]		Peak Load [N]	
	Granite Mix	Taconite Mix	Granite Mix	Taconite Mix
1	484.34	381.69	4078.02	3838.64
2	483.07	423.09	4716.75	3694.50
3	574.43	373.33	4703.24	3801.89
4	---	513.40	---	4246.24
Average	513.95	422.88	4499.34	3895.32
CoV [%]	10.19	15.17	8.11	6.21

Table G4: DCT results for 10 F-T cycle conditioned granite and taconite mixtures

Sample	Fracture Energy [J/m^2]		Peak Load [N]	
	Granite Mix	Taconite Mix	Granite Mix	Taconite Mix
1	507.33	759.47	4710.88	4089.85
2	510.61	598.03	4569.22	4078.38
3	532.74	664.84	4317.71	4037.04
Average	516.89	674.11	4532.61	4068.42
CoV [%]	2.67	12.03	4.39	0.68

Table G5: DCT results for 20 F-T cycle conditioned granite and taconite mixtures

Sample	Fracture Energy [J/m^2]		Peak Load [N]	
	Granite Mix	Taconite Mix	Granite Mix	Taconite Mix
1	727.93	558.49	4417.43	3156.51
2	1161.36	421.58	4632.71	4081.78
3	1228.43	770.14	3888.11	3652.60
Average	1039.24	583.41	4312.75	3630.30
CoV [%]	26.14	30.10	8.88	12.75

Table G6: DCT results for unconditioned granite and taconite mixtures tested at -18^{o}C

	Fracture Energy [J/m^2]		Peak Load [N]	
Sample	Granite Mix	Taconite Mix	Granite Mix	Taconite Mix
A-T	510.78	619.80	3889.48	3695.05
A-B	1293.54	2566.81	4258.56	3086.59
B-T	2290.77	2151.07	3247.95	2585.69
B-B	2133.98	971.94	3740.07	3545.51
Average	1557.27	1577.41	3784.02	3228.21
COV [%]	52.89	58.92	11.06	15.50

Table G7: DCT results for field conditioned granite and taconite mixtures tested at -18^{o}C

	Fracture Energy [J/m^2]		Peak Load [N]	
Sample	Granite Mix	Taconite Mix	Granite Mix	Taconite Mix
C-T	1445.14	991.04	3406.80	3779.13
C-B	1177.46	1737.68	3602.79	2934.26
Average	1311.30	1364.36	3504.80	3356.70
COV [%]	14.43	38.70	3.95	17.80

Appendix H: Load-CMOD Curves for Granite-Taconite Samples

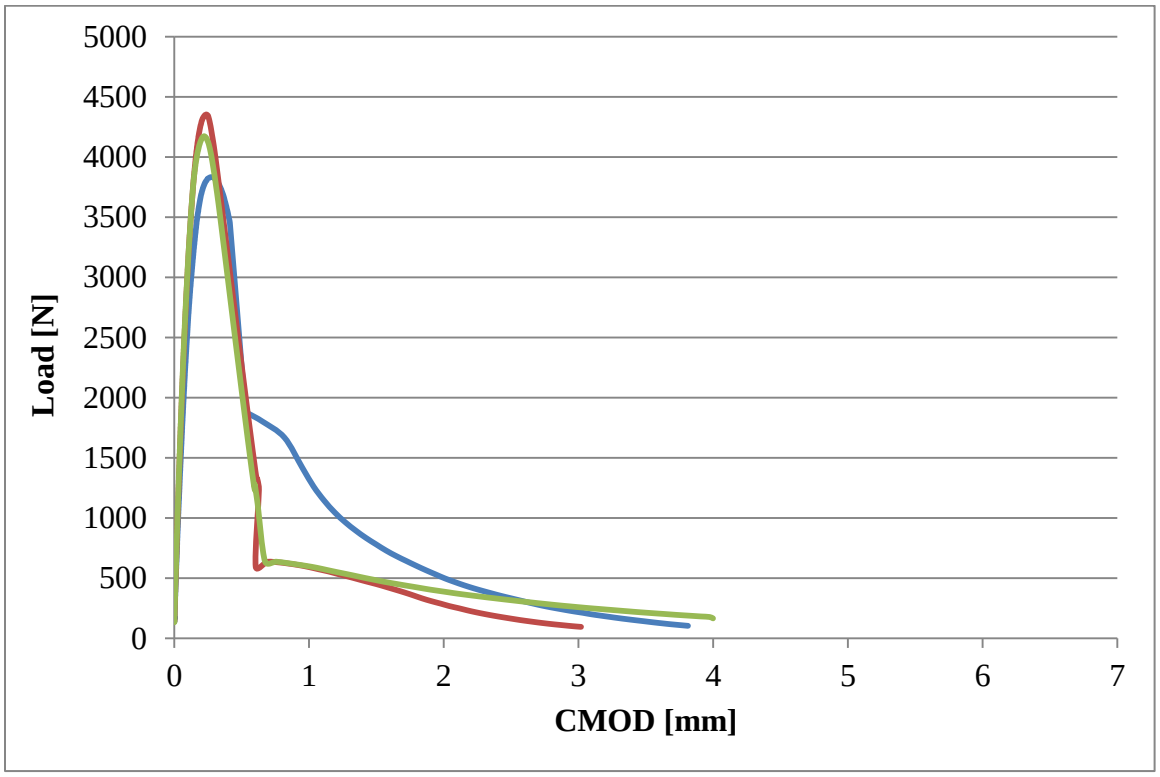

Figure H1: Load-CMOD curves for unconditioned granite samples

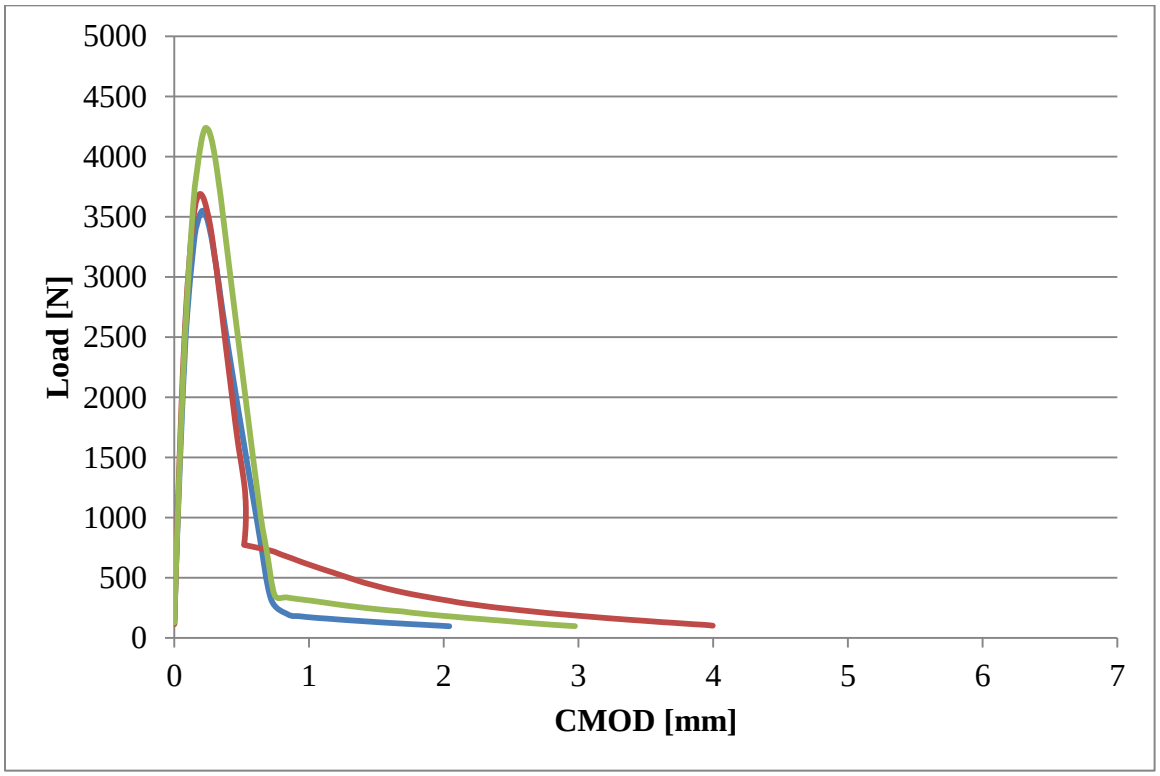

Figure H2: Load-CMOD curves for unconditioned taconitesamples

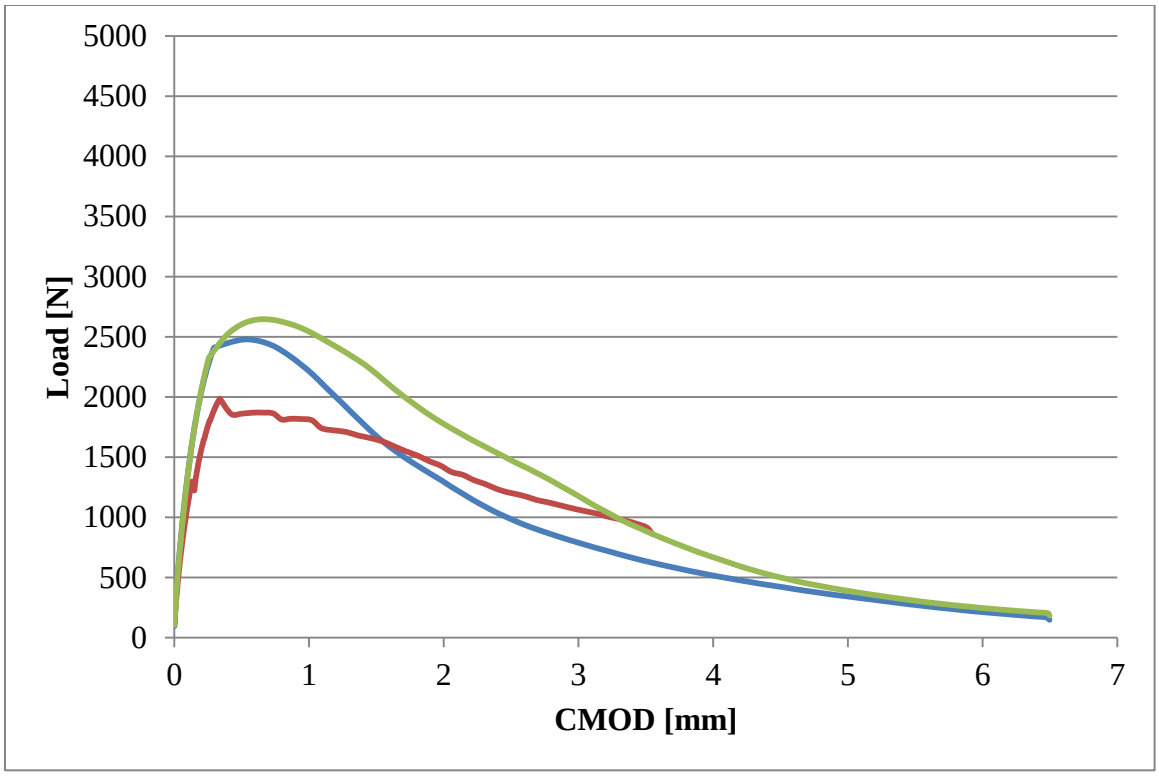

Figure H3: Load-CMOD curves for AASHTO T-283 conditioned granite samples

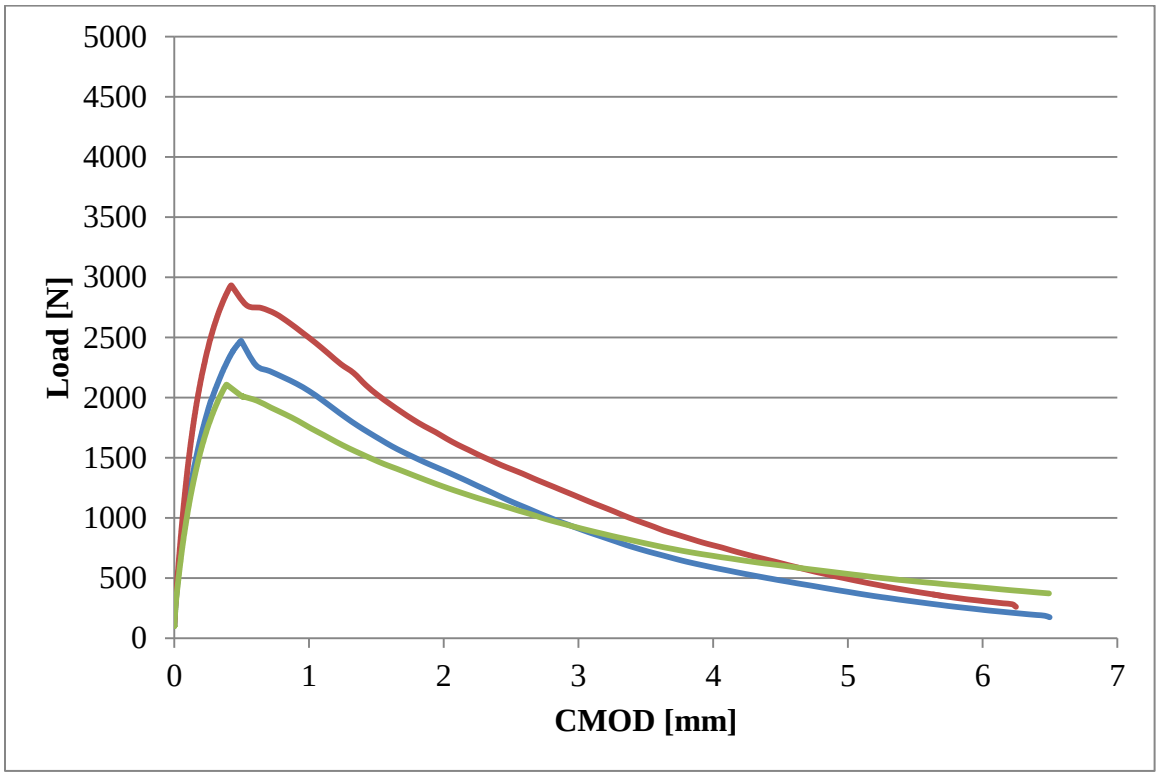

Figure H4: Load-CMOD curves for AASHTO T-283 conditioned taconitesamples

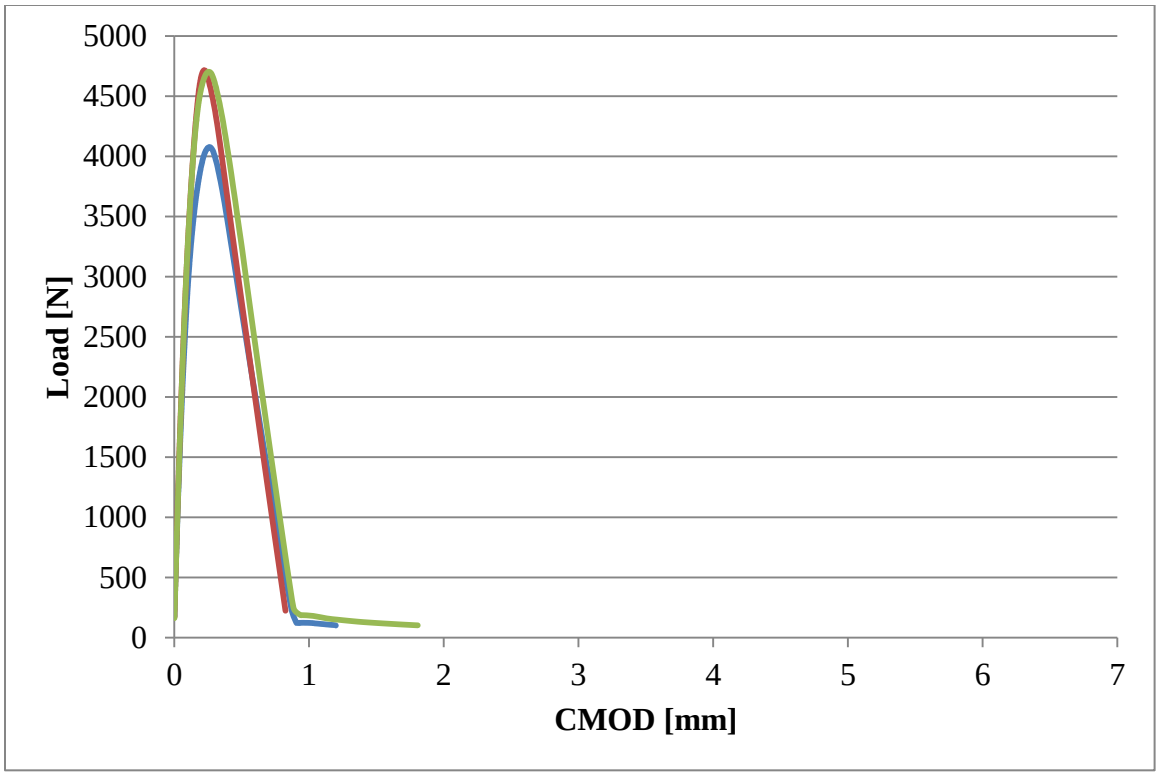

Figure H5: Load-CMOD curves for field conditioned granite samples tested at -24°C

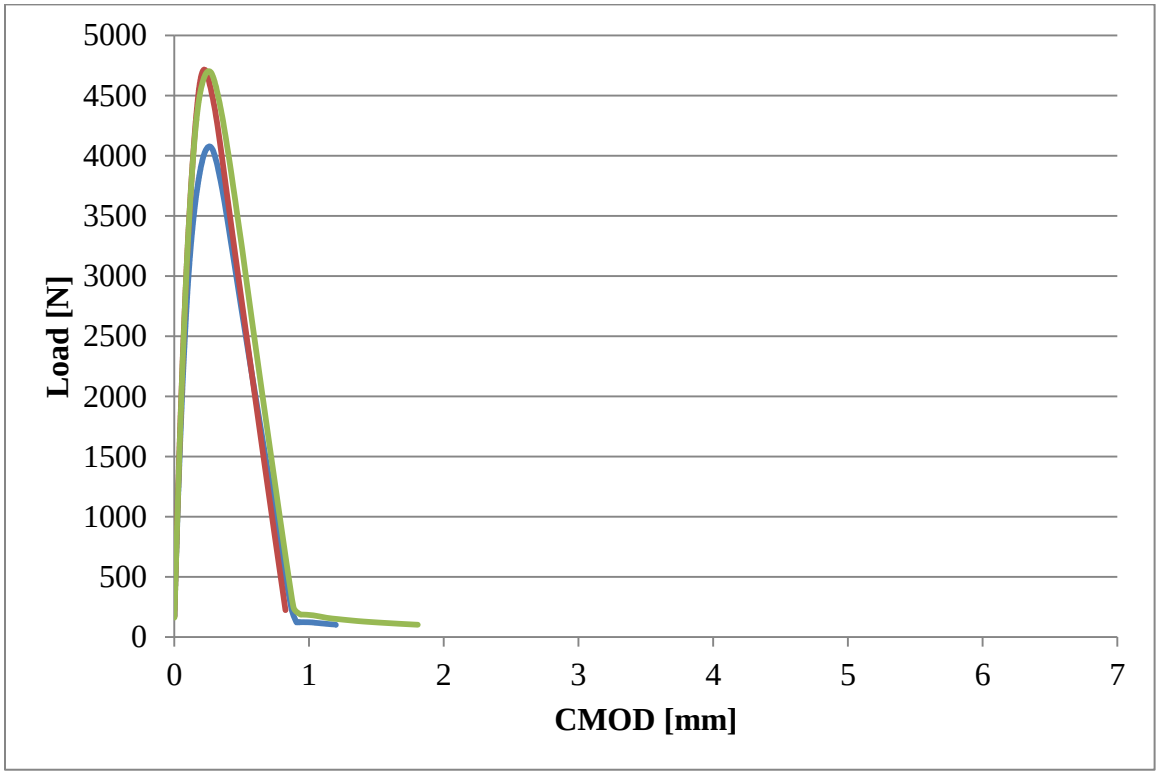

Figure H6: Load-CMOD curves for field conditioned taconite samples tested at -24°C

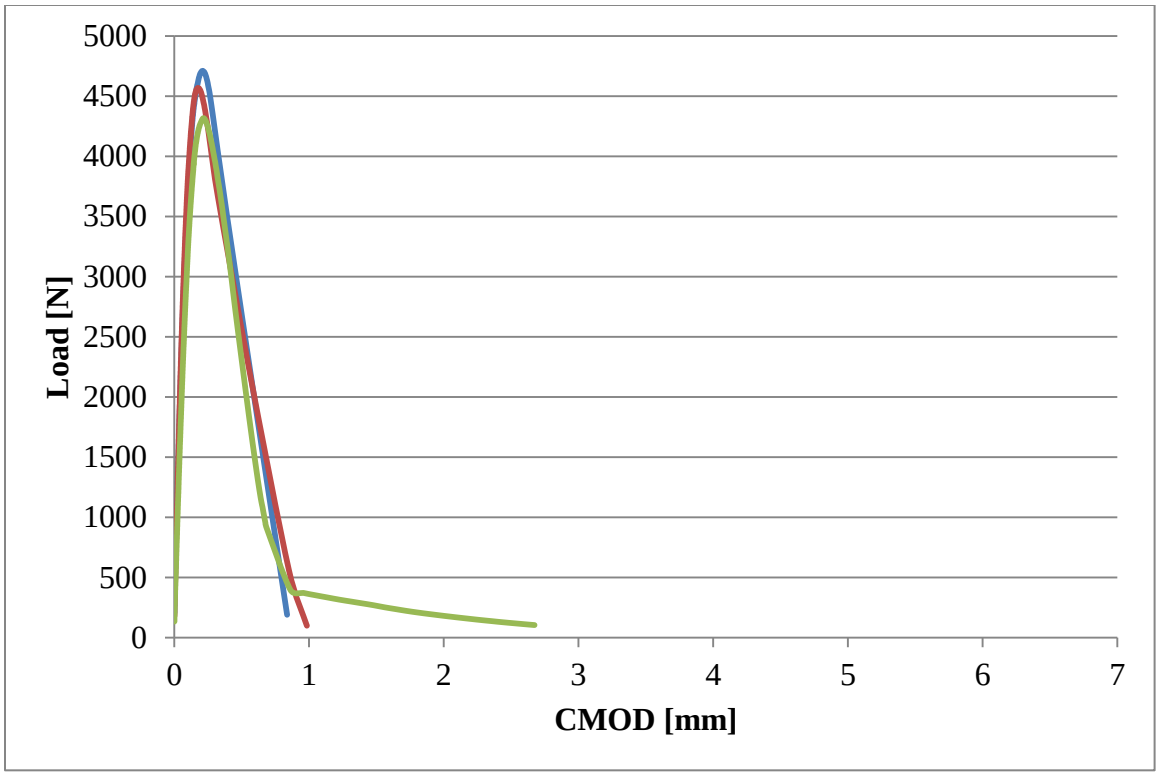

Figure H7: Load-CMOD curves for 10 FT cycle conditioned granite mixture

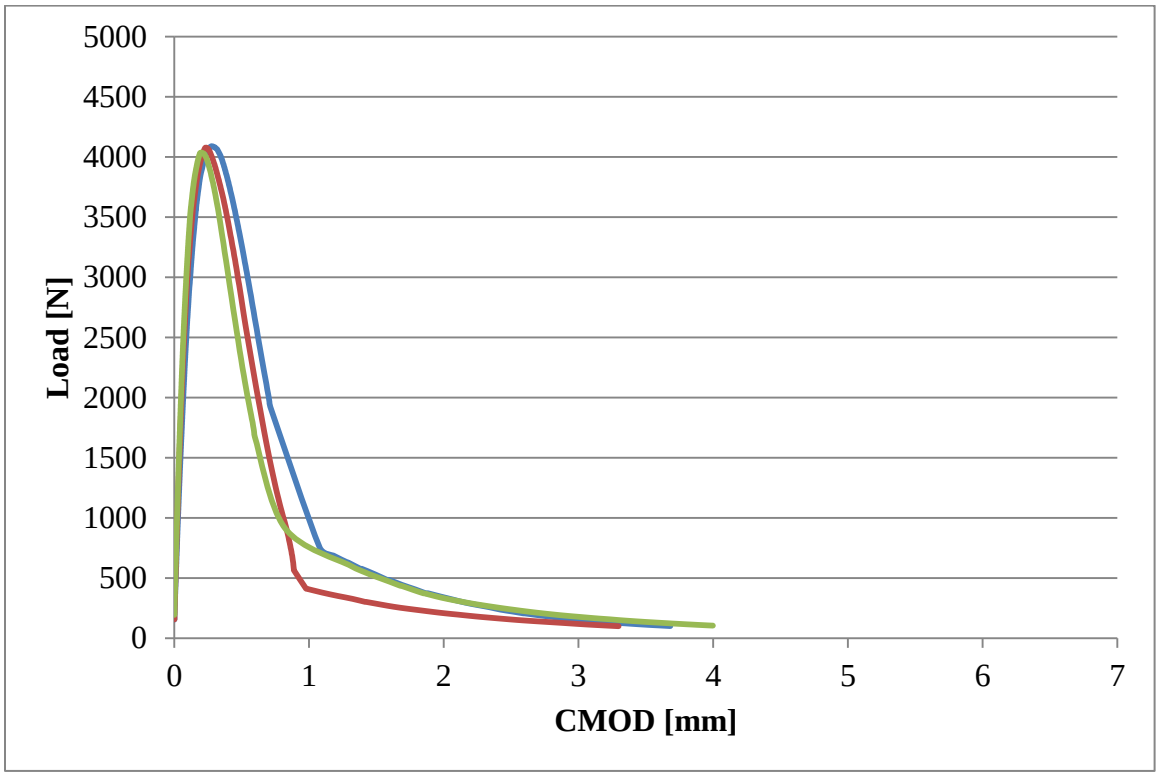

Figure H8: Load-CMOD curves for 10 FT cycle conditioned taconite mixture

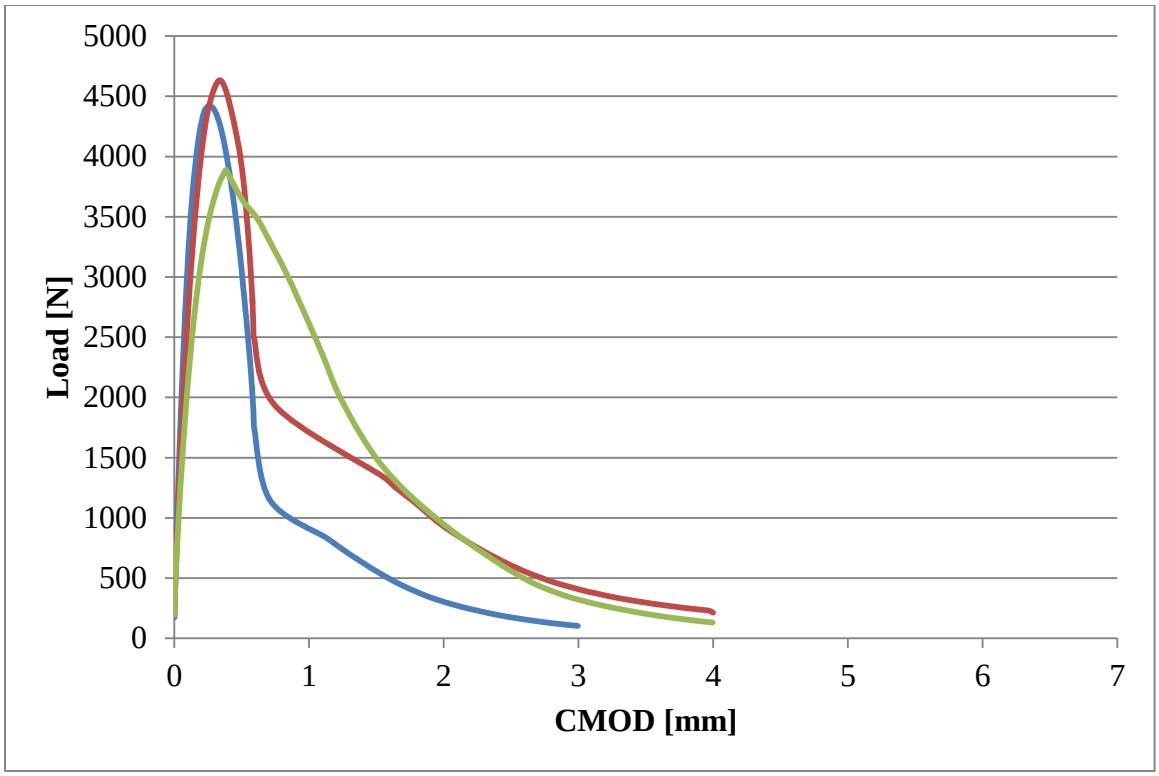

Figure H9: Load-CMOD curves for 20 FT cycle conditioned granite mixture

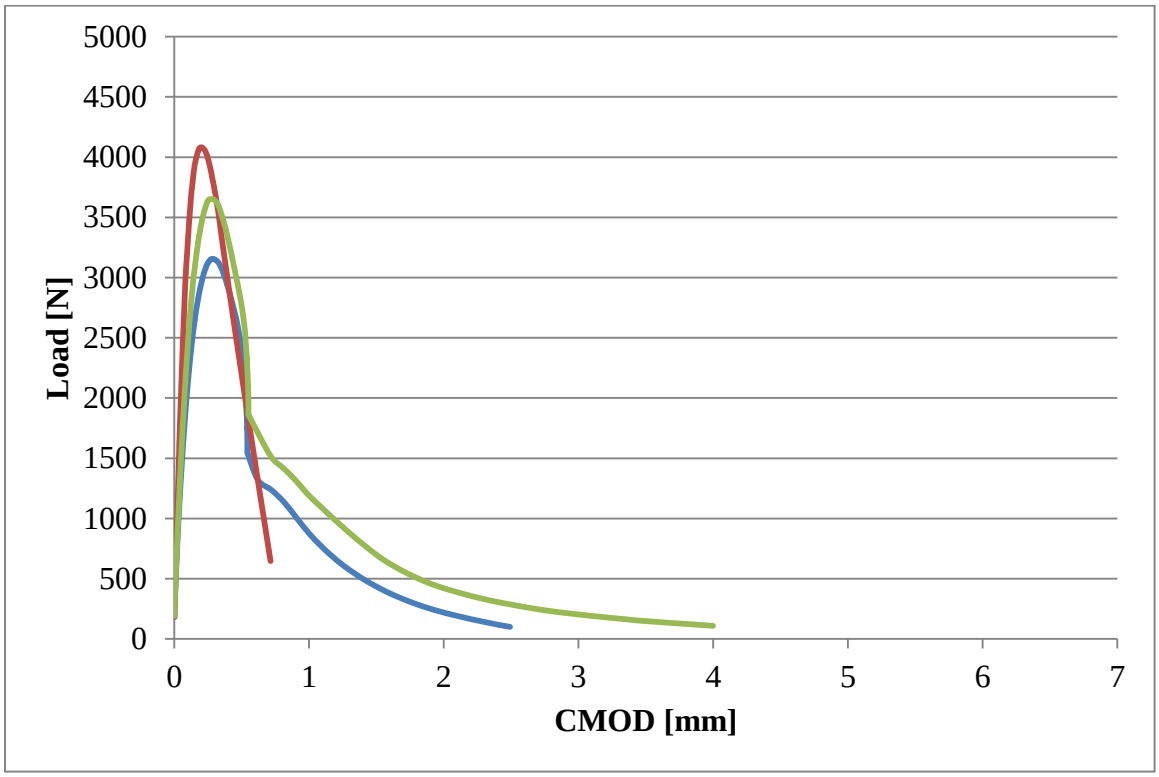

Figure H10: Load-CMOD curves for 20 FT cycle conditioned taconite mixture

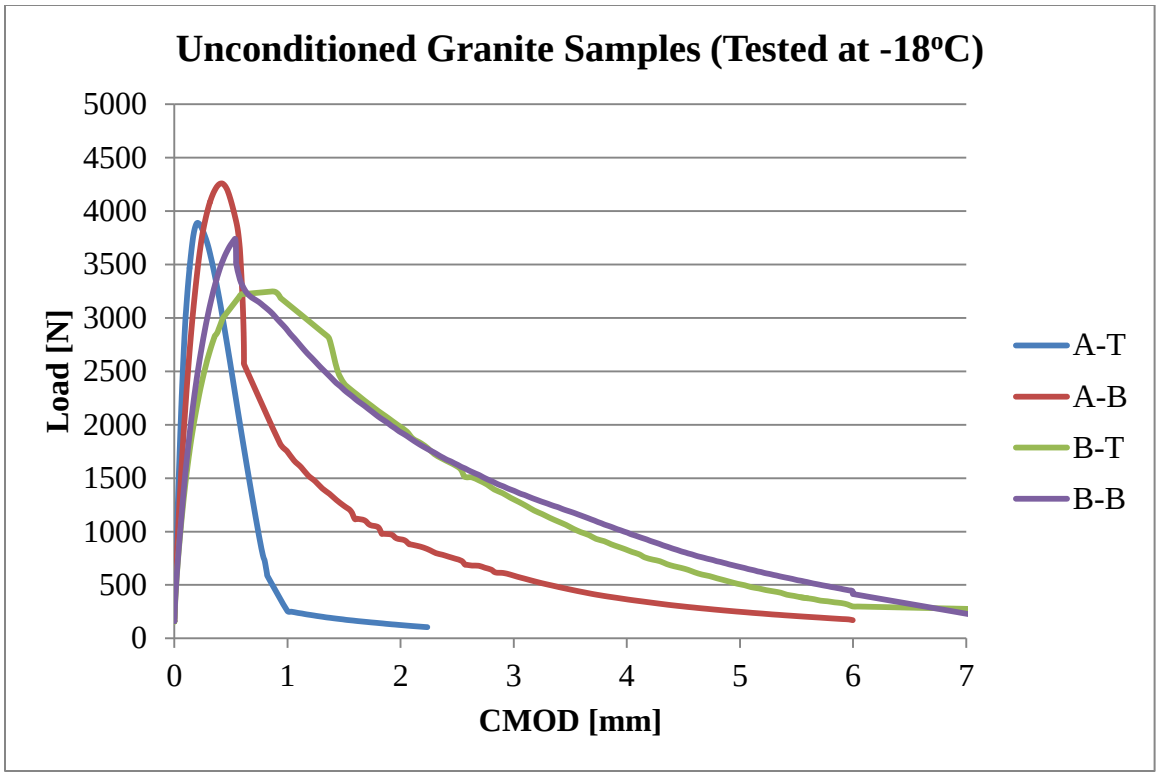

Figure H11: Load-CMOD curves for unconditioned granite mixture tested at -18°C

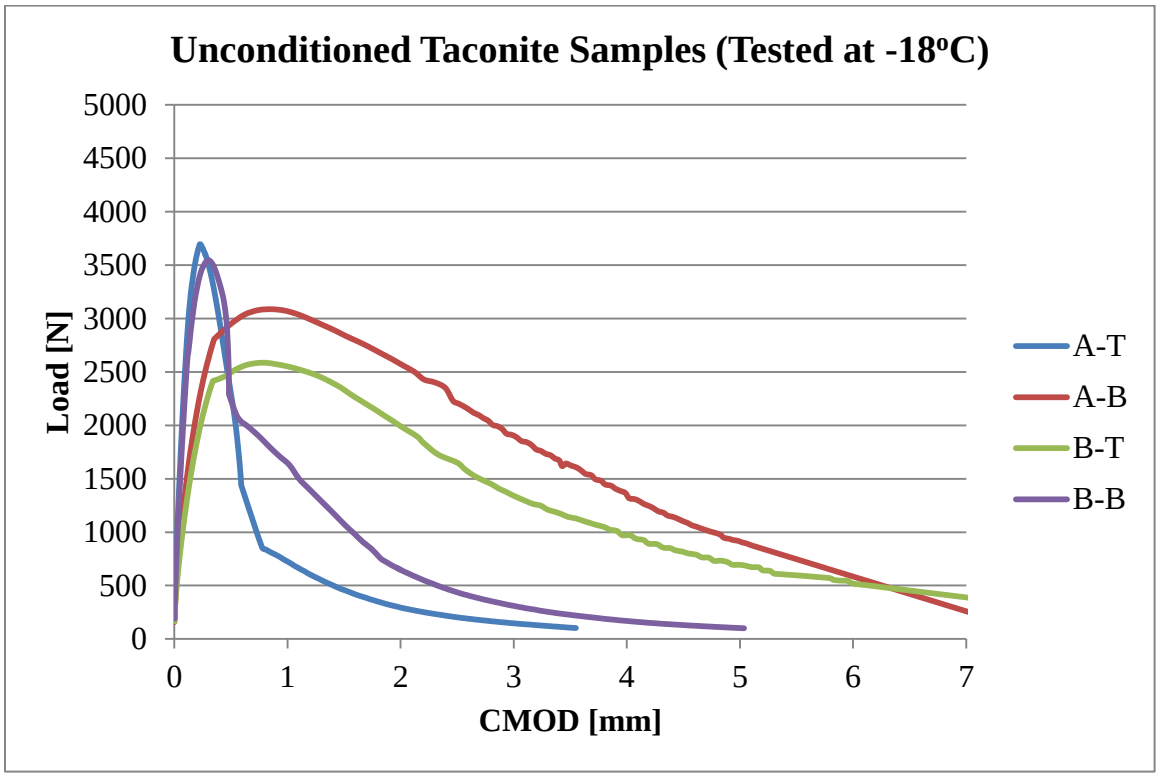

Figure H12: Load-CMOD curves for unconditioned taconite mixture tested at -18°C

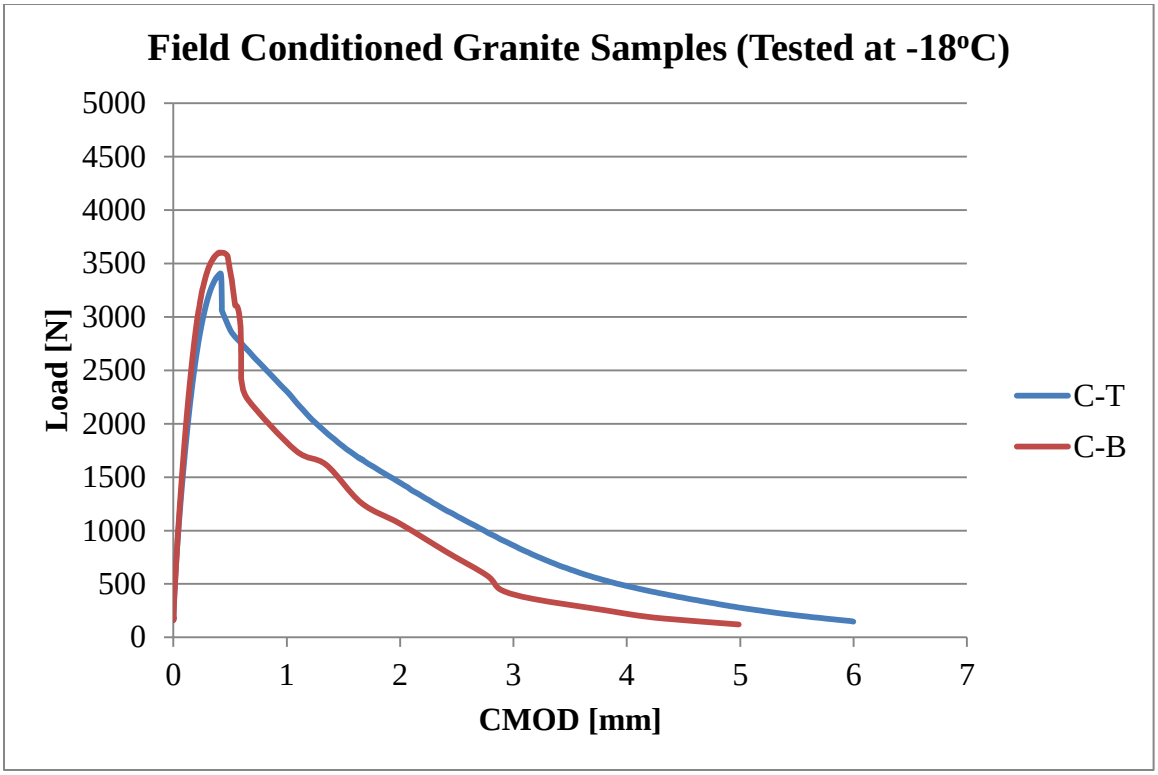

Figure H13: Load-CMOD curves for field conditioned granite mixture tested at -18°C

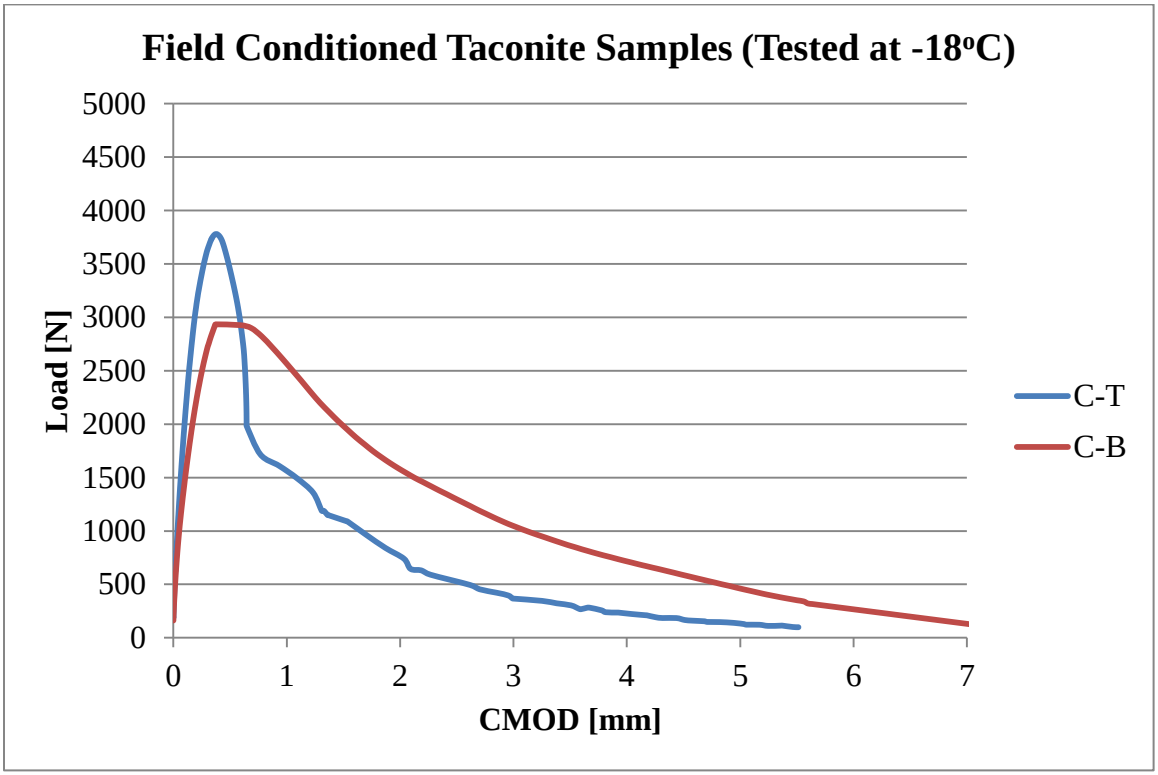

Figure H14: Load-CMOD curves for field conditioned taconite mixture tested at -18°C

Appendix I: DCT Results for Field and Plant Samples

Table I1: DCT results for parking lot samples

	Fracture Energy [J/m^2]		Peak Load [N]	
Sample	Base	Wearing	Base	Wearing
1-T	412.77	538.17	3089.71	2986.73
1-B	428.60	467.98	3408.69	2885.98
2-T	401.11	457.74	3420.69	2917.93
2-B	465.02	535.52	3038.27	2822.13
3-T	385.14	442.64	2953.68	2924.64
3-B	512.62	515.80	3443.73	3495.32
Average	434.21	492.97	3225.79	3005.46
CoV [%]	10.85	8.50	6.89	8.18

Table I2: DCT results for TH9 samples

	Fracture Energy [J/m^2]		Peak Load [N]	
Test Temperature	-24^{o}C	-18^{o}C	-24^{o}C	-18^{o}C
1	264.94	823.26	3953.07	4003.96
2	398.54	610.77	3727.83	4307.98
3	502.63	---	2974.20	---
4	373.12	---	3174.73	---
Average	384.81	717.02	3457.46	4155.97
CoV [%]	25.36	20.95	13.28	5.17

Table I3: DCT results for TH70 samples

	Fracture Energy [J/m^2]		Peak Load [N]	
Test Temperature	-24^{o}C	-18^{o}C	-24^{o}C	-18^{o}C
1	874.13	797.11	3368.81	4073.45
2	745.09	792.91	3533.66	4379.51
3	359.12	---	3911.38	---
4	469.67	---	3405.21	---
Average	612.00	795.01	3554.77	4226.48
CoV [%]	38.97	0.37	6.98	5.12

Table I4: DCT results for TH371 RP 6 samples

	Fracture Energy [J/m^2]		Peak Load [N]	
Sample	Wear	Non-wear	Wear	Non-wear
A	294.86	432.59	3924.84	3542.71
B	552.92	436.16	3932.04	3844.68
C	512.53	541.29	3747.02	3825.32
Average	453.44	470.02	3867.97	3737.57
COV [%]	30.61	13.14	2.71	4.52

Table I5: DCT results for TH371 RP 17 samples

	Fracture Energy [J/m^2]		Peak Load [N]	
Sample	Wear	Non-wear	Wear	Non-wear
A	454.25	425.99	3510.50	3952.32
B	381.73	451.59	3591.01	4228.03
C	232.55	427.57	3389.20	3809.39
Average	356.18	435.05	3496.90	3996.58
CoV [%]	31.74	3.30	2.91	5.32

Table I6: DCT results for TH371 RP 21.5 samples

	Fracture Energy [J/m^2]		Peak Load [N]	
Sample	Wear	Non-wear	Wear	Non-wear
A	392.62	484.87	3392.44	3909.17
B	334.51	476.58	3542.71	3949.76
C	264.64	449.91	3145.20	3905.14
Average	330.59	470.45	3360.12	3921.36
COV [%]	19.38	3.88	5.97	0.63

Appendix J: Load-CMOD Curves for Field and Plant Samples

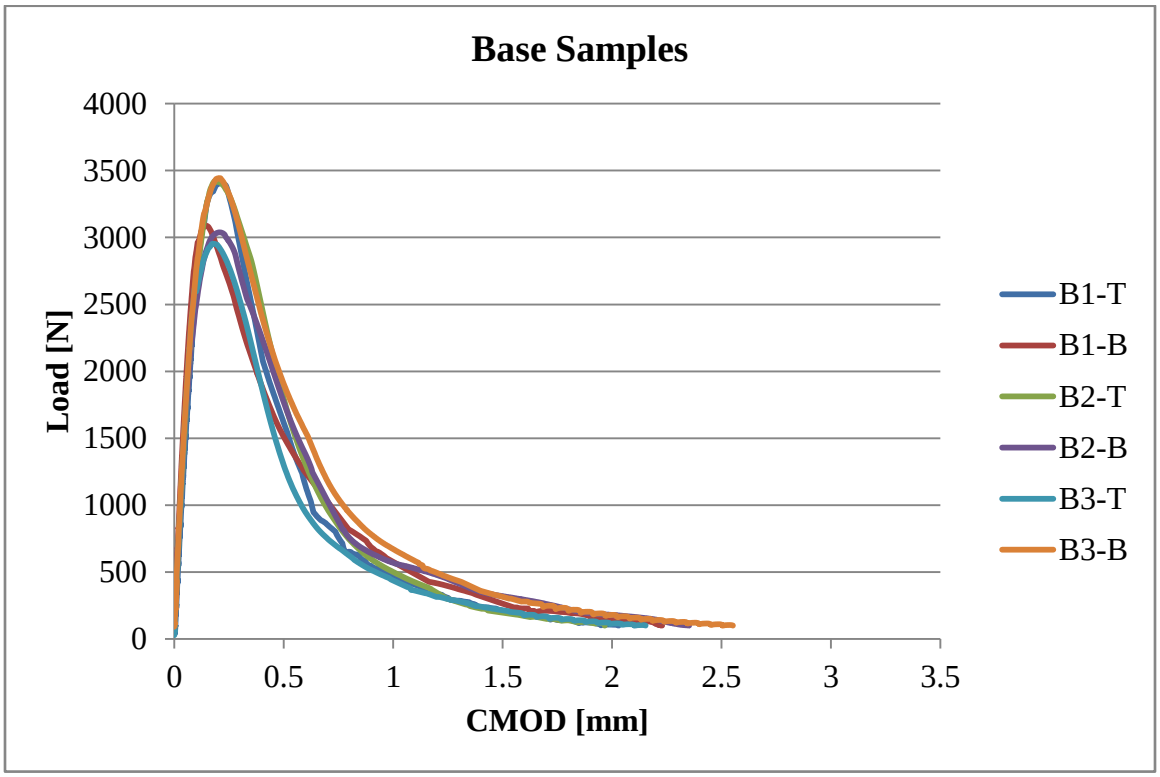

Figure J1: Load-CMOD curves for parking lot base mixture

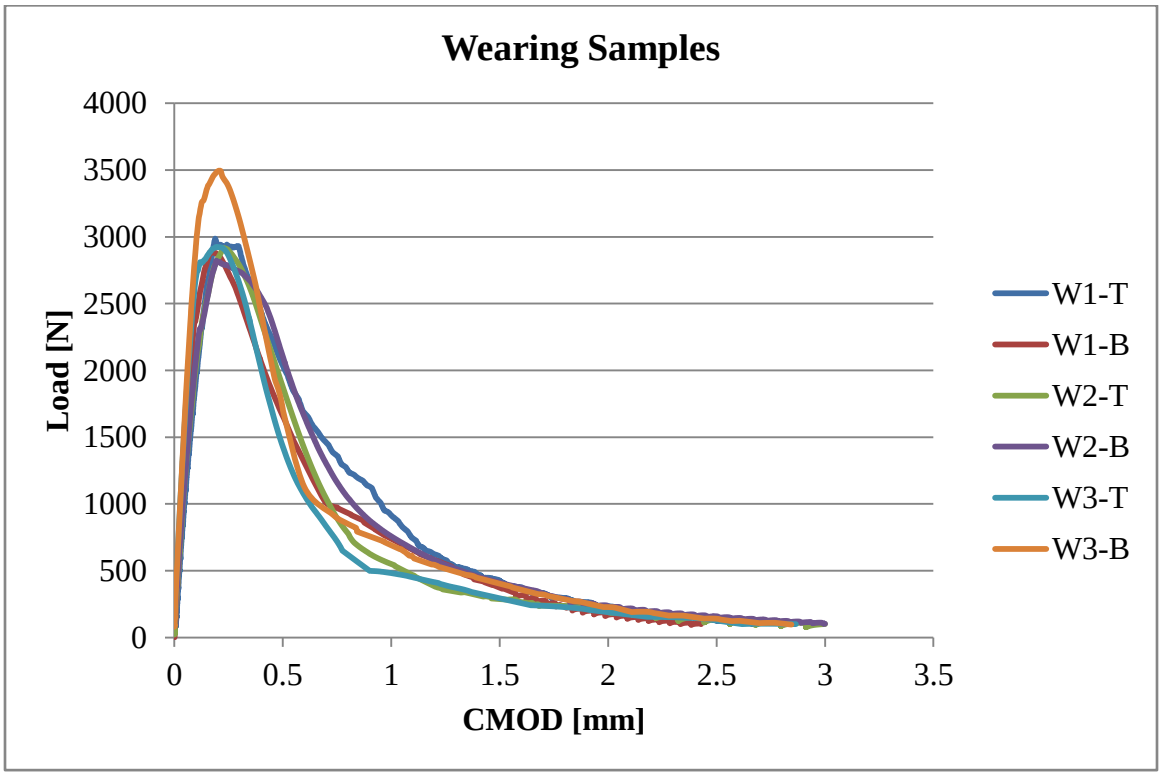

Figure J2: Load-CMOD curves for parking lot wearing mixture

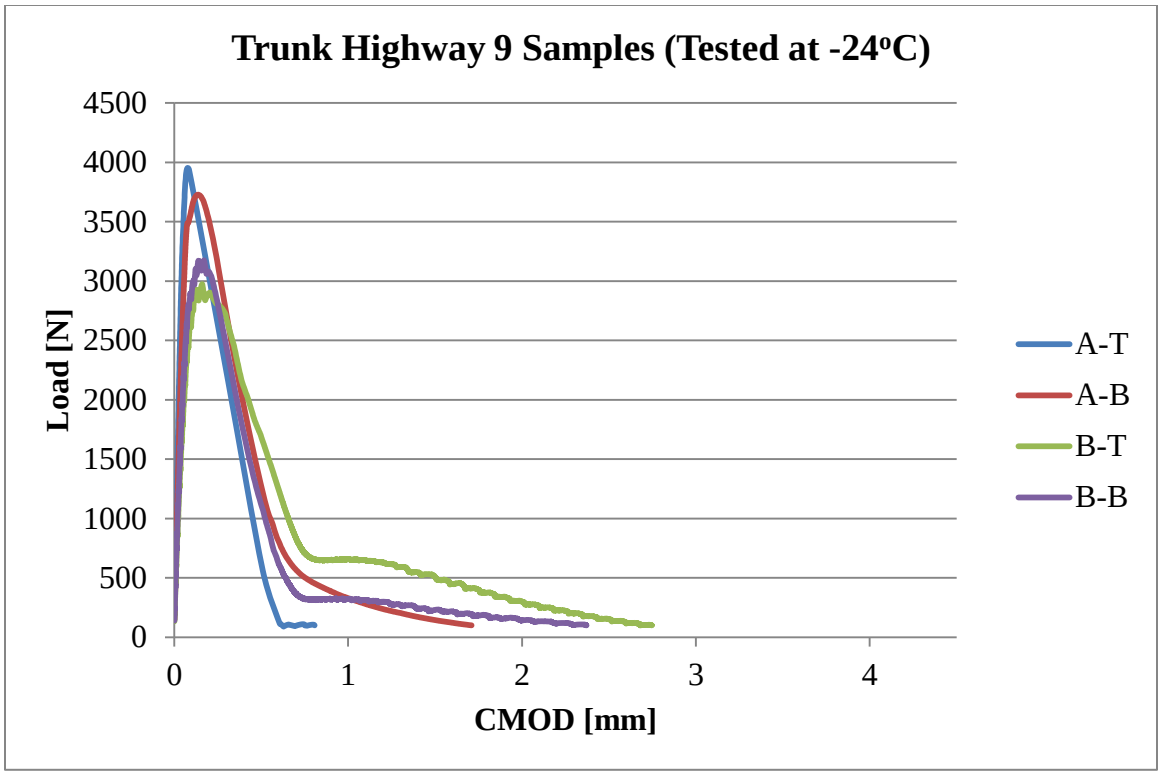

Figure J3: Load-CMOD curves for TH9 samples tested at -24°C

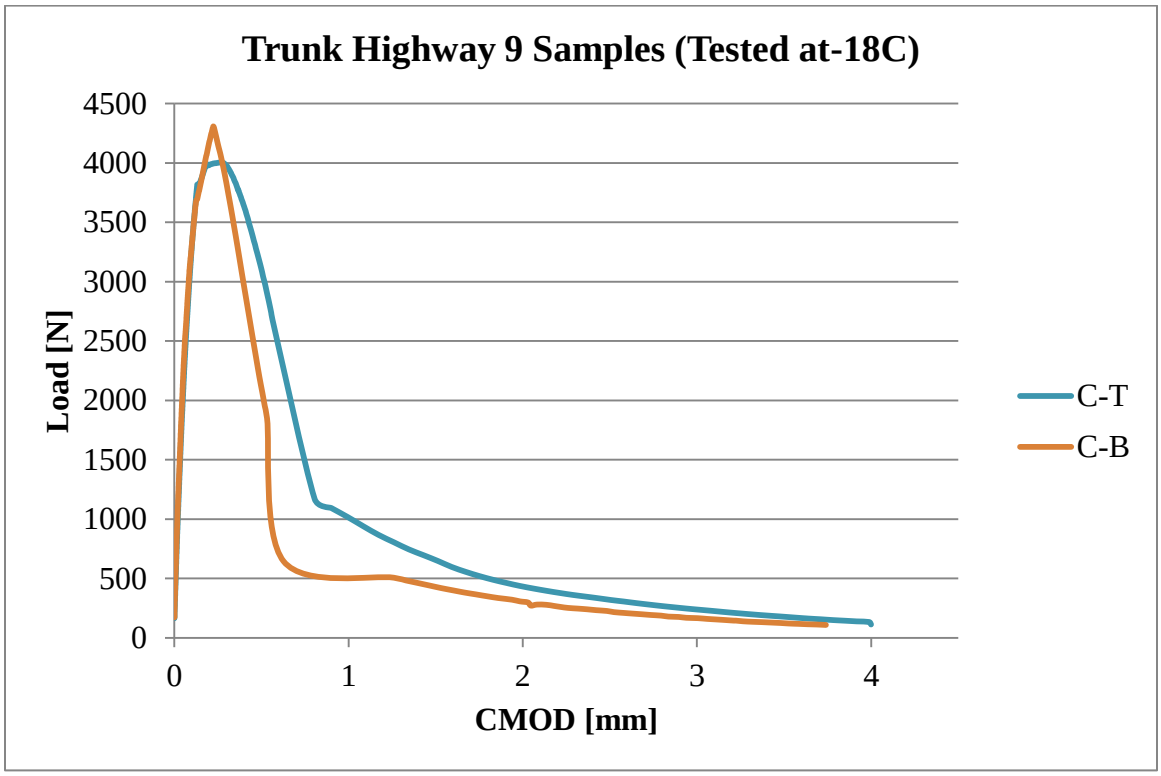

Figure J4: Load-CMOD curves for TH9 samples tested at -18°C

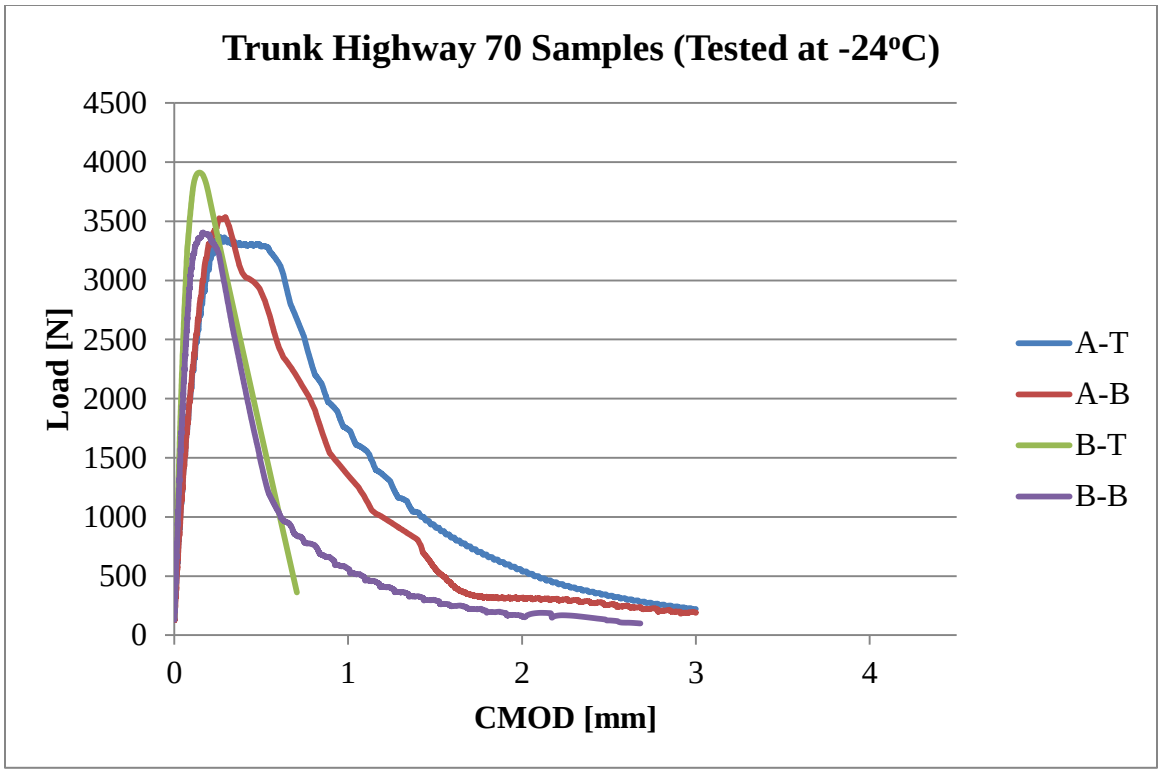

Figure J5: Load-CMOD curves for TH70samples tested at -24°C

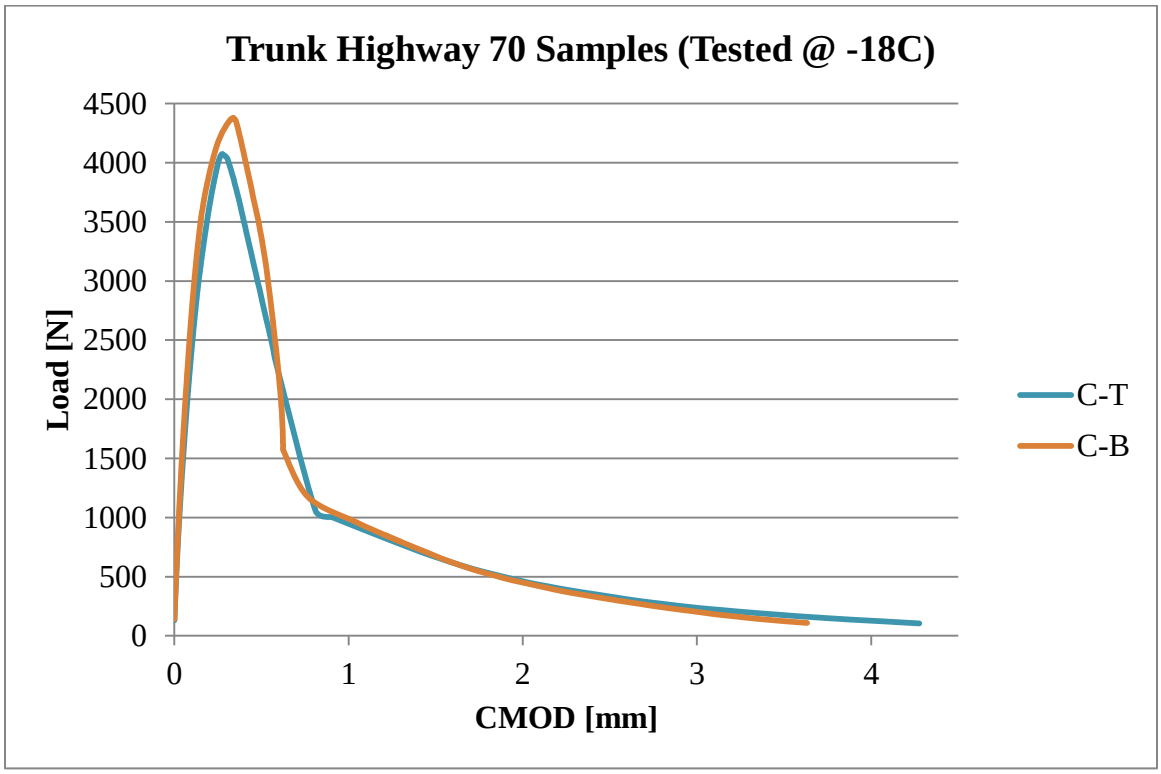

Figure J6: Load-CMOD curves for TH70samples tested at -18°C

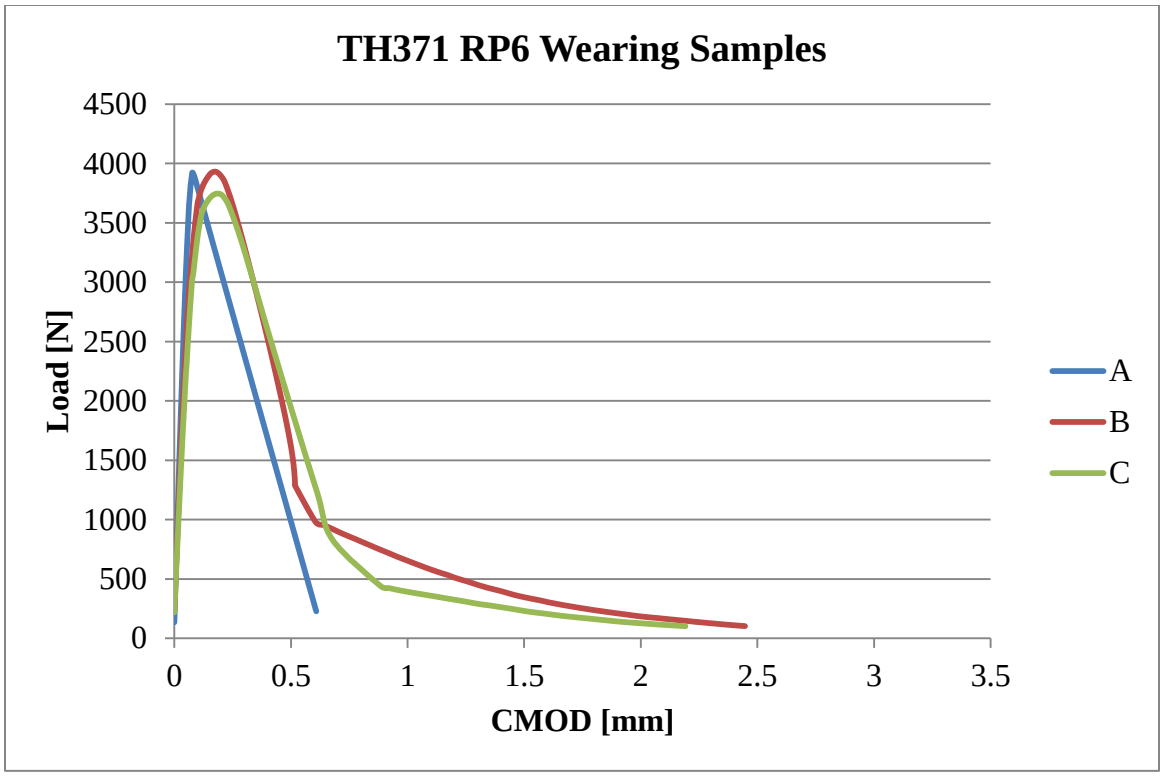

Figure J7: Load-CMOD curves for TH371 RP6 wearing samples

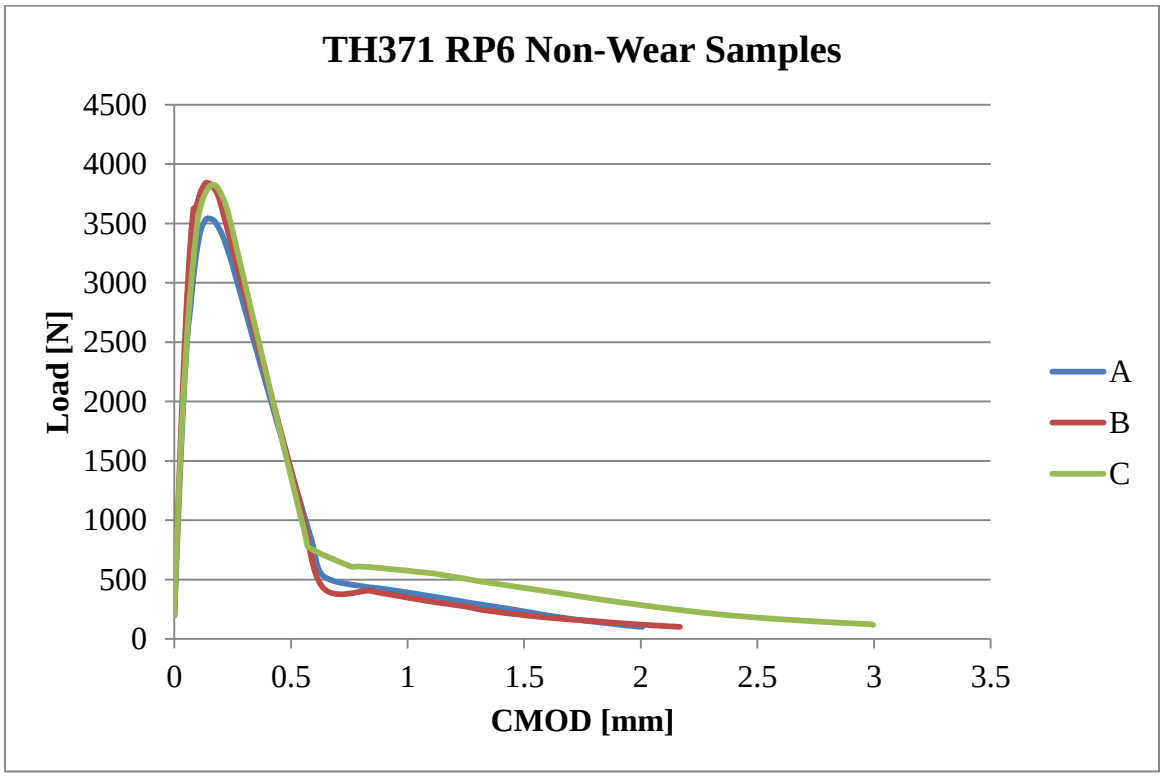

Figure J8: Load-CMOD curves for TH371 RP6 non-wearing samples

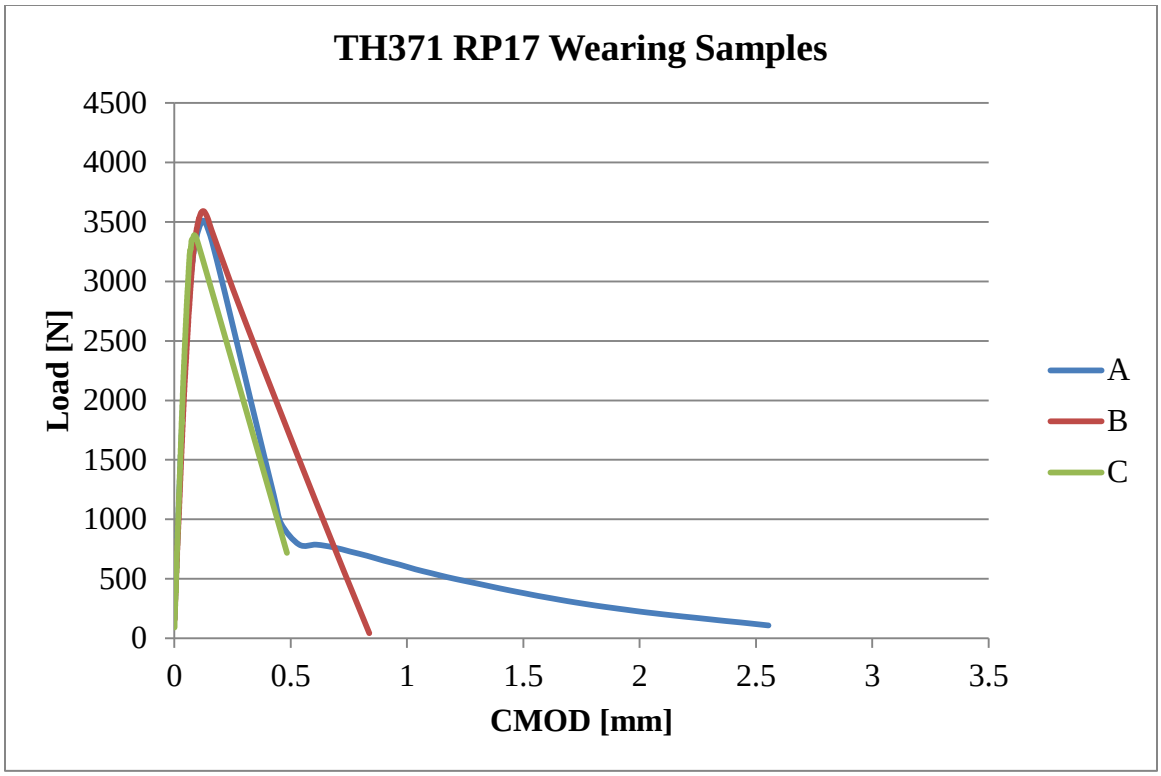

Figure J9: Load-CMOD curves for TH371 RP17 wearing samples

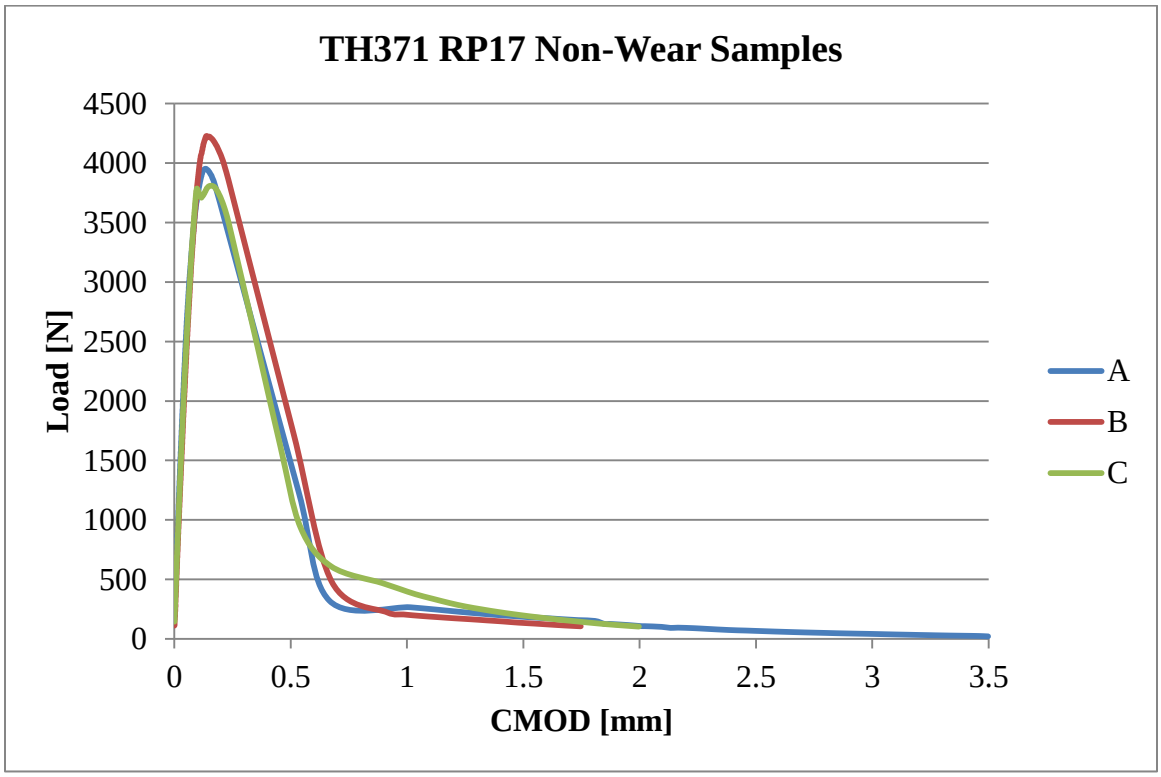

Figure J10: Load-CMOD curves for TH371 RP17 non-wearing samples

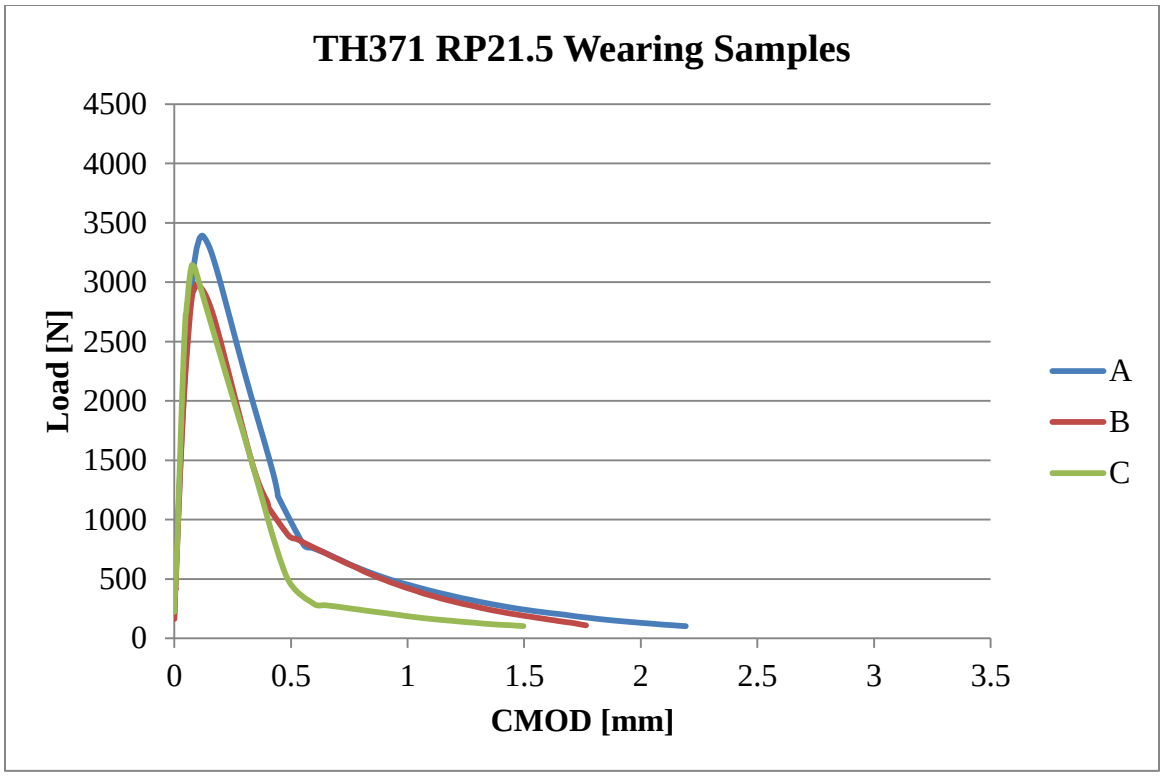

Figure J11: Load-CMOD curves for TH371 RP21.5 wearing samples

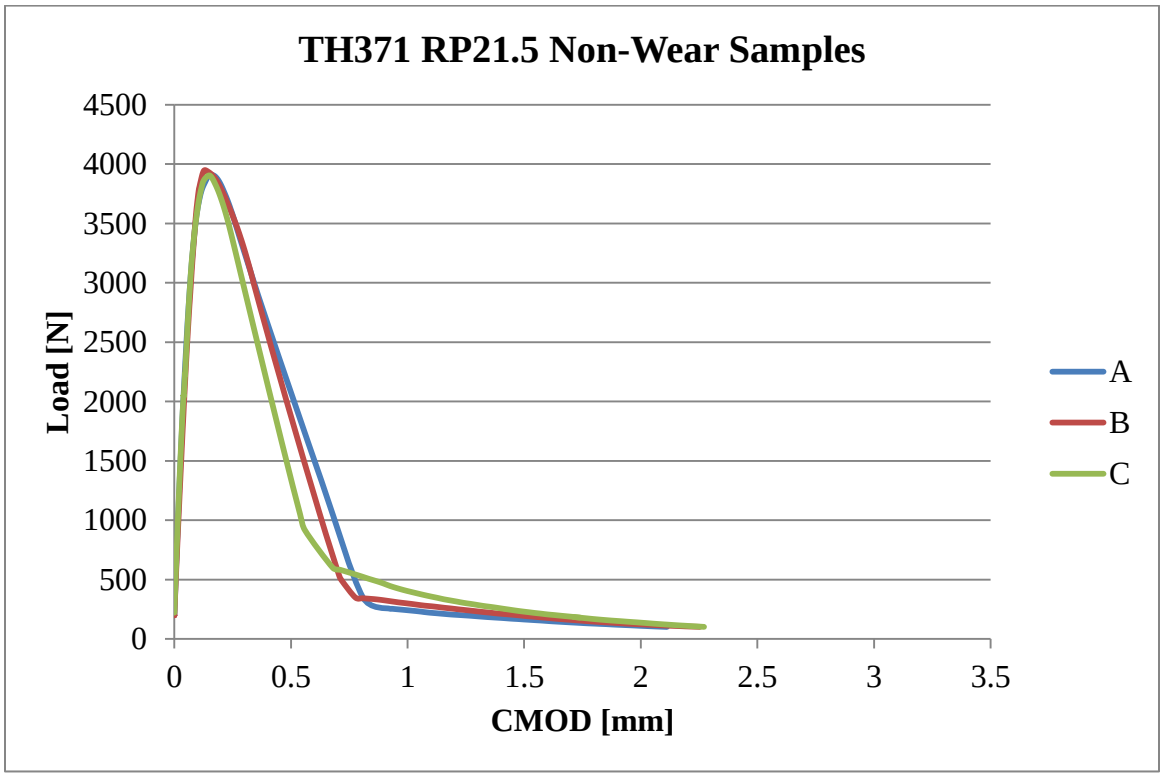

Figure J12: Load-CMOD curves for TH371 RP21.5 non-wearing samples

Appendix K: Parking Lot Mix Designs

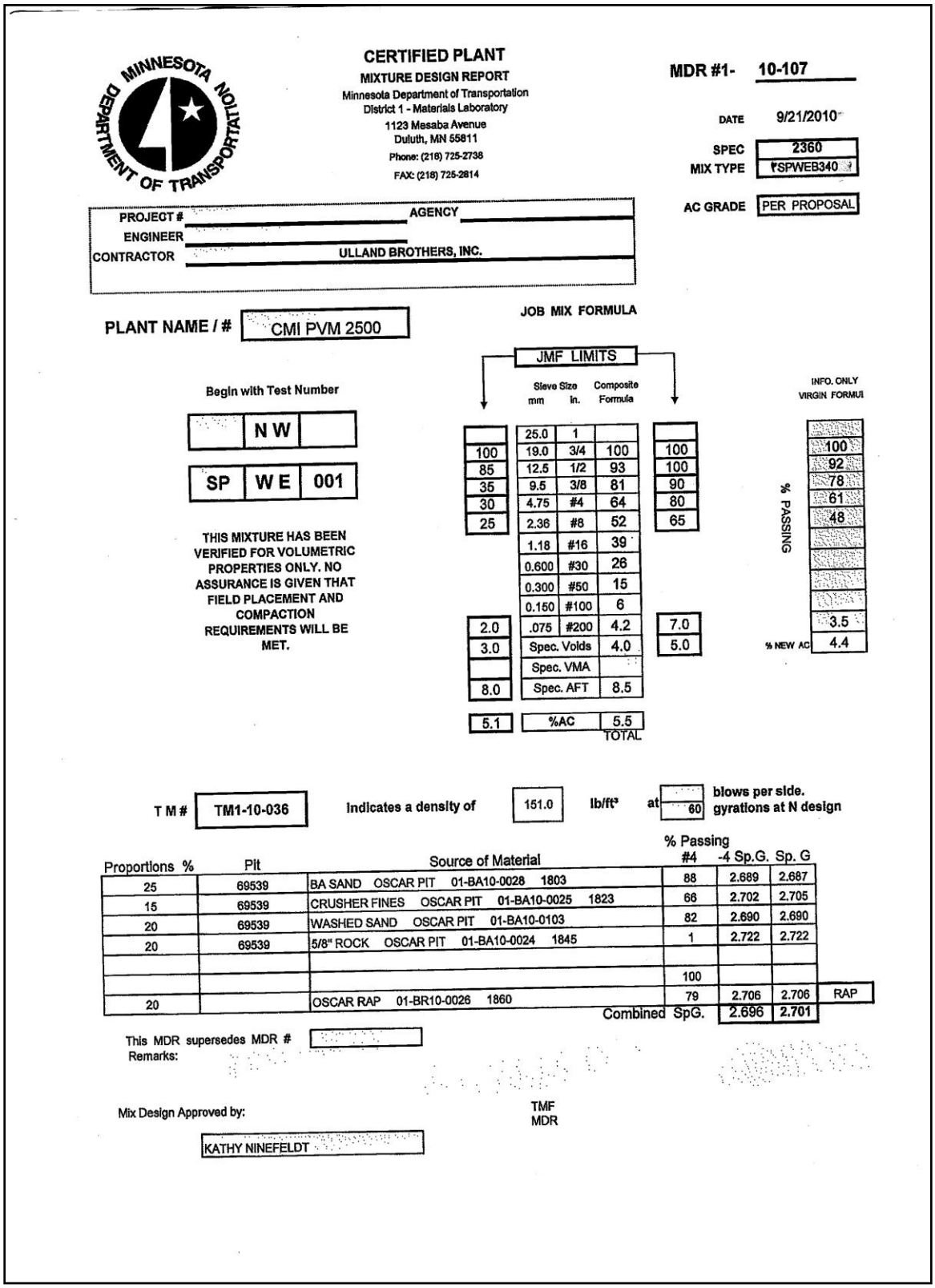

CERTIFIED PLANT
MIXTURE DESIGN REPORT
Minnesota Department of Transportation
District 1 - Materials Laboratory
1123 Mesaba Avenue
Duluth, MN 55811
Phone: (218) 725-2738
FAX: (218) 725-2814

MDR #1- 10-107
DATE 9/21/2010
SPEC 2360
MIX TYPE SPWEB340
AC GRADE PER PROPOSAL

PROJECT #
AGENCY
ENGINEER
CONTRACTOR ULLAND BROTHERS, INC.

PLANT NAME / # CMI PVM 2500

JOB MIX FORMULA

Begin with Test Number

N W
SP W E 001

THIS MIXTURE HAS BEEN VERIFIED FOR VOLUMETRIC PROPERTIES ONLY. NO ASSURANCE IS GIVEN THAT FIELD PLACEMENT AND COMPACTION REQUIREMENTS WILL BE MET.

JMF LIMITS	Sieve Size mm	Sieve Size in.	Composite Formula	JMF LIMITS	INFO. ONLY VIRGIN FORMUI
	25.0	1			
100	19.0	3/4	100	100	100
85	12.5	1/2	93	100	92
35	9.5	3/8	81	90	78
30	4.75	#4	64	80	61
25	2.36	#8	52	65	48
	1.18	#16	39		
	0.600	#30	26		
	0.300	#50	15		
	0.150	#100	6		
2.0	.075	#200	4.2	7.0	3.5
3.0	Spec. Voids		4.0	5.0	% NEW AC 4.4
	Spec. VMA				
8.0	Spec. AFT		8.5		
5.1	%AC		5.5 TOTAL		

% PASSING

TM # TM1-10-036 Indicates a density of 151.0 lb/ft³ at 60 blows per side. gyrations at N design

Proportions %	Pit	Source of Material	% Passing #4	-4 Sp.G.	Sp. G	
25	69539	BA SAND OSCAR PIT 01-BA10-0028 1803	88	2.689	2.687	
15	69539	CRUSHER FINES OSCAR PIT 01-BA10-0025 1823	66	2.702	2.705	
20	69539	WASHED SAND OSCAR PIT 01-BA10-0103	82	2.690	2.690	
20	69539	5/8" ROCK OSCAR PIT 01-BA10-0024 1845	1	2.722	2.722	
			100			
20		OSCAR RAP 01-BR10-0026 1860	79	2.706	2.706	RAP
			Combined SpG.		2.696	2.701

This MDR supersedes MDR #
Remarks:

Mix Design Approved by:

KATHY NINEFELDT

TMF
MDR

CERTIFIED PLANT

MIXTURE DESIGN REPORT

Minnesota Department of Transportation
District 1 - Materials Laboratory
1123 Mesaba Avenue
Duluth, MN 55811
Phone: (218) 725-2738
FAX: (218) 725-2814

MDR #1- 10-110

DATE 9/23/2010

SPEC 2360
MIX TYPE SPNWB330

AC GRADE PER PROPOSAL

PROJECT #
ENGINEER AGENCY
CONTRACTOR ULLAND BROTHERS

PLANT NAME / # CMI PVM 2500

JOB MIX FORMULA

Begin with Test Number

SP	N W	001
	W E	

THIS MIXTURE HAS BEEN VERIFIED FOR VOLUMETRIC PROPERTIES ONLY. NO ASSURANCE IS GIVEN THAT FIELD PLACEMENT AND COMPACTION REQUIREMENTS WILL BE MET.

JMF LIMITS	Sieve Size mm	Sieve Size in.	Composite Formula		INFO. ONLY VIRGIN FORMUI
	25.0	1			
100	19.0	3/4	100	100	100
85	12.5	1/2	92	100	91
35	9.5	3/8	80	90	77
30	4.75	#4	63	80	59
25	2.36	#8	51	65	48
	1.18	#16	39		
	0.600	#30	27		
	0.300	#50	15		
	0.150	#100	7		
2.0	.075	#200	4.6	7.0	4.0
2.0	Spec. Voids		3.0	4.0	% NEW AC 4.4
	Spec. VMA				
8.0	Spec. AFT		8.5		
5.1	%AC		5.5 TOTAL		

% PASSING

T M # 1-10-038 **Indicates a density of** 152.9 **lb/ft³** **at** 60 **blows per side. gyrations at N design**

Proportions %	Pit	Source of Material	% Passing #4	-4 Sp.G.	Sp. G
33	69539	OSCAR PIT BA SAND (1803) BA1-10-028	88	2.689	2.687
15	69539	OSCAR PIT CRUSHER FINES (1823) BA1-10-025	66	2.702	2.705
10	69539	OSCAR PIT WASHED SAND BA1-10-103	82	2.690	2.690
22	69539	OSCAR PIT 5/8 ROCK (1845) BA1-10-024	1	2.722	2.722
	-				
	69539	BAG HOUSE FIHES	100	2.698	2.698
20	69539	OSCAR RAP (1860) BR1-10-026	79	2.706	2.706 RAP
			Combined SpG.	2.696	2.701

This MDR supersedes MDR #
Remarks:

Mix Design Approved by:

DENISE ANDERSON

TMF
MDR

Appendix L: Mix Designs for Highways 9, 70, And 371

Table L1: Volumetric Properties for TH9 and TH70 Mixtures

	TH9	TH70
Project #	SP6010-26	SP3310-11
Mix Type	SPWEB340C	SPWEB340C
Gradation	coarse	fine
Design Gyrations	60	60
Binder	PG58-34	PG58-34
RAP [%]	20	20
Total AC [%]	4.0	5.2
New AC Ratio [%]	73	76
AFT [microns]	8.5	8.4
VMA [%]	13.2	15.9
G_{mm}	2.53	2.512
G_{mb}	2.428	2.375

Table L2: Highway 371 Mix Design Specifications

	RP 6		RP 17 / RP 21.5	
	Wearing	Non-wear	Wearing	Non-wear
Mix Type	WEB440F	NWC430H	WEB440F	NW430B
NMAS [mm]	12.5	19.0	12.5	19.0
Design Traffic Level	4	4	4	4
Binder Type	PG58-34	PG70-28	PG64-34	PG58-28
Design Air Void Level [%]	4.0	3.0	4.0	3.0
HMA Thickness [in]	3.5	2.5	4.0	2.5
Base	7" Class 6		10" Class 6	
Subbase	12" Select Granular		12" Select Granular	